Zeitschrift: IABSE reports of the working commissions = Rapports des commissions de travail AIPC = IVBH Berichte der Arbeitskommissionen

Band: 16 (1974)

Rubrik: Theme II: Simple design procedures

II

Accuracy of Simple Design Procedures for Concrete Columns

Précision des méthodes simples de dimensionnement des colonnes en béton

Über die Genauigkeit einfacher Bemessungsverfahren für Betonstützen

Urs H. OELHAFEN
Dr.sc.techn., Prof.
ITR Rapperswil Engineering College
Rapperswil, Switzerland

1. INTRODUCTION

Design methods for slender reinforced concrete columns based on allowable stresses have been prooved to be inadequate. As a consequence of the non-linear relation between lateral deflections and cross-section forces these methods may claim safety levels which, in reality, are much smaller than the methods suggest. Thus, the prediction of ultimate load capacity is an essential point in most of the recent design procedures. Safety is vouched for by safety factors introduced where uncertainties are present: at the loads, at the strengths, at the stiffnesses, etc. The moment magnifier method as it is recommended in the ACI Building Code 318-71 (1) is an example of such a procedure. The accuracy of the moment magnifier method has been studied in recent investigations (2, 3) based on extensive computer analyses and comparisons with test results. It has been found that the accuracy of the method can be improved only within limits because the method does not distinguish properly between columns which might fail due to a material failure and those which might fail due to a stability failure.

This paper will outline ways of developing an alternative procedure which accounts for both types of failure by a step-by-step computation of the load-moment-curve (or load-deflection curve). Only the behavior of the hinged ended column bent in single curvature is considered. The investigation of the moment magnifier method (2, 3) will be quoted repeatedly because it is the basis of the method presented in this paper.

2. ANALYSIS OF SHORT TERM LOAD CAPACITY OF SLENDER COLUMNS

2.1 Method of Analysis

The computer analysis described briefly in this section was used to predict the strength and behavior of slender columns. The

results of design procedures were then compared to the results of this rigorous analysis. A more detailed description of the method of analysis is given in Refs. 2 and 4 .

Material Properties

1. Steel: idealized elastoplastic material
2. Concrete: stress-strain relationship
   - linear in the range $f'_t/E_c \leq \varepsilon \leq 0$
   - quadratic parabola in the range $0 < \varepsilon < 2f'_c/E_c$
   - perfectly plastic in the range $2f'_c/E_c \leq \varepsilon \leq \varepsilon_u$

Method of Analysis

1. The cross-section of a column subjected to uniaxial bending and compression is divided into a number of concrete and steel fibres parallel to the neutral axis.
2. The ultimate compression strain ε_u is divided into a number of segments which are selected as strain increments at the compressed edge of the cross-section.
3. By varying the strain distribution over the depth of the cross-section the sum of the internal forces (computed from the basic stress-strain relationships) is made equal to the external force P_i by means of a trial and error procedure.
4. By repeating of 3.) for all given values of P_i (i=1,2...NP) and all given values of ε_j (j=1,2...NE) the moment curvature relationship $M_{i,j}$, $\Phi_{i,j}$ results.
5. The influence of the concrete tensile zone will be included by subtracting a correction $\Delta\Phi$ from the computed curvature, Φ . The following corrections are applied:

$$M \leq M_o : \quad \Delta\Phi = 0$$

$$M_o < M < M_{cr} : \quad \Delta\Phi = \Delta\Phi_{cr} \frac{M - M_o}{M_{cr} - M_o}$$

$$M_{cr} \leq M : \quad \Delta\Phi = \Delta\Phi_{cr} \frac{M_{cr} - M_o}{M - M_o}$$

where: M_o is the moment for zero strain at the tensile edge

M_{cr} is the cracking moment

$\Delta\Phi_{cr}$ is the difference between the curvature computed for the cracked cross-section and the curvature computed for the uncracked cross-section both evaluated for the moment $M = M_{cr}$.

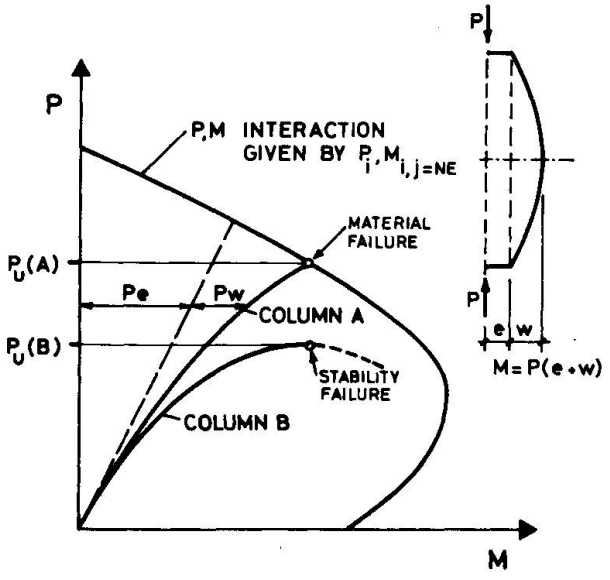

FIG. 1: BEHAVIOR OF SLENDER COLUMNS

6. The moment curvature relationships $M_{i,j}$, $\Phi_{i,j}$ are used in an iterative numerical integration procedure to determine the deflections, w, of the column subjected to P_i.
7. By repeating the computation of deflections for different values of P_i a load-moment relationship P,M representing the column behavior, can be found where M is the maximum moment at midheight given by M = P(e + w). Failure is assumed to occur at the intersection of this P,M curve with the P,M interaction curve (material failure) or at the point on the P,M curve where dP/dM becomes zero (stability failure) as shown in Fig. 1. The interaction curve is given by P_i, $M_{i,j=NE}$ and follows for j = NE from the moment curvature relationships.

2.2 Design of Computer Experiment

The variables listed in Table 1 were found to have the most effect on the column stiffness EI. To study the effects of these variables the eight values of each variable listed in Table 1 were chosen.

A fully factorial six factor experimental design with eight factor levels for each variable would call for 8^6 computer analyses or experiments. A Graeco-Latin square design allows to reduce this excessive number to 64 by an efficient combination of the variables. Each of the 64 cells in Table 2 represents one "computer experiment" and each of the first seven numbers in each cell represents the level of one variable listed in Table 1. For example, the combination 327458216 for cross-section shape B and slenderness ratio l/h = 15 means that the properties of this column were:

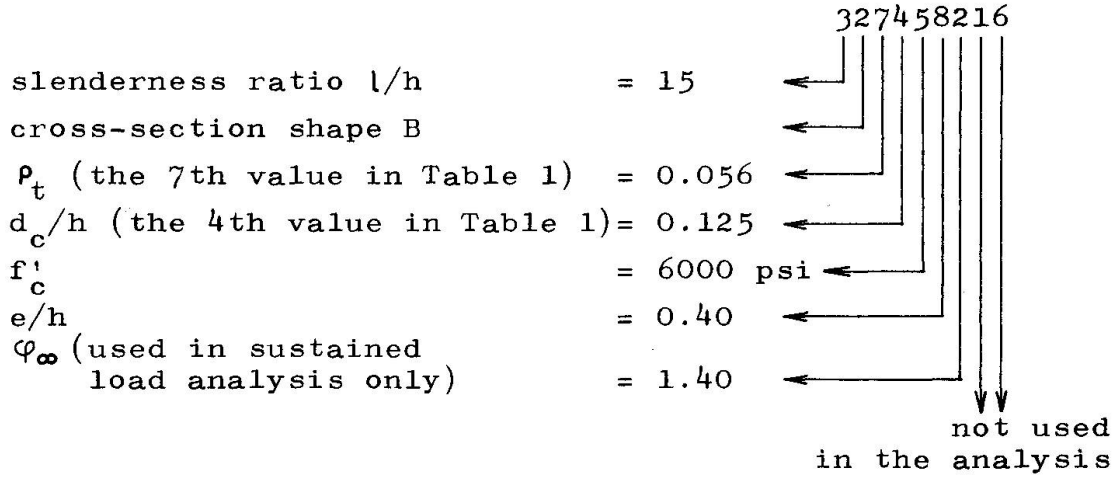

It is a feature of the Graeco-Latin square variable arrangement that each variable appears once with each value of every other variable (5). The Graeco-Latin square may therefore be considered as a representative sample of the fully factorial experiment. A residual sum of squares exists in the present case because the 8 x 8 Graeco-Latin square could contain nine instead of the six or seven variables used. The residual sum of squares in the Analysis of Variance allows an estimation of the total interaction of the variables.

TABLE 1

VARIABLES USED IN COMPUTER EXPERIMENT

Order in Cell	Variable	Level of Variable 1	2	3	4	5	6	7	8
1.	Slenderness Ratio l/h	5	10	15	20	25	30	35	40
2.	Cross-Section Shape	A	B	C	D	E	F	G	H
3.	Reinforcement Ratio ρ_t	0.008	0.016	0.024	0.032	0.040	0.048	0.056	0.064
4.	Reinforcement Cover d_c/h	0.050	0.075	0.100	0.125	0.150	0.175	0.200	0.225
5.	Concrete Strength f'_c (psi)	2000	3000	4000	5000	6000	7000	8000	9000
6.	Load Eccentricity e/h	0.05	0.10	0.15	0.20	0.25	0.30	0.35	0.40
7.	Creep Coefficient φ_∞ (used in section 5)	0.8	1.4	2.0	2.6	3.2	3.8	4.4	5.0

Values of factors held constant: $f_y = 60'000$ psi, $E_s = 29.0 \times 10^6$ psi,

$f'_t = 6\sqrt{f'_c}$ (psi), $E_c = 62726\sqrt{f'_c}$ (psi), $\epsilon_u = 0.0035$

TABLE 2

8 x 8 GRAECO-LATIN SQUARE EXPERIMENTAL DESIGN (REF.(5))

Slenderness Ratio l/h	Cross-Section Shapes (See Table 1) A	B	C	D	E	F	G	H
5	111111111	122546738	133268547	144387265	155734826	166475382	177823654	188652473
10	212222222	221864375	237145863	246753148	258376514	264638751	273517486	285481637
15	313333333	327458216	331786452	345162784	354215678	368524167	372671845	386847521
20	414444444	426312857	435627318	441578623	453851762	462183576	478765231	487236185
25	515555555	528137642	534872136	543426871	551643287	567361428	576284713	582718364
30	616666666	624721583	638413725	642835417	657582341	661257834	675348172	683174258
35	717777777	723685124	732354681	748241356	756128435	765816243	771432568	784563812
40	818888888	825273461	836531274	847614532	852467153	863742615	874156327	881325746

3. ACCURACY OF THE MOMENT MAGNIFIER METHOD

3.1 Results of the ACI Moment Magnifier Method

The load capacity of the columns considered in the computer experiment has been computed from the moment magnifier method of the ACI Building Code 318-71. Following this method the maximum moment in a column with equal end-eccentricities can be calculated with sufficient accuracy for design purposes using Eqn. (1) (Ref. 7):

$$M_u = P_u e \frac{1}{1 - \frac{P_u}{P_{cr}}} \qquad (1) \qquad \text{where:} \quad P_{cr} = \frac{\pi^2 EI}{l^2} \qquad (2)$$

EI has been assumed as suggested by ACI Equations (10-7) and (10-8). The ratios of theoretical to calculated ultimate loads were analyzed using an Analysis of Variance as shown in Table 3. F represents a statistical measure of the level of significance of the variance due to a certain variable. In the case considered the critical F value for the 1 % probability level is $F_{0.01} = 3.66$. An F value greater than $F_{0.01}$ means that the probability is greater than 99 % that the variances are of a systematic character. It may be concluded that the variable in question will not be properly allowed for in the design procedure. This is the case for e/h if ACI Eqn. (10-7) is used and for ρ_t, e/h and l/h if ACI Eqn. (10-8) is used. The trend of the ratio P_u^{Th}/P_u^C is shown in Fig. 2. Each point in Fig. 2 represents the mean of eight columns having the same factor level of the variable considered. A frequency distribution of P_u^{Th}/P_u^C is shown in Fig. 3.

3.2 Evaluation of Improved EI Equations

The columns analyzed in the computer experiment were used to derive more reliable EI Equations. From the results P_u and M_u for each column one stiffness value EI can be found by substituting P_u and M_u into Eqn. (1) and solving Eqns. (1) and (2) for EI:

$$EI = \frac{P_u M_u}{M_u - eP_u} \cdot \frac{l^2}{\pi^2} \qquad (3)$$

In the case of a stability failure the ultimate moment was taken from the point on the interaction diagram corresponding to the computed ultimate load. The population of these EI values from all the columns analyzed represents the basis for an evaluation of simplified EI equations containing the most significant variables.

From a stepwise multiple regression analysis incorporating the three most important variable-combinations the following regression equation resulted:

$$EI = E_c I_g \left(0.205 + 0.000622 \frac{l}{e} + 0.731 \frac{E_s I_s}{E_c I_g}\right) \qquad (4)$$

For Eqn. (4) the multiple correlation coefficient is 0.908. Only minor improvements could be achieved by taking further variables into the regression. The Analysis of Variance (Table 3) shows a much smaller total sum of squares and a more adequate consideration of all the variables as can be seen from the F-values.

Equation (4) was considered impractical in design practice because the term l/e leads to an overestimation of EI for very small eccentricities and because the same term is not clearly defined for unequal end-eccentricities. Finally, an EI equation well suited for design practice was found by a number of simplifications (2):

$$EI = E_c I_g \left(0.25 + \frac{E_s}{E_c} \rho_t\right) \qquad (5)$$

For this equation the mean ratio of theoretical to calculated ultimate load was 1.043, the coefficient of variation was 18.7 %. The lower coefficient of variation indicates a better level of prediction and a better fit into the data than ACI Equations (10-7) and (10-8) but the eccentricity ratio e/h has still a significant effect on the ratio P_u^{Th}/P_u^C. The frequency distribution of P_u^{Th}/P_u^C is shown in Fig. 3.

It is improbable that the moment magnifier method can be improved substantially by further developments of stiffness formulas in a manner similar to the one described above. A major portion of the variances are attributable to the fact that stability failures are practically reduced to material failures. Thus, it is the aim of the following section to develop a procedure which takes proper account of both types of failure.

4. STEP-BY-STEP ANALYSIS PROCEDURE FOR COLUMN DESIGN

4.1 A Simplified Step-by-Step Analysis Procedure

A design procedure which accounts for the influence of the internal forces on the column stiffness was found to produce much better results. The simplified strain-controlled procedure described in this section proved to be efficient and able to cover both types of failure.

TABLE 3

MOMENT MAGNIFIER METHOD

ANALYSIS OF VARIANCE FOR P_u^{Th}/P_u^C ($\frac{\text{THEORETICAL}}{\text{COMPUTED}}$ ULTIMATE LOADS = $\frac{P_u^{Th}}{P_u^C}$)

		ACI Eqn.(10-7)			ACI Eqn.(10-8)			Eqn.(4)		
Source of Variation	Degrees of Freedom	Sums of Squares	Mean Square	F	Sums of Squares	Mean Square	F	Sums of Squares	Mean Square	F
Shapes	7	0.287	0.0410	1.26	0.396	0.0566	1.46	0.0712	0.0102	1.18
l/h	7	0.444	0.0635	1.95	1.153	0.1647	4.26	0.0367	0.0052	0.61
ρ_t	7	0.323	0.0461	1.42	1.913	0.2733	7.06	0.0454	0.0065	0.75
d_c/h	7	0.174	0.0248	0.76	0.303	0.0433	1.12	0.0359	0.0051	0.59
f'_c	7	0.309	0.0442	1.36	0.323	0.0462	1.19	0.0525	0.0075	0.87
e/h	7	1.482	0.2117	6.52	1.888	0.2697	6.97	0.1401	0.0200	2.32
Residuals	21	0.682	0.0325		0.813	0.0387		0.1811	0.0086	
Total	63	3.701			6.789			0.5629		
Total Sample										
Mean		1.099			1.168			1.001		
Coef. of Variation		22.0 %			28.1 %			9.4 %		

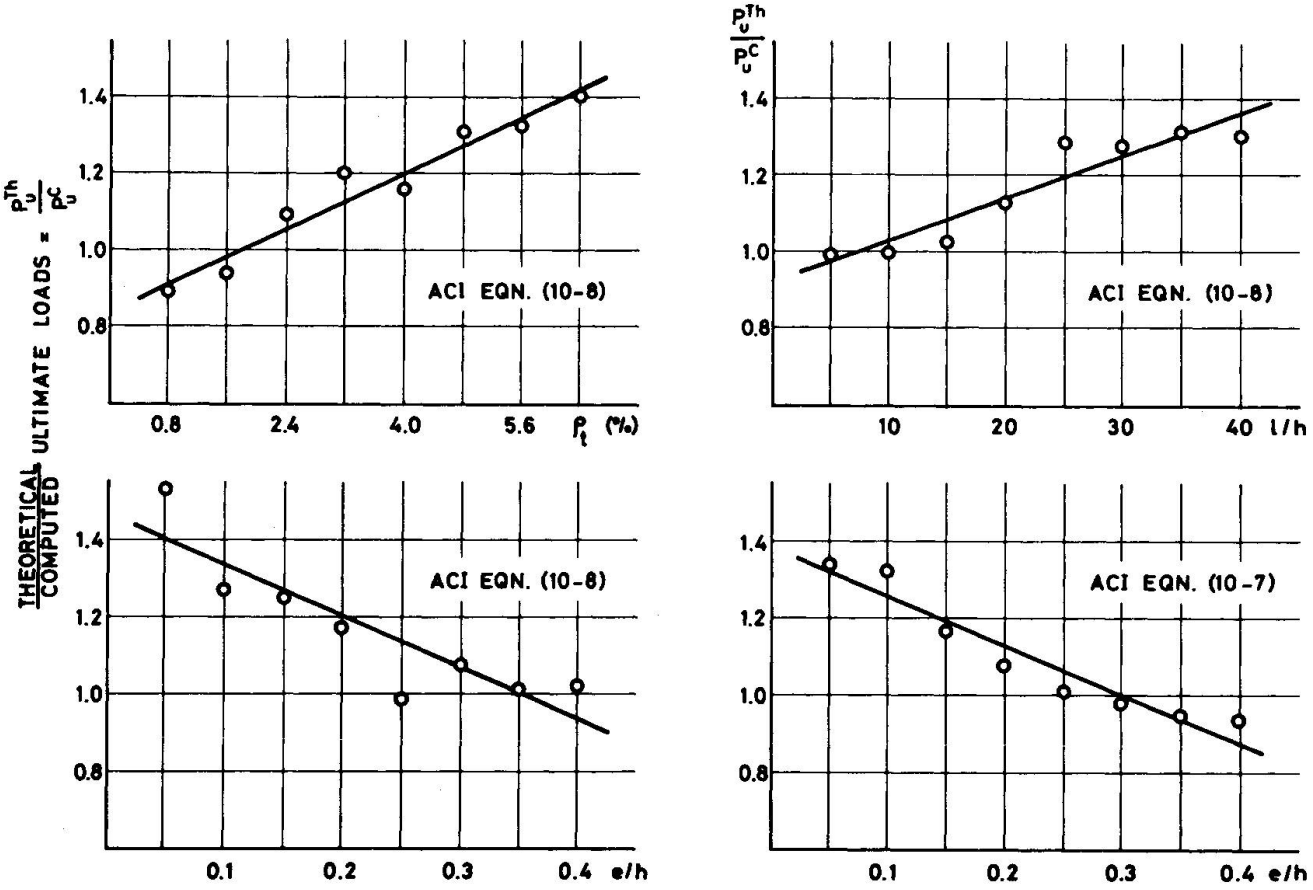

FIG. 2: SIGNIFICANT EFFECTS OF VARIABLES

In the critical cross-section a strain ε_1 at the compressed edge is chosen and by assuming a strain distribution over the depth of the cross-section the axial load P, the internal moment M_i and the external moment $M_e = P(e+w)$ may be computed. The strain at the compressed edge is held constant and the strain distribution is varied until M_i and M_e are made equal. Usually this can be achieved by assuming two or three strain distributions as a design example will show. In the next step the procedure described is repeated for an increased strain ε_1. Very few steps are required to allow an accurate prediction of the ultimate load capacity.

The following example of a slender column subjected to short-term loading may illustrate the method. Table 4 contains the data of a column tested in a short-term loading experiment (4,17). The broken line in Fig. 5 shows the experimental relationship between load and moment at midheight.

To start the computation the values $\varepsilon_1/\varepsilon_o = 0.25$ and $\varepsilon_2/\varepsilon_1 = 0.20$ are assumed. For these values the diagrams in Fig. 4 yield the following coefficients:

$$k_c = 0.280 \quad , \qquad k_y = 0.105$$

$$k_s = 0.334 \quad , \qquad k'_s = 0.865$$

Eqn. (6) gives the force P associated with the assumed strain distribution:

$$P = \int_{A_c} \sigma_c dA_c + \sigma_s' A_s' + \sigma_s A_s \qquad (6)$$

and in the case of the rectangular cross-section considered with $A_s' = A_s$:

$$\begin{aligned} P &= P_c + P_s' + P_s \\ &= k_c \cdot P_o + (k_s' + k_s) \cdot \varepsilon_1 \cdot E_s \cdot A_s \qquad (6a) \\ &= 0.28 \cdot 86.25 + (0.334 + 0.865) \cdot 0.0005 \cdot 2100 \cdot 3.14 = 28.1 \text{ Mp} \end{aligned}$$

The restrictions

$$\varepsilon_s' = k_s' \varepsilon_1 \leq f_y/E_s$$

and $|\varepsilon_s| = |k_s \varepsilon_1| \leq f_y/E_s$ are fullfilled.

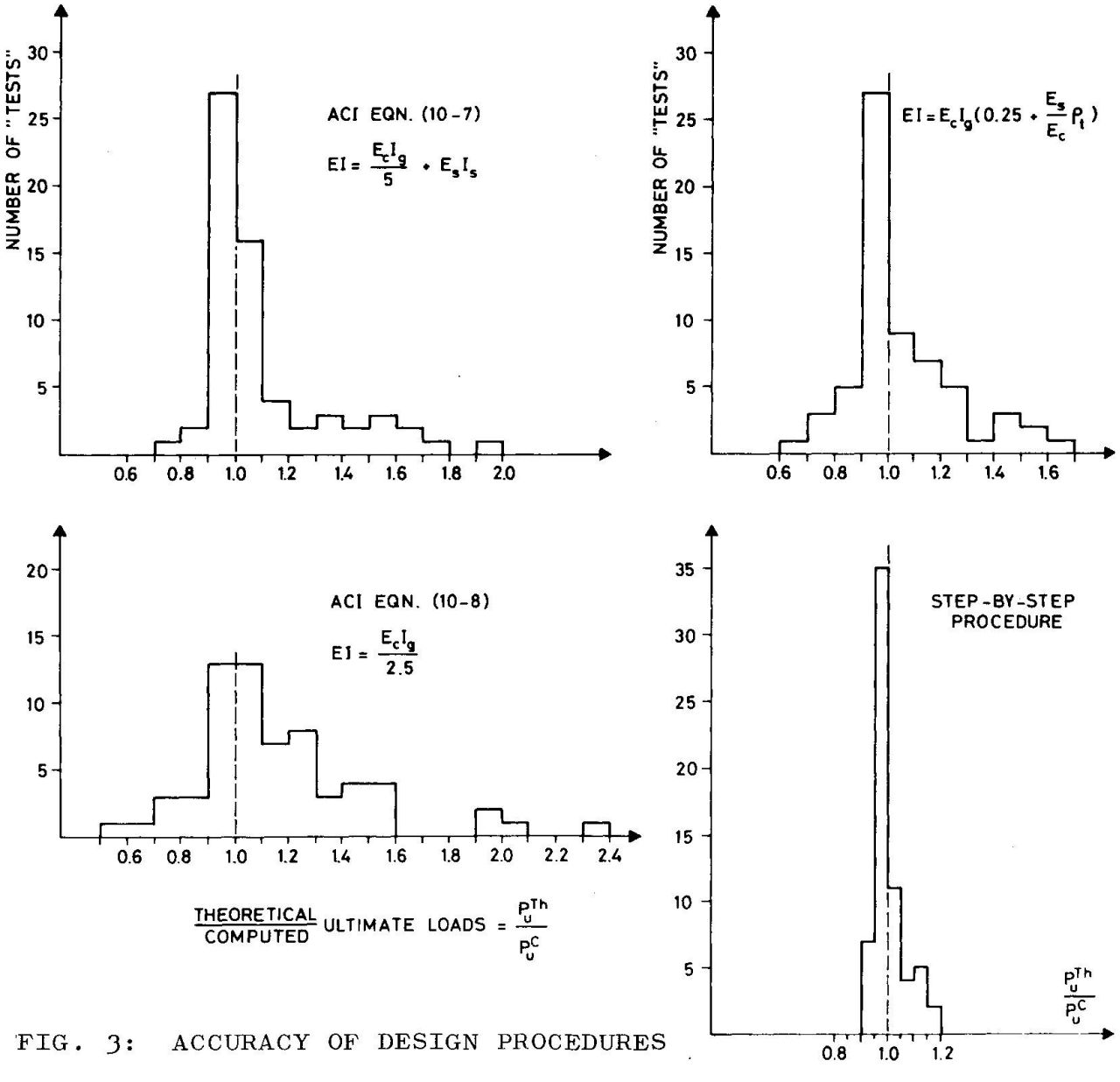

FIG. 3: ACCURACY OF DESIGN PROCEDURES

TABLE 4

COLUMN DATA USED IN DESIGN EXAMPLE

Column Test No.41; Refs.(4),(17); Short-Term Loading

Cross-Section and Dimensions

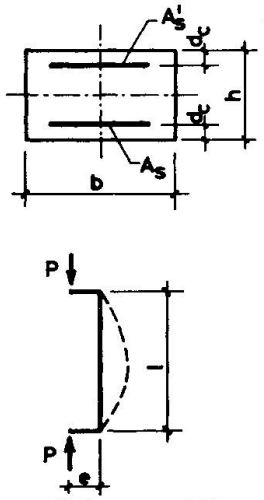

b = 25.0 cm
h = 15.0 cm
d_c = 2.5 cm
A_s = 3.14 cm^2
A'_s = 3.14 cm^2
l = 432.6 cm
e = 0.5 cm

Material Properties and Design Data

Concrete: $f'_c = 0.75\, f'_{cube\ 28} = 230$ kp/cm^2

$E_c = 229'000$ kp/cm^2

$P_o = f'_c\, bh = 86.25$ Mp

$\varepsilon_o = \frac{2 f'_c}{E_c} = 2.0 \cdot 10^{-3}$

$\varepsilon_u = 3.5 \cdot 10^{-3}$

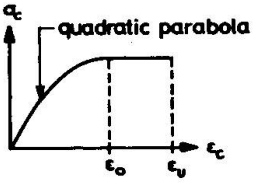

Steel: $f_y = 4'600$ kp/cm^2

$E_s = 2.1 \cdot 10^6$ kp/cm^2

$P_{sy} = P'_{sy} = f_y\, A_s = 14.45$ Mp

Eqn. (7) gives the moment M_i associated with the assumed strain distribution:

$$M_i = \int_{A_c} \sigma_c y_c \, dA_c + (\sigma'_s A'_s - \sigma_s A_s)\, y_s \qquad (7)$$

and for the rectangular cross-section:

$$M_i = P_c \cdot k_y \cdot h + (P'_s - P_s) \cdot y_s \qquad (7a)$$
$$= 24.15 \cdot 0.105 \cdot 15 + (2.85 - 1.10) \cdot 5 = 46.8 \text{ Mpcm}$$

EI and P_{cr} may be computed from M_i:

$$EI = \frac{M_i\, h}{\varepsilon_1 - \varepsilon_2} \quad (8) \quad \text{and} \quad P_{cr} = \frac{\pi^2 EI}{l^2} = \pi^2 \frac{h}{l^2} \frac{M_i}{(\varepsilon_1 - \varepsilon_2)} \qquad (9)$$

In the example: $P_{cr} = 7.91 \cdot 10^{-4} \dfrac{46.8}{(0.5 - 0.1) \cdot 10^{-3}} = 92.5$ Mp

By Eqn. (8) the stiffness EI is computed from moment and curvature at the critical cross-section. Idealized, EI is assumed to be constant over the entire column length. As a further idealization the influence of the tensile zone is neglected.

Eqn. (10) gives the external moment M_e somewhat more accurate than Eqn. (1) as section 4.2 will show

$$M_e = Pe \frac{1 + 0.234 \frac{P}{P_{cr}}}{1 - \frac{P}{P_{cr}}} \qquad (10)$$

Example: $M_e = 28.1 \cdot 0.5 \dfrac{1 + 0.234 \dfrac{28.1}{92.6}}{1 - \dfrac{28.1}{92.6}} = 21.6$ Mpcm

Compared to the internal moment, M_i, the calculation yields a smaller value for the external moment, M_e. A smaller value of M_i and a larger value of M_e is obtained by an increase of the axial load; this can be achieved by an increase of the strain ε_2 if ε_1 is held constant. For $\varepsilon_2/\varepsilon_1 = 0.5$ the resulting moments $M_i = 23.5$ Mpcm and $M_e = 35.2$ Mpcm are listed in the second row of Table 5. Now, M_i is the smaller and M_e the larger value.

In the P,M diagram of Fig. 5 values of M_i and M_e belonging to the axial load values P=28.1 Mp and P=34.3 Mp are entered. The P,M_i curve and the P,M_e curve are approximated by two straight lines within the load range.

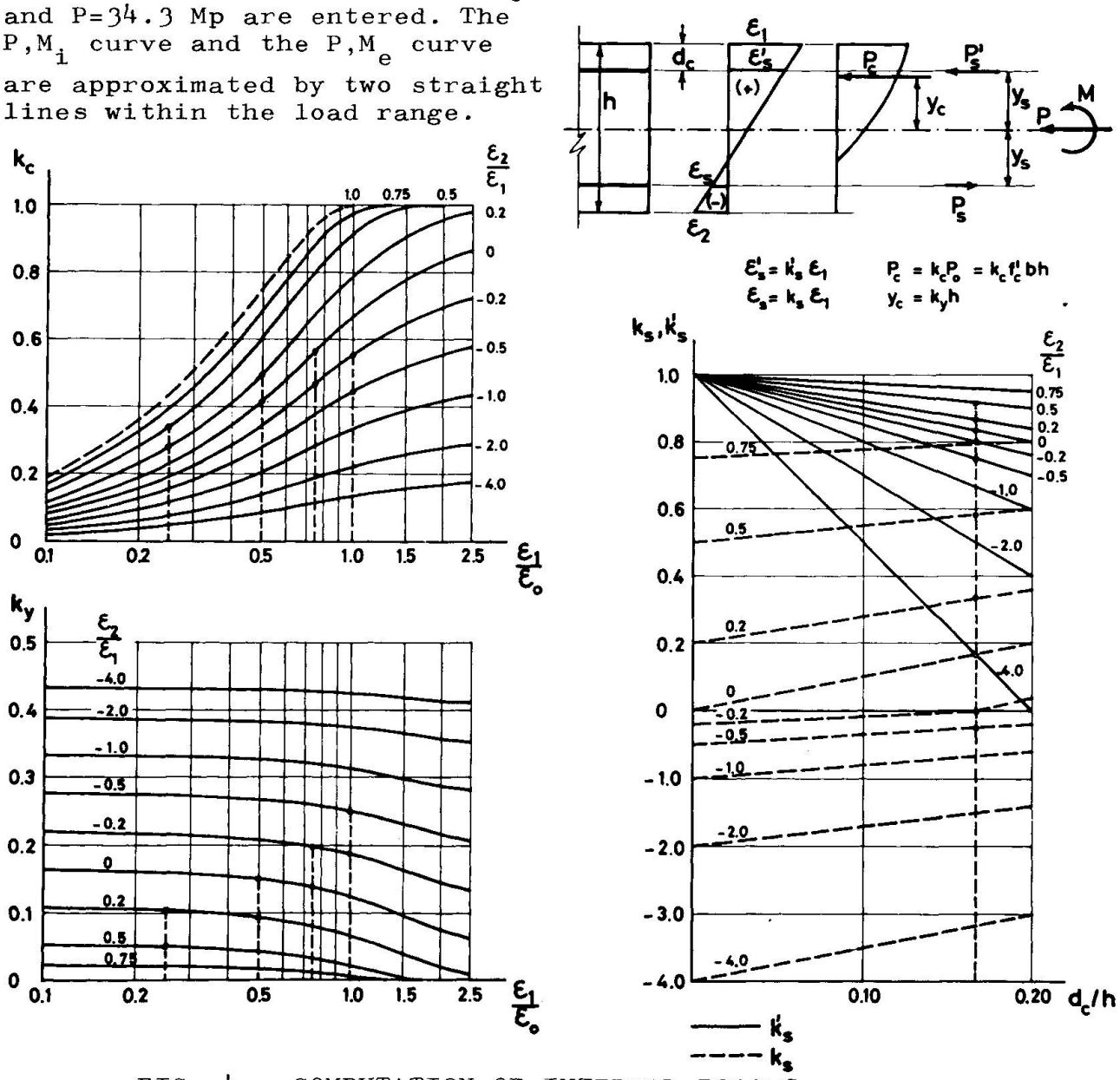

FIG. 4: COMPUTATION OF INTERNAL FORCES; COEFFICIENTS FOR RECTANGULAR CROSS-SECTIONS

The first point of the P,M relationship follows from the intersection of these two straight lines.

In the next step the strain ε_1 is increased to $\varepsilon_1 = 0.5\ \varepsilon_o$ and the computational procedure described above is repeated. As a result a second point of the P,M relationship is found. With two more values of ε_1 the P,M curve can be plotted sufficiently accurate as Fig. 5 indicates.

TABLE 5

COMPUTATION OF P, M_i AND M_e

$\frac{\varepsilon_1}{\varepsilon_o}$	$\frac{\varepsilon_2}{\varepsilon_1}$	P Eqn. (6a)	M_i Eqn. (7a)	P_{cr} Eqn. (9)	M_e Eqn. (10)
0.25	0.2	28.1	46.8	92.5	21.6
0.25	0.5	34.3	23.5	74.5	35.2
0.50	0.0	43.3	104.5	82.6	50.9
0.50	0.2	50.8	77.3	76.5	87.4
0.75	-0.2	48.5	160.0	70.3	90.5
0.75	0.0	58.8	134.2	70.8	207.7
1.00	-0.5	45.1	210.6	55.3	146.2
1.00	-0.2	58.5	187.3	61.5	731.3

The resulting ultimate load capacity is $P_u^C = 53.3$ Mp. The corresponding value measured in the experiment was $P_u^{Test} = 52.5$ Mp. It is interesting to compare this result with the moment magnifier method described previously using different EI equations:

	Ratio of P_u^{Test}/P_u^C
Step-by-Step Procedure:	0.985
EI from ACI Eqn.(10-7):	1.64
EI from ACI Eqn.(10-8):	1.64
EI from Eqn. (4) :	0.83
EI from Eqn. (5) :	1.64

As Figures 3 and 5 show the step-by-step procedure is in any case a much better approach to the column behavior than the moment magnifier method.

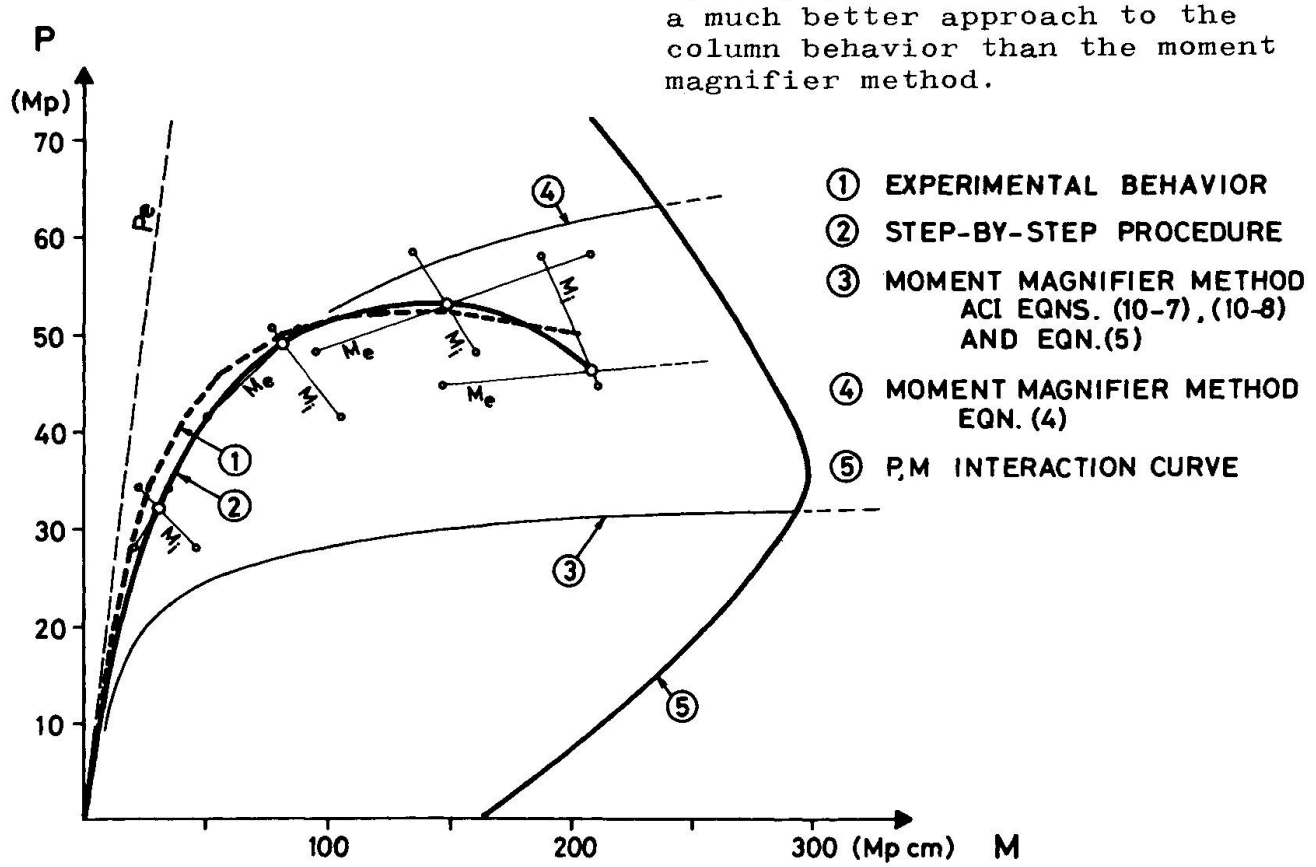

FIG. 5: EXPERIMENTAL BEHAVIOR OF A SLENDER COLUMN AND COMPUTATIONAL APPROACH

The use of a programmable desk calculator makes the method described more efficient; because of an automatic trial and error procedure the results are also more accurate. A program for general cross-section shapes and positions of reinforcement developed on a HP 9810A desk calculator requires about 1000 program steps and less than 50 data storage registers.

4.2 Comparison of the Analysis Procedure with Computer Tests

The analysis procedure described in the preceding section has been used to compute the ultimate load capacity of the 64 columns investigated in the computer experiment. In addition to Eqn. (10) the following equations have been used to compute the moment M_e:

$$M_e = Pe \frac{1}{1 - \frac{P}{P_{cr}}} \qquad (11)$$

and

$$M_e = \frac{Pe_2}{\sin \lambda l} \sqrt{\alpha^2 - 2\alpha \cos \lambda l + 1} \qquad (12)$$

$$\lambda = \sqrt{\frac{P}{EI}} \quad , \quad \alpha = \frac{e_1}{e_2} \quad : \text{ratio of end-eccentricities } -1 \leqslant \alpha \leqslant 1 \text{ (in the case considered: } \alpha = 1)$$

Eqn. (11) represents a simple approximative solution of the maximum moment in an elastic beam-column bent in single curvature with equal end-eccentricities. More accurate for that type of column is Eqn.(10). Finally, Eqn.(12) represents the solution of the differential equation including the case of unequal end-eccentricities.

TABLE 6

STEP-BY-STEP ANALYSIS PROCEDURE

ANALYSIS OF VARIANCE FOR p_u^{Th}/p_u^C ($\frac{\text{THEORETICAL}}{\text{COMPUTED}}$ ULTIMATE LOADS = $\frac{p_u^{Th}}{p_u^C}$)

		Eqn.(10)			Eqn.(11)			Eqn.(12)		
Source of Variation	Degrees of Freedom	Sums of Squares	Mean Square	F	Sums of Squares	Mean Square	F	Sums of Squares	Mean Square	F
Shapes	7	0.0171	0.00244	1.40	0.0091	0.00130	1.14	0.0176	0.00251	1.40
l/h	7	0.0656	0.00937	5.39	0.0215	0.00308	2.69	0.0743	0.01061	5.90
ρ_t	7	0.0432	0.00617	3.55	0.0220	0.00314	2.74	0.0446	0.00638	3.55
d_c/h	7	0.0055	0.00079	0.45	0.0050	0.00072	0.63	0.0056	0.00080	0.45
f'_c	7	0.0093	0.00132	0.76	0.0052	0.00075	0.65	0.0098	0.00140	0.78
e/h	7	0.0272	0.00388	2.23	0.0171	0.00245	2.14	0.0284	0.00405	2.25
Residuals	21	0.0365	0.00174		0.0240	0.00114		0.0378	0.00180	
Total	63	0.2044			0.1039			0.2181		
Total Sample										
Mean		1.005			0.958			1.008		
Coef. of Variation		5.7 %			4.2 %			5.8 %		

Eqn. (11) was found to show the smallest variances (Table 6). All variables may be considered as adequately taken into account because all F-values are smaller than $F_{0.01}$. However, the low mean of 0.958 indicates a distinct tendency to overestimate the ultimate load capacity. The variances are larger for Eqns. (10) and (12) and the influence of the slenderness is on a significant level. As a general trend the load capacity of a slender column tends to be underestimated. Thus, the design is slightly more conservative for slender columns; a fact which may not be undesirable. Preference should be given to Eqns. (10) and (12) because the mean is much more clearly illustrated by these equations than by Eqn. (11) (Table 6).

The evaluation of ε_u is difficult, since ε_u depends on a wide range of factors (Ref. 6). As an alternative approach, Ref. 6 suggests to allow the stress-strain curve to extend indefinitely and to identify failure when the rate of increase of applied load is zero. The results of a computation based on this assumption was only unessentially different. The mean of P_u^{Th}/P_u^C was 0.996, the coefficient of variation was 6.6 %, maximum and minimum values were 1.179 and 0.831. Eqn. (10) was used to compute M_e. About 30 % of the columns investigated were affected by ε_u, all other columns failed before ε_u = 0.0035 was reached.

TABLE 7

COMPARISON OF DESIGN METHODS WITH COLUMN TESTS

Investigator	Reference	No. of Tests	Ratio of P_u^{Test}/P_u^C							
			Moment Magnifier Method						Step-by-Step Method	
			EI from ACI Eqn.(10-7)		EI from ACI Eqn.(10-8)		EI from Eqn.(5)		M_e from Eqn.(10)	
			Mean	Coef. of Var.	Mean	Coef. of Var.	Mean	Coef. of Var.	Mean	Coef. of Var.
				%		%		%		%
Thomas	9	12	1.584	27.5	1.424	31.7	1.163	24.0	0.917	16.5
Ernst, Hromadik, Riveland	12	7	1.092	24.5	1.007	20.9	1.064	23.4	0.989	15.3
Goyal, Jackson	19	26	1.015	8.0	1.035	7.6	1.012	7.0	0.942	3.6
Ferguson, Chang	14	6	1.210	22.2	1.139	23.1	1.192	23.2	0.849	10.0
Drysdale, Huggins (Rectangular)	18	4	1.171	2.5	1.470	22.0	1.283	2.4	1.057	2.8
Drysdale, Huggins (Diamond)	18	10	1.212	4.9	1.155	5.4	1.307	5.0	1.084	4.5
Baumann	8	13	1.212	28.8	1.079	22.7	1.215	26.1	1.040	21.6
Ramboll	11	29	1.208	22.8	1.089	16.2	1.148	19.4	1.202	13.7
Hanson, Rosenstrom	10	3	1.664	5.9	1.202	6.4	1.511	4.5	1.119	6.1
Kordina	20	4	1.199	13.1	1.030	12.6	1.199	13.1	1.019	9.9
Thürlimann	17	6	1.105	27.2	1.036	25.1	1.084	26.5	0.805	9.1
Gaede (Rectangular)	13	8	0.884	13.0	0.787	10.7	0.888	13.2	0.897	6.4
Gaede (Diamond)	15	11	1.093	11.1	0.986	10.0	1.093	11.1	1.071	13.5
Robinson, Modjabi (Channel)	16	4	1.388	14.8	1.671	16.0	1.526	15.0	1.138	18.8
Tal, Chistiakov	21	60	1.253	22.6	1.222	16.6	1.345	18.2	1.075	12.4
Mehmel	22	14	-	-	-	-	-	-	0.952	10.3
Overall		217	1.202	24.1	1.162	22.9	1.202	21.2	1.035	15.6

4.3 Comparison of the Analysis Procedure with Tests

The analysis procedure described in section 4.1 has been used to compute the ultimate load capacity of 217 columns tested in short-term tests in 16 investigations (Refs. 8-22). The comparisons have been limited to hinged columns bent in symmetrical single curvature. All but 25 of the columns were rectangular. The same assumptions made in Ref. 2 concerning concrete strength have been used in the present investigation. The external moment M_e has been computed from Eqn. (10).

The results are presented in Fig. 6 and Table 7. The mean, the coefficient of variation and the frequency distribution of the proposed procedure are distinctly improved compared to the results of the moment magnifier method reported in Ref. 2.

5. EFFECT OF LOAD DURATION

5.1 Sustained Load Behavior of Columns

The knowledge of the effect of sustained loads on the strength of slender columns has been improved in the past two decades by experiments (Refs. 13, 15, 17, 18, 19, 20) and analyses of the problem (Refs. 3, 4, 18, 19, 20, 23, 24).

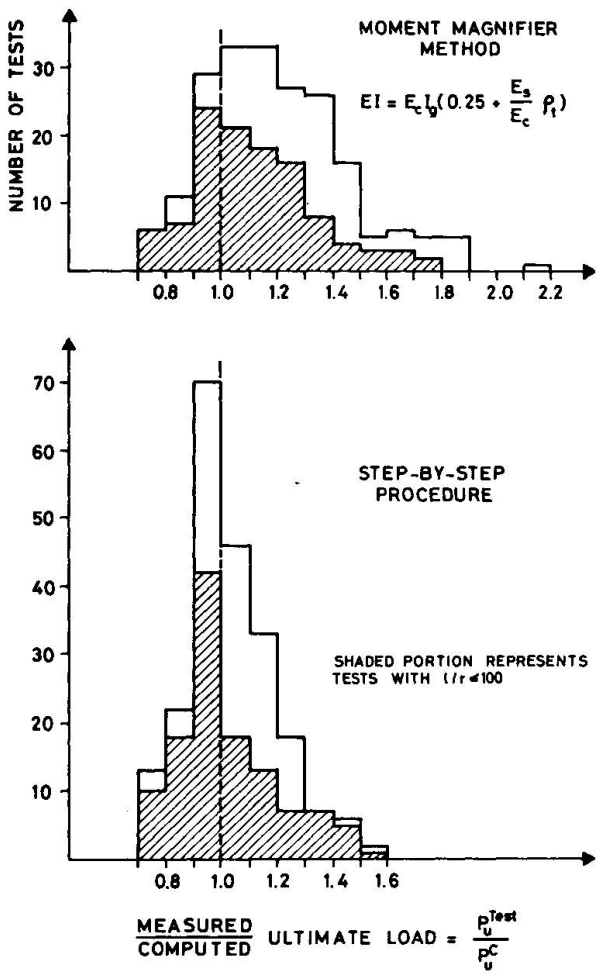

FIG. 6: COMPARISON OF DESIGN PROCEDURES WITH TESTS

In Ref. 3 an incremental rate-of-creep analysis has been developed and used to generate data for a statistical evaluation of the effect of creep on the stiffness, EI. Each of the 64 columns investigated in the computer experiment described in section 2.2 was analyzed to determine the critical sustained load capacity and the remaining short-term load capacities after the column had been subjected to sustained loads. An average of 7 or 8 sustained load levels P_i was chosen for each column and the resulting total population included 482 values of $P_{u\infty,i}$ and $M_{u\infty,i}$.

The behavior of a slender column under short-term and sustained loads is shown qualitatively in Fig. 7. Curve (A) shows the instantaneous short-term behavior expressed in terms of load and moment at midheight. Curve (B) shows the behavior of a column loaded up to failure after being subjected to a sustained load P_i during a period of time, t. Failure is assumed to occur at the intersection with a P,M-interaction curve ($\bar{B}$) computed with a slightly increased

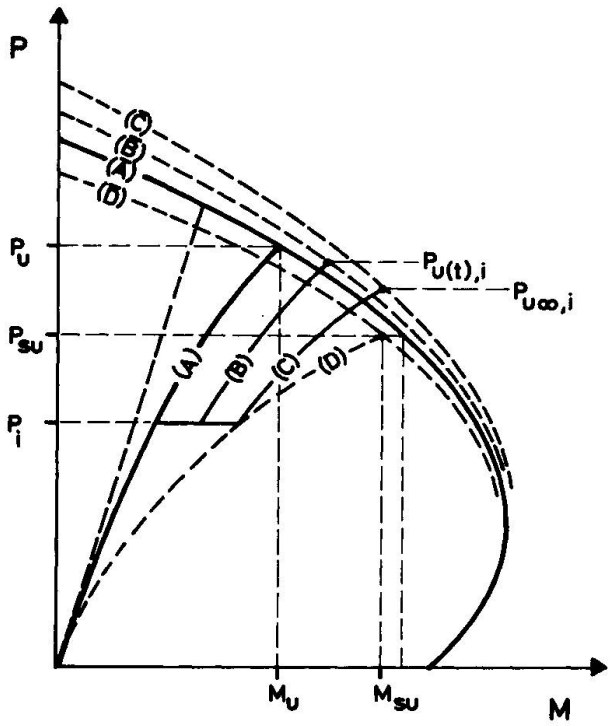

FIG. 7: BEHAVIOR OF A COLUMN UNDER SHORT TERM AND SUSTAINED LOADS

concrete strength due to maturing. The basic P,M-interaction curve ($\bar{A}$) is computed with the initial (28 days age) concrete strength. Curve (C) shows the behavior of a column loaded up to failure after the total amount of creep possible under the sustained load P_i has occured. Curve (D) represents the maximum possible increase in the moment at failure section due to creep. The intersection of this limiting curve and the interaction curve ($\bar{D}$) yields the critical sustained load P_{su} which is the lowest load that can cause a creep failure. Because the strength of concrete tends to decrease under sustained high stresses (26) interaction curve ($\bar{D}$) is situated slightly lower than interaction curve ($\bar{A}$).

For sustained loads less than P_{su} the column load can be increased to failure at time $t = \infty$ as shown by curve (C). For sustained loads greater than P_{su} the column will fail under the sustained load (4, 23).

It is important to note that the design of a column subjected to sustained loads requires two separate safety checks. The column would first be proportioned for the total design (ultimate) load. In a second step the designer ought to check whether the column would fail during the sustained load period when subjected to sustained loads only.

5.2 Analysis of Sustained Load Capacity of Columns

A more complete description of the method of analysis is given in Ref. 3. The assumptions made for the material behavior and for the step-by-step Rate-of-Creep analysis are summarized briefly in the following.

The creep function $\varphi(t)$ is defined as the ratio between creep strain and initial strain:

$$\varphi(t) = \frac{\varepsilon_{CR}(t)}{\varepsilon} \tag{13}$$

ε is given by the equation of the short-term stress-strain curve:

$$\varepsilon = \frac{2f'_c}{E_c}\left(1 - \sqrt{1 - \frac{f_c}{f'_c}}\right) \tag{14}$$

The function $\varphi(t)$ has been derived from tests on plain concrete specimens subjected to different load levels (Refs. 3, 4); it was found that the stress dependency of the creep function at

any time t can be expressed by

$$\varphi(t) = C_1(t) + C_2(t) \frac{f_c}{f'_c} \tag{15}$$

where

$$C_{1,2}(t) = \bar{C}_{1,2} \left[1 - \exp(-\kappa_{1,2} t^{\delta_{1,2}})\right] \tag{16}$$

$$\bar{C}_1 = \frac{[\varphi(\infty,0.40) - 0.8]}{3} \tag{17}$$

$$\bar{C}_2 = 2.5 [\varphi(\infty,0.40) - \bar{C}_1] \tag{18}$$

In these expressions $\varphi(\infty,0.40)$ refers to time $t=\infty$ and $f_c/f'_c=0.40$ and is taken equal to the value of φ given by the CEB Recommendations (25).

Preliminary studies on columns with an equal amount of reinforcement on both faces have shown that the effect of shrinkage was insignificant and consequently it has not been considered in this study.

The increase in the strength of the concrete due to maturing was included and conservatively assumed to be 1.10 times the 28 day strength at time infinity. The decrease in concrete strength in the presence of high sustained stresses was assumed to be 20 percent of the short time strength (26).

In 2.1 the computation of the moment-curvature relationship $M_{i,j}$, $\Phi_{i,j}$ has been described. To include the effect of creep, this relationship had to be expanded to $M_{i,j}$, $\Phi_{i,j,k}$. The index k stands for time, where k=1 indicates values for the short-term loading situation so far referred to as $\Phi_{i,j}$. The values $\Phi_{i,j,k}$ for k=2,3...NT are computed by a Rate-of-Creep Method considering the viscoelastic behavior of any single fibre in the cross-section and using time as a discrete variable (3). The time dependent deflections of a column subjected to a sustained load were computed by the Rate-of-Creep Method making use of the $M_{i,j}$, $\Phi_{i,j,k}$ relationship.

5.3 Design Methods Accounting for the Effect of Creep

As discussed in Ref. 28 for design purposes there are essentially three major methods of accounting for sustained load effects. These are the Reduced E-Modulus Method used in the ACI Code (1), the Dischinger Method (27) and the Sustained Load Eccentricity Method (29). For these methods creep parameters have been derived statistically from computer experiments similar to the evaluation of EI equations discussed in section 3.2 (Ref. 3).

The 1971 ACI Code includes the effect of creep by reducing the flexural stiffness to $EI_R = EI/(1 + \beta_d)$. The load transfer to the reinforcement due to creep may cause premature yielding of the compression reinforcement and for this reason both the concrete and the steel terms in the ACI equations were reduced. With the trend to higher steel percentages this procedure was found to be excessively conservative (3). Accordingly Eqns. (19) and (20) have been used in Ref. 3 to define the reduced modulus:

$$EI_R = E_c I_g \left(\frac{0.25}{\beta} + \frac{E_s}{E_c}\rho_t\right) \quad (19)$$

or

$$EI_R = \frac{E_c I_g}{5\beta} + E_s I_s \quad (20)$$

Eqn. (19) or Eqn. (20) may be substituted into Eqn. (21) to obtain the magnified moment

$$M(t) = \frac{Pe}{1 - \frac{Pl^2}{\pi^2 EI_R}} \quad (21)$$

Eqn. (21) can be solved for EI_R and β using the values of $P_{u\infty,i}$ and $M_{u\infty,i}$. By computing β for all the columns analyzed in the computer experiment, a population of 482 β values is created which can be used to derive design equations for β by stepwise multiple regression analysis. The resulting linear regression equation was

$$\beta = 1.016 - 11.45\ \rho_t + 0.107\varphi_\infty - 0.0126\ \frac{l}{h} + 0.318\beta_P^2 \geq 1.0 \quad (22)$$

The variables included in Eqn. (22) are the most significant of 13 variables and variable combinations considered. For design practice Eqn. (22) then has been simplified to Eqn. (23)

$$\beta = 0.9 + 0.5\ \beta_P^2 - 12\ \rho_t \geq 1.0 \quad (23)$$

where β_P is the ratio of design dead load to design total load

ρ_t is the total reinforcement ratio $= (A_s + A'_s)/A_c$

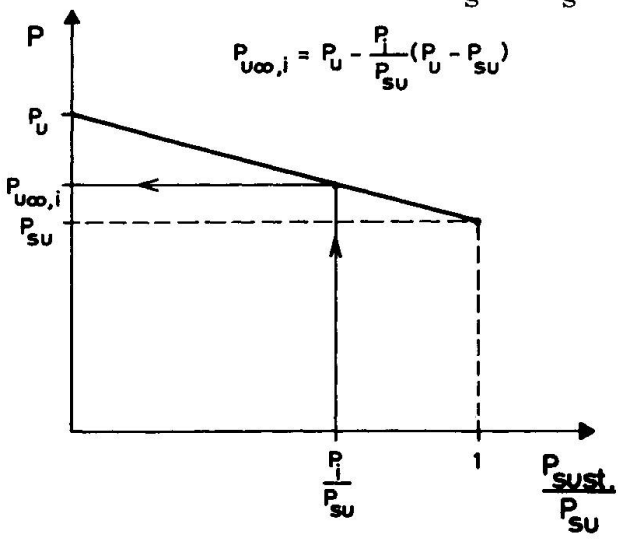

FIG. 8: REDUCED ULTIMATE LOAD CAPACITY DUE TO SUSTAINED LOAD (APPROXIMATION)

As pointed out in 5.1, columns subjected to high sustained loads may fail under the sustained load. In order to find the critical ultimate sustained load, P_{su}, the creep parameter β_s had to be derived from the value P_{su} found in the computer tests. β_s was derived in the same manner as β except that $P_{u\infty,i}$ and $M_{u\infty,i}$ had to be replaced by P_{su} and M_{su}. For M_{su}, the moment on interaction curve ($\bar{A}$) (Fig. 7) at the level of P_{su} was chosen because ($\bar{A}$) is the only interaction curve available to the designer and therefore the use of M_{su} from curve ($\bar{D}$)

would have led to creep parameters which would overestimate P_{su}. Eqn. (24) represents a simplified regression equation for design use:

$$\beta_s = 0.06\ l/h \geq 1.0 \qquad (24)$$

In the procedure considered, the column would first be proportioned for the design (ultimate) load using Eqns. (19, 21 and 23). The check whether the column would fail during the sustained load period would then be carried out using Eqns. (19, 21 and 24) with $\beta = \beta_s$ in Eqn. (19).

The Reduced E-Modulus Method is well suited to be used in the simplified step-by-step analysis procedure discussed in 4.1. The critical sustained load capacity, P_{su}, may be computed exactly in the same manner as the ultimate load capacity P_u replacing E_c by the reduced modulus $E_c(t=\infty)$ computed from Eqn. (25)

$$E_c(t) = \frac{E_c}{1 + \varphi(t)} \qquad (25)$$

The creep coefficient $\varphi_\infty = \varphi(t=\infty)$ follows from Eqn. (15) inserting $t=\infty$ and assuming an average ratio $f_c/f'_c = 0.40$. For the computation of the internal forces the diagrams in Fig. 4 can be used again but prior to the evaluation of k_c and k_y the assumed strain distribution has to be divided by $(1 + \varphi_\infty)$. The ultimate concrete strain under sustained loads, ε_{su}, has been limited to $(1 + \varphi_\infty)$ times the instantaneous strain given by Eqn. (14) on the stress level $f_c/f'_c = 0.88$. The strength of concrete has been assumed in the computation as 80 % of the short time strength of concrete of the same age. Since the short time strength at time infinity has been assumed equal to $1.10\ f'_{c28}$, the critical sustained stress will be $0.8 \cdot 1.10\ f'_{c28} = 0.88\ f'_{c28}$. The assumed ultimate strain

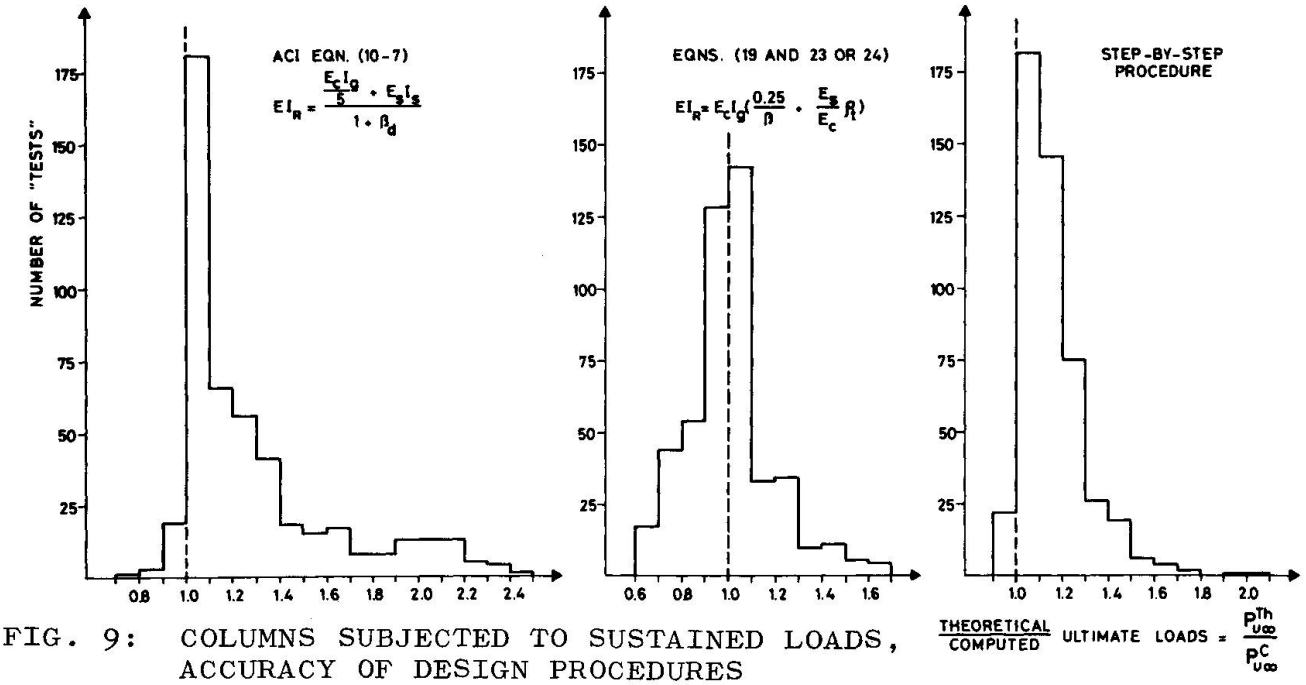

FIG. 9: COLUMNS SUBJECTED TO SUSTAINED LOADS, ACCURACY OF DESIGN PROCEDURES

TABLE 8

COMPARISON OF DESIGN PROCEDURES WITH COMPUTER EXPERIMENTS
(Columns Subjected to Sustained Loads)

Design Method (Total Sample-482 Columns)	Ratio of $P^{Th}_{u\infty}/P^{C}_{u\infty}$ Mean	Coef. of Var. %
Reduced E-Modulus Concept used in Moment Magnifier Method Ref.(3)		
ACI Eqn.(10-7)	1.290	26.4
ACI Eqn.(10-8)	1.373	33.6
Eqn.(19 and 23 or 24)	1.013	17.9
Eqn.(20 and 23 or 24)	1.045	20.3
Dischinger Method(Ref.(3))	1.063	16.5
Magnified Eccentricity Method Ref.(3)	1.109	16.8
Creep Eccentricity Method Ref.(3)		
CEB Version	1.568	30.0
Version proposed in Ref.(3)	1.115	17.6
Reduced E-Modulus Concept used in Step-by-Step Analysis Procedure	1.156	12.1

was reached by four columns only. Moreover, this limitation of the strain appears to be of minor importance because P_{su} increased by not more than 0.35 % for an unlimited stress-strain curve.

P_u represents an upper bound on the ultimate load capacity and P_{su} represents a lower bound (Fig. 7). An increase of the sustained load portion results in a gradual decrease of the ultimate load capacity from P_u to P_{su}. As a simplification for design it has been assumed that the ultimate load decreases proportionally to the increase of the sustained load portion as shown in Fig. 8. This assumption is slightly overconservative.

In the Step-by-Step Design Method it is advisable to compute P_{su} first if the sustained load portion is considerable. If the check shows that there is no danger of a creep failure, P_u is computed and the ultimate load capacity for the total design load is found by linear interpolation between P_u and P_{su} as shown in Fig. 8.

Table 8 shows the accuracy of different design procedures in the case of the computer experiment including 482 columns. The design methods proposed in Ref. 3 are clearly more accurate than the 1971 ACI Method. However, neither the Dischinger Method nor the Creep Eccentricity Method was found to be superior to the Reduced E-Modulus Method. Compared to all the methods considered the Step-by-Step Method described in this paper is clearly the most accurate procedure as shown by Table 8 and Fig. 9. In addition, less values are on the unsafe side ($P^{Th}_{u\infty}/P^{C}_{u\infty} < 1.0$) as shown by Fig. 9.

As for short-term tests a comparison between design procedures and tests on reinforced concrete columns investigated by several authors (Refs. 15, 17, 18, 19, 20) has been carried out. The usual

TABLE 9

COMPARISON OF DESIGN METHODS WITH SUSTAINED LOAD COLUMN TESTS

Design Method (Total Number of Tests - 53 Columns)	Ratio of $P^{Test}_{u(t)}/P^{C}_{u(t)}$ Mean	Coef. of Var. %
Reduced E-Modulus Concept used in Moment Magnifier Method		
ACI Eqn.(10-7)	1.278	20.5
Eqn.(19 and 23 or 24)	0.997	18.7
Reduced E-Modulus Concept used in Step-by-Step Analysis Procedure	1.069	12.8

Investigators and Number of Tests*

Thürlimann, Ref.(17), N = 12
Kordina, Ref.(20), N = 12
Goyal, Jackson, Ref.(19), N = 20
Gaede (Diamond), Ref.(15), N = 1
Drysdale, Huggins (Diamond), Ref.(18) N = 8

*) The investigation includes columns which failed in a final short-term test after a period of sustained loading. Columns which failed under sustained load (Refs.(15,17,18)) have been excluded.

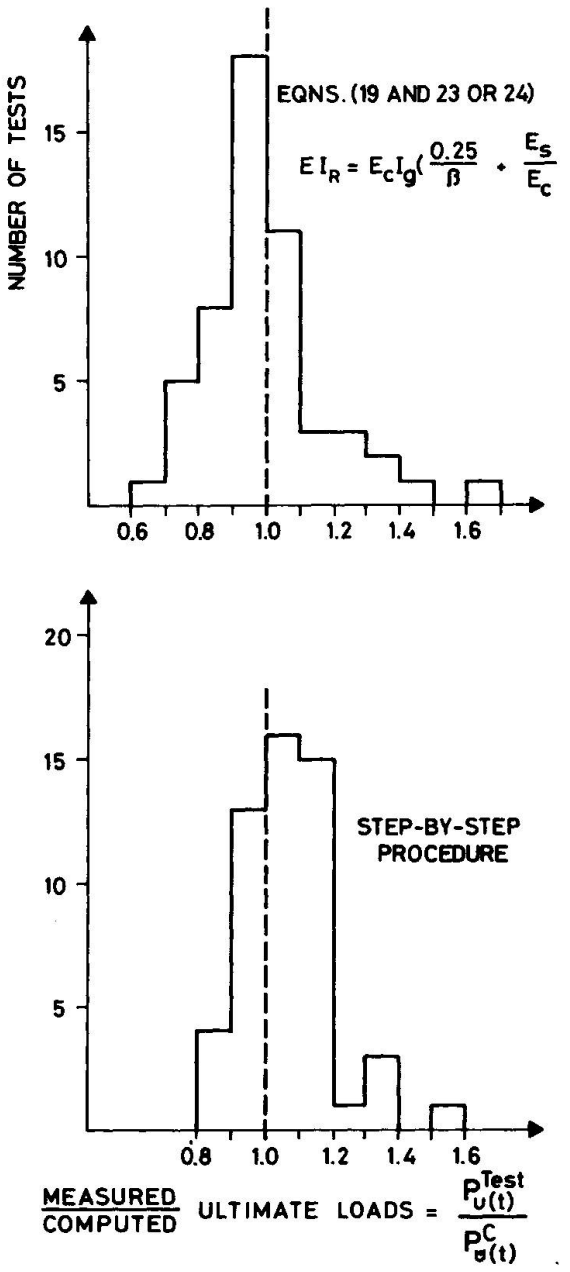

FIG. 10: COMPARISON OF DESIGN PROCEDURES WITH SUSTAINED LOAD COLUMN TESTS

test procedure is to subject a column to a constant sustained load; if no creep failure occurs within a certain time period the column is loaded up to failure in a final short-term test. To compute the ultimate load of these columns the time dependent development of the creep parameter was taken as $\gamma(t)$ times the values at $t=\infty$, where:

$$\gamma(t) = 1 - \exp(-0.1325\sqrt{t}) \qquad (26)$$

Columns which failed under sustained load have not been considered in this investigation. The ratio between measured and computed ultimate loads is shown by histograms in Fig. 10 for 53 sustained load column tests. The characteristic values of the distributions including the 1971 ACI Method, the improved Moment Magnifier Method from Ref. 3 and the Step-by-Step Method are shown in Table 9. Considering the coefficient of variation the ACI Method is poorer than the method based on Eqns. (19 and 23 or 24) but both methods gave much poorer prediction than the Step-by-Step Method (Table 9).

6. CONCLUDING REMARKS

Economically the columns account in most cases for a rather small part of the total structural costs but structurally they constitute a vital part of the structure (Ref. 30). As a consequence relatively simple and conservative design procedures are preferable as they will usually not lead to an appreciable increase of the total structural costs (30). Sophisticated computer oriented incremental analysis procedures such as described in sections 2.1 and 5.2 are therefore not suited to be used in common design practice.

The comparisons of approximate column design methods with computer analyses and column tests presented in this paper confirm that the simplest methods also prove to be the least accurate (6) and in a few cases the prediction of the ultimate load capacity is found to be considerably unsafe.

The general trend to make use of programmable desk calculators in design practice allows the development of simple step-by-step

analysis procedures for design purposes. Compared to moment magnifier method or complementary eccentricity method (31) the step-by-step analysis method provides more accurate predictions of the behavior and load carrying capacity of concrete columns. The application of the method to columns which are components of frames or structural subassemblages needs further research.

REFERENCES

1. ACI Committee 318, "Building Code Requirements for Reinforced Concrete (ACI 318-71)", American Concrete Institute, Detroit, 1971.
2. MacGregor, J.G., Oelhafen, U.H. and Hage, S., "A Re-examination of the EI Value for Slender Columns", Reinforced Concrete Columns, Special Publication, American Concrete Institute (in Press - 1974)
3. Oelhafen, U.H. and MacGregor, J.G., "The Design of Slender Columns Subjected to Sustained Loads", Reinforced Concrete Columns, Special Publication, American Concrete Institute (in Press - 1974)
4. Oelhafen, U.H., "Formänderungen von Stahlbetonstützen unter exzentrischer Druckkraft", Institut für Baustatik, ETH, Bericht No. 31, Zürich, 1970.
5. Fisher, R.A., "The Design of Experiments", Hafner Publishing Company, New York, 1960.
6. Warner, R.F., "Physical-Mathematical Models and Theoretical Considerations", Theme Paper I, Preliminary Report, IABSE-CSCE Symposium on Design and Safety of Reinforced Concrete Compression Members, Zürich, 1973.
7. MacGregor, J.G., Breen, J.E., Pfrang, E.O., "Design of Slender Concrete Columns", ACI Journal, Proceedings Vol. 67, No. 1, January 1970.
8. Baumann, O., "Die Knickung der Eisenbeton-Säulen", Eidg. Materialprüfungsanstalt an der ETH, Zürich, Bericht No. 89, Zürich, 1934.
9. Thomas, F.G., "Studies in Reinforced Concrete VII. Strength of Long Reinforced Concrete Columns in Short Period Tests to Destructions", Department of Scientific and Industrial Research, Building Research Technical Paper No. 24, London, 1939.
10. Hanson, R. and Rosenstrøm, S., "Trykkforsøk med slanka betongpelare", Betong, Vol. 32, No. 3, Stockholm, 1947.
11. Rambøll, B.J., "Reinforced Concrete Columns", Teknisk førlag, Copenhagen, 1951.
12. Ernst, G.C., Hromadik, J.J., Riveland, A.R., "Inelastic Buckling of Plain and Reinforced Concrete Columns, Plates and Shells", University of Nebraska Engineering Experiment Station Bulletin No. 3, Lincoln, Nebraska, 1953.
13. Gaede, K., "Knicken von Stahlbetonstäben unter Kurz- und Langzeitbelastung", Deutscher Ausschuss für Stahlbeton, Heft No. 129, Berlin, 1958.
14. Chang, W.F. and Ferguson, P.M., "Long Hinged Reinforced Concrete Columns", ACI Journal, Proceedings Vol. 60, No.1, January 1963.
15. Gaede, K., "Knicken von Stahlbetonstäben mit quadratischem Querschnitt in Richtung einer Diagonalen unter Kurz- und Langzeitbelastung", Institut für Materialprüfung u. Forschung des Bauwesens, Universität Hannover, 1968.

16. Robinson, J.R. and Modjabi, S.S., "La Prévision des Charges de Flambement des Poteaux en Béton Armé par la Méthode de M.P. Faessel", Annales de l'Institut Téchnique du Bâtiment et des Travaux Publics, No. 249, Paris, September 1968.
17. Ramu, P., Grenacher, M., Baumann, M., Thürlimann, B., "Versuche an gelenkig gelagerten Stahlbetonstützen unter Dauerlast", Institut für Baustatik, ETH, Bericht No. 6418-1, Zürich 1969.
18. Drysdale, R.G., Huggins, M.W., "Sustained Biaxial Load on Slender Concrete Columns", Journal of the Structural Division, ASCE, Vol. 97, ST5, May 1971.
19. Goyal, B.B., Jackson, N., "Slender Conrete Columns Under Sustained Load", Journal of the Structural Division, ASCE, Vol. 97, ST11, November 1971.
20. Kordina, K., "Langzeitversuche an Stahlbetonstützen", Deutscher Ausschuss für Stahlbeton, (in press)
21. Kukulski, W. and Lewicki, B., "Contribution to the Discussion about the Simplified Calculations Methods for Eccentrically Loaded Columns", Memorandum to CEB Commission 8, Flambement, Warsaw, September 1969. (This memorandum summarizes the results of tests by Tal and Chistiakov).
22. Mehmel, A., Schwarz, H., Kasparek, K.H., Makovi, J., "Tragverhalten ausmittig beanspruchter Stahlbetondruckglieder", Deutscher Ausschuss für Stahlbeton, Heft No. 204, Berlin, 1969.
23. Mauch, S.P. and Holley, M.J., "Creep Buckling of Reinforced Concrete Columns", Journal of the Structural Division, Vol. 89, ST4, August 1963.
24. Manuel, R.F. and MacGregor, J.G., "Analysis of Restrained Reinforced Concrete Columns Under Sustained Load", ACI Journal, Proceedings Vol. 64, No. 1, January 1967.
25. Comité Européen du Béton, "CEB-FIP International Recommendations for the Design and Construction of Concrete Structures", FIP Sixth Congress, Prague, June 1970.
26. Rüsch, H., "Researches Toward a General Flexural Theory for Structural Concrete", ACI Journal, Proceedings Vol. 57, No. 1, July 1960.
27. Dischinger, F., "Untersuchungen über die Knicksicherheit, die elastische Verformung und das Kriechen des Betons bei Bogenbrücken", Bauingenieur, Vol. 18 and 20, Berlin 1937 and 1939.
28. MacGregor, J.G., "Simple Design Procedures for Concrete Columns", Theme Paper II, Preliminary Report, IABSE-CSCE Symposium on Design and Safety of Reinforced Concrete Compression Members, Zürich, 1973.
29. Commission 8, "Manuel de Calcul CEB-FIP, Buckling-Instability", Bulletin d'Information No. 79, Comité Européen du Béton, Paris, Jan. 1972.
30. Thürlimann, B., Summary Report, Technical Committee No. 21, Elastic Analysis-Strength of Members and Connections, Volume III, IABSE-ASCE Joint Committee on Planning and Design of Tall Buildings, ASCE, New York, 1972.
31. Cranston, W.B., "Analysis and Design of Reinforced Concrete Columns", Research Report 20, Cement and Concrete Association, 41.020, London, 1972.

SUMMARY

The accuracy of simple design procedures for concrete columns under short-term and sustained loads is investigated. Statistical comparisons of design method with computer analyses and column tests show limited improvement capacity of the common Moment Magnifier Method (ACI Code 318-71). However, a design procedure based on a step-by-step analysis of the load-moment relationship of the column takes proper account of material failure and stability failure; therefore it is considerably more accurate.

RESUME

On étudie la précision des méthodes simples de dimensionnement des colonnes en béton soumises à des sollicitations instantanées ou de longue durée. On effectue des comparaisons statistiques avec des calculs d'ordinateur et des résultats d'essais: il s'avère qu'on ne peut guère améliorer la méthode des "Moment Magnifier" (ACI 318-71). Un procédé qui permet un calcul pas-à-pas de la courbe charge-moment de la colonne s'avère par contre plus précis, car il tient exactement compte des processus de rupture, qu'il soient dûs ou non au flambement.

ZUSAMMENFASSUNG

Die Zuverlässigkeit einfacher Berechnungsverfahren für Betonstützen unter Kurz- und Langzeitbeanspruchung wird untersucht. Statistische Vergleiche mit Computerberechnungen und Stützenversuchen zeigen eine beschränkte Verbesserungsfähigkeit der bekannten "Moment Magnifier"-Methode (ACI Code 318-71). Ein Verfahren, bei dem die Last-Moment-Kurve der Stütze schrittweise berechnet wird, erweist sich dagegen als bedeutend zuverlässiger, da dieses Verfahren sowohl den Festigkeits- als auch den Stabilitätsbruch qualitativ richtig erfasst.

Leere Seite
Blank page
Page vide

II

Effects of Slenderness and Sustained Load on the Capacity of Reinforced Concrete Columns: An Analysis of the Design Parameters

Effets de l'élancement et de charges soutenues sur la capacité des colonnes en béton armé: Une Analyse des Paramètres de Dimensionnement

Der Einfluss von Schlankheit und Dauerlast auf die Tragfähigkeit von Stahlbetonstützen: Eine Untersuchung über die Bemessungsparameter

R.G. DRYSDALE
Associate Professor
McMaster University
Hamilton, Ontario, Canada

S. SALLAM
Ph.D. Student
McMaster University
Hamilton, Ontario, Canada

K.B. TAN
Assistant Structural Engineer
Housing and Development Board
Republic of Singapore

1. INTRODUCTION

The design of column cross sections for known axial loads and moments has reached the stage where practical methods give results which agree very closely with tests and with accurate analyses. However considerable uncertainty exists with regard to methods employed to take into account the effects of column length. It is generally agreed[2,6] that the rational way to compute the reduced capacity is to include directly the effects of the additional moments caused by deflection of columns (PΔ effects). Theoretical calculations[3] can be used to accurately predict the loads at which material failure or column instability will occur. However designers require simpler techniques which are sufficiently general in nature to be equally applicable to the large variety of design cases.

The effect of column slenderness which is further complicated by consideration of creep under sustained load is the main topic of this paper. It is suggested that a realistic appraisal of design methods must be based on the idea of consistent safety factors. Thus slender columns subjected to sustained load must retain sufficient reserve capacity so that failure loads when compared to design loads provide equal safety factors. The National Building Code of Canada is being revised to include the relevant provisions of ACI 318-71[1]. Therefore the columns analysed in this paper were designed in accordance with ACI 318-71.

2. DESIGN PARAMETERS

The magnitude and effect of the additional moments due to deflection must be determined for the full range and combinations of design parameters. Such a comprehensive evaluation was not attempted here. The values of the design parameters chosen were selected to be representative of normal design practice. Those

parameters which are included in this study are briefly discussed below.

2.1 Column Properties

For simplicity of interpretation square cross sections with symmetric reinforcing in exterior layers were analysed. The reinforcement was positioned so that the distance, g, between the exterior layers was 0.8h. Most of the results presented are for P_t =3.0% although some results for 1.5% of steel are provided for comparison. The concrete strength used is f'_c=27.5 MN/m^2 and the steel yield stress is σ_y=412 MN/m^2.

Individual columns with slenderness ratios, $^l/_r$, from 0 to 100 were analysed for various combinations of end eccentricities. Also an example of the behaviour of columns in frames is presented.

2.2 Loading Conditions

The columns to be analysed were designed according to ACI 318 -71[1,7] where, in addition to knowing the section properties, the values of the end moments, the effective length and the level of sustained load were required. For the analyses of individual columns (kl=1.0) the majority of the results are for the case of symmetric single curvature where the effect of PΔ should be largest. The eccentricities used in the investigation are 0.1h, 0.4h and balanced eccentricity, e_{bal}.

The short term capacity of each column was determined. This only has meaning if live load, L, is 100% of the total loading. Two cases which are more realistic (D=L and D=100% of the total load) were analysed to find the effect of sustaining the dead load, D. The remaining capacities after sustained loading were also determined. Finally analyses were performed for the case of D=100% of the total load and with the ultimate dead load of 1.4D being sustained.

3. DESCRIPTION OF THE METHOD OF ANALYSIS

A computer program has been developed to predict the behaviour and capacity of reinforced concrete frame structures[8]. Details of the major features of the method of analysis have been reported elsewhere[3,4]. The accuracy of this method has been verified by the comparison[3,4,9] of the analytical results with tests of columns and frames subjected to short term and sustained loading. Therefore only a brief description with emphasis on those aspects which are particularly important to this study will be provided.

3.1 General Description

The response of cross sections to axial load and moment is found by dividing the section into strips. For any plane distribution of strain the stress on each strip is calculated taking into account the amount of creep and shrinkage which has occurred at the centre of each strip. The sum of the forces and the moments of the forces from each cross section strip and from the reinforcing steel are compared to the applied axial load and moment. The magnitude

and slope of the plane strain distribution are varied until the internal forces balance the applied forces. Failure of the cross-section is defined when the internal forces cannot be increased to balance the applied forces.

The strain distributions for equilibrium of internal and applied forces provide values of equivalent stiffnesses ($M/K=EI$ and $P/\varepsilon=EA$) which can be used in the elastic structural analysis of a column or frame. In this analysis the members are divided into short elements. These elements are assigned stiffnesses which are the average of those calculated for the cross sections at each end. Using a matrix analysis format the forces and displacements at the ends of each element are computed. For the axial load and moment (including the $P\Delta$ effect calculated using the displacement information) at the ends of each element the new stiffnesses are found and compared to the previous values. Using an iterative process for changing the stiffnesses of each element, convergence for equilibrium and compatible displacements is achieved when all calculated values of stiffness coincide with the values used in the previous structural analysis.

For sustained load the magnitudes of creep and shrinkage are calculated and accumulated at regular intervals. The externally applied loads may change according to any predetermined pattern. Usually a period of constant sustained load is followed by short term loading to failure. Material failure is defined as before and instability is identified when the stiffness values for a particular element do not converge.

3.2 Material Properties

The stress strain properties for the reinforcing steel are idealized as being elastic-plastic. Inclusion of the effect of strain hardening would increase the column cross section capacity.

The properties of the concrete were based on test results[3] for a particular concrete which was specifically designed to have a lower than average aggregate to cement ratio and therefore a higher than average creep and shrinkage. The compressive failure strain was taken as .0038. In this analysis no increases of concrete strength or modulus of elasticity were taken into account after 28 days. Also the tensile strength of the concrete was disregarded. These factors plus the fact that creep and shrinkage values were found for 50% relative humidity and a temperature of 24°C create the situation where the calculated strains in the concrete will be greater than would actually occur. Thus the analysis will underestimate the resistance of the concrete section.

For this study sustained load was maintained for only 2 years. Previous analyses[3] had shown that most of the effects of creep and shrinkage will have occurred during this time. This is because the rate of creep is nearly proportional to the logarithm of time and because the stresses in the concrete decrease as the reinforcement carries a larger share of the load. A modified superposition method for calculating creep strain on each cross section strip was used to account for stress history.

Load	L=100%, D=0% P_ϕ=0			L=D=50% P_ϕ=D			L=0%, D=100% P_ϕ=D			L=0, D=100% P_ϕ=1.4D		
l/r \ e	0.1h	0.4h	e_{bal}	0.1h	0.4h	e_{bal}	0.1h	0.4h	e_{bal}	0.1h	0.4h	e_{bal}
0	2.73	2.68	2.66	2.50	2.37	2.36	2.20	2.15	2.13	2.20	2.06	1.97
20	2.70	2.65	2.63	2.42	2.33	2.33	2.18	2.11	2.09	2.17	2.03	1.96
40	2.83	2.72	2.66	2.45	2.50	2.52	2.38	2.38	2.35	2.31	2.20	2.10
60	2.95	2.82	2.76	2.90	2.60	2.60	3.00	2.54	2.50	2.94	2.31	2.37
80	3.45	2.95	2.81	3.62	3.00	2.75	4.20	3.12	2.80	4.14	3.01	2.65
100	4.20	3.42	3.09	5.00	3.50	3.05	5.80	3.70	3.20	5.74	3.66	3.15

Table 1 Comparison of Computed Safety Factors for Columns Designed by ACI 318-71[1]. ($M_1=M_2$, $P_t=0.03$, $f'_c=27.5$ MN/m^2, $\sigma y=412$ MN/m^2)

4. ANALYTICAL RESULTS

4.1 Comparison of Safety Factors

Table 1 contains the safety factors for different combinations of P_ϕ, e, and l/r. The safety factor was determined by dividing the computed capacity after sustained loading by the design load found from ACI 318-71[1]. The nominal ACI safety factor is (1.4D + 1.7L)/0.7 which gives values of 2.43, 2.21, 2.0 and 2.0 for the 4 cases of loading. The safety factors for l/r=0 were up to 13% higher than the ACI values. The difference is mainly due to the ACI's use of a rectangular approximation for the stress distribution. This difference (which is less for larger eccentricities) is considered to be acceptable for calculation of cross section capacities. Therefore the design provisions to account for the additional moment, PΔ, should be evaluated in terms of the change in safety factor compared to the computed value for l/r=0.

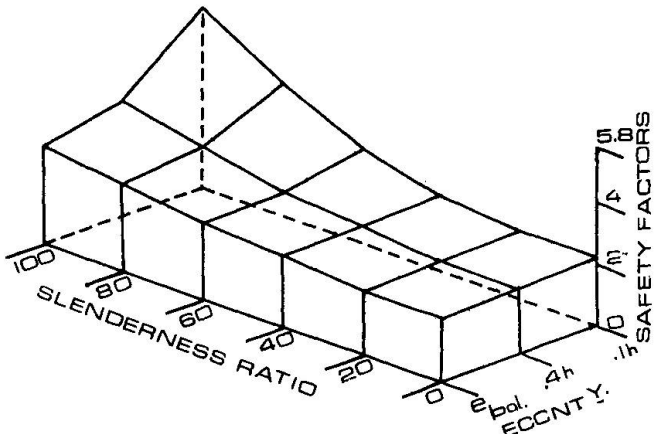

Fig. 1. Variation in Safety (p_t=3%, D=100%, L=0, P_ϕ=D, $M_1=M_2$)

The results show that the ACI design is most conservative for high l/r ratios, low e/h and high sustained loads. Even for the unrealistic case of sustaining 1.4D where L=0, the safety is not affected much. Reasons for these trends are suggested in the Conclusions.

The variation in the actual safety factor is shown graphically in Figure 1 for the case where L=0, D=100% and the design D is sustained. The safety factors for P_t=1.5% and e=0.4h are shown in Figure 2 for the same loading conditions. A similar trend is observed.

4.2 Evaluation of Moment Magnification

Figure 3 contains a graph of the computed moment magnifications, F, at failure versus $^{l}/_{r}$ for e=0.1h and e=0.4h. The computed F values at the ACI failure load are substantially less than the ACI values. Because the computed failure loads are much greater the moment magnifications at failure are closer to the ACI values. The differences between computed and ACI values are even more pronounced for lower levels of sustained load.

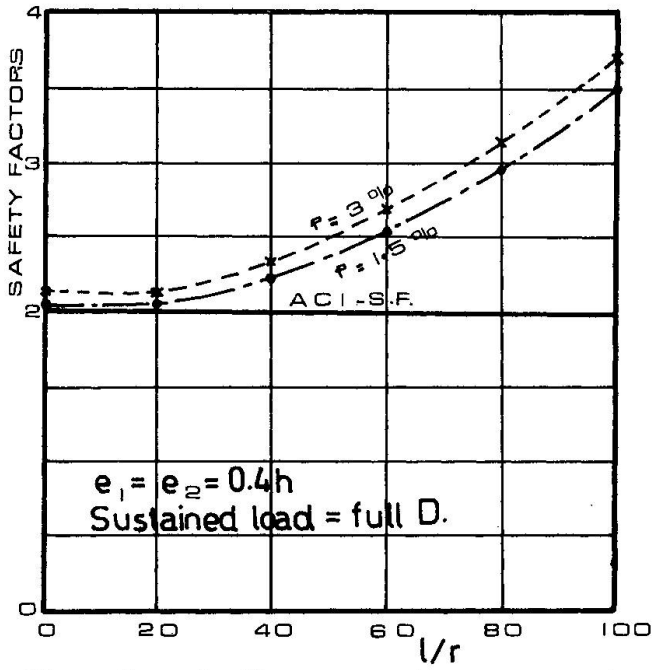

Fig. 2. Influence of p_t on Safety (D=100%, L=0)

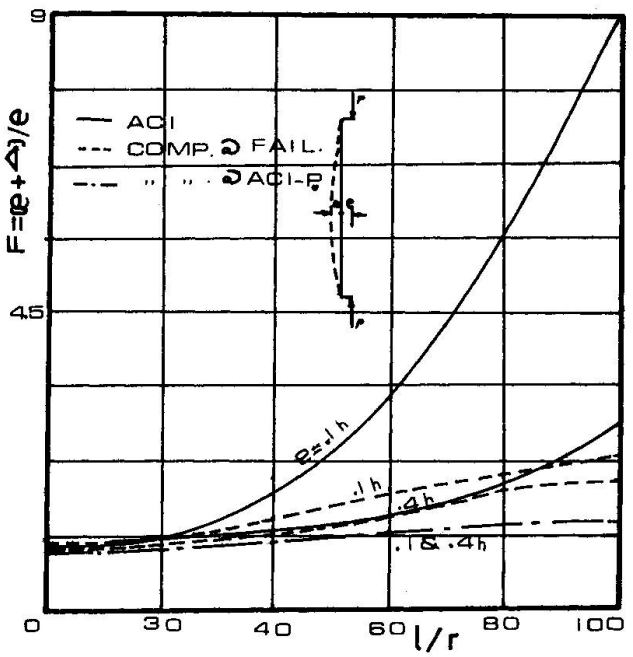

Fig. 3. Comparison of Moment Magnification (D=100%, L=0, P_ϕ=D, p_t=3%)

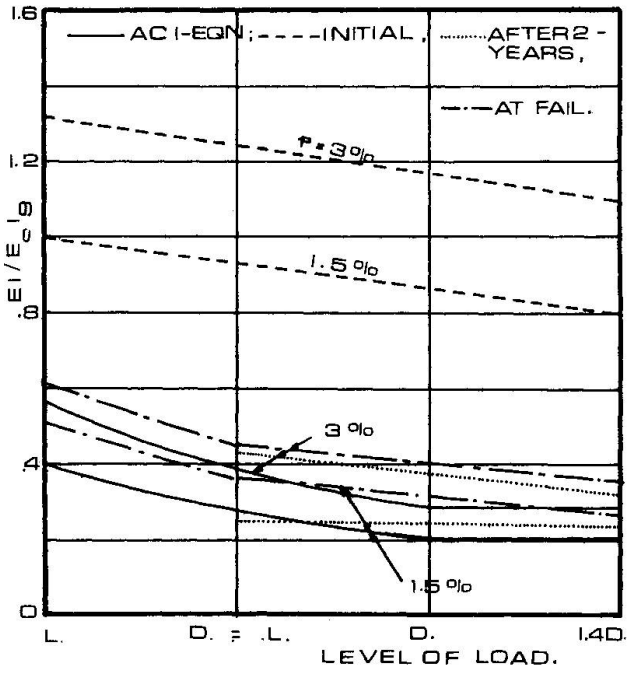

Fig. 4. Comparison of EI Values (e_1=e_2=0.4h, P_ϕ=D, $^{l}/_{r}$=60)

One of the main features in the calculation of the PΔ effect is the determination of the flexural stiffness, EI, of the cross section. For e=0.4h, the computed values of EI=Pe/K for different combinations of loading are shown in Figure 4 along with the ACI values. Computed values are shown for the following cases:

a) initial application of the design load
b) after two years of sustained dead load
c) at failure as the load was increased after the period of sustained loading.

The EI values after sustained load are slightly higher than the ACI values. As more load is applied to determine failure, the concrete again

begins to carry a greater share of the load and the computed EI values show large increases. Even as the failure load is reached the EI values remain higher than they were at the sustained load stage. The influence of EI will be discussed in the Conclusions.

4.3 Effect of End Conditions

Analyses performed for different ratios of M_1/M_2 indicate that some variation in safety factor occur where the ACI provision for modifying the magnification factor, F, to account for this effect is used. The effect of multiplying F by the term $(0.6 + 0.4 M_1/M_2) > 0.4$ did not seem to create major changes in the spread of safety factor values.

One of the structures which have been analysed[8] is presented in Figure 5 to illustrate behaviour. A portion of the frame was analysed for sustained load followed by short term loading to failure. The dimensions, initial stiffnesses and loading are shown. Using ACI 318-71 the nominal safety factor for column 1 is 2.31. The computed safety factor is 3.15. Since this column had a low slenderness ratio the reserve strength is partially due to the

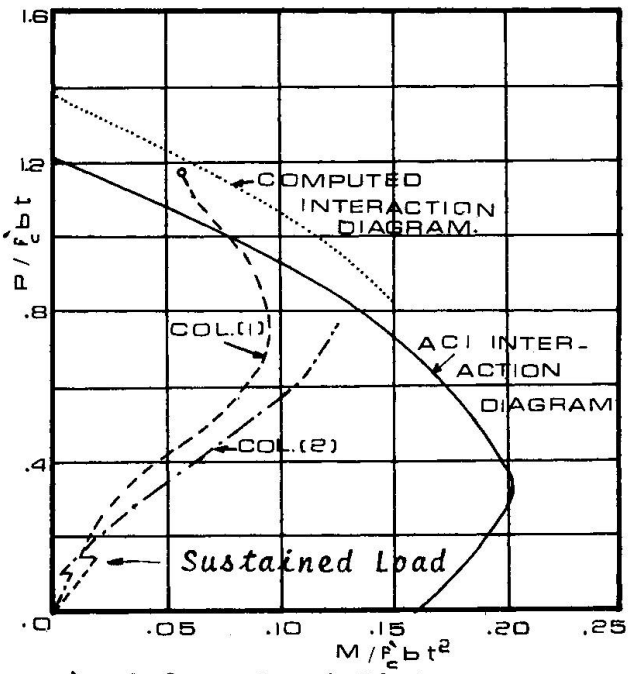

a) Column Load History

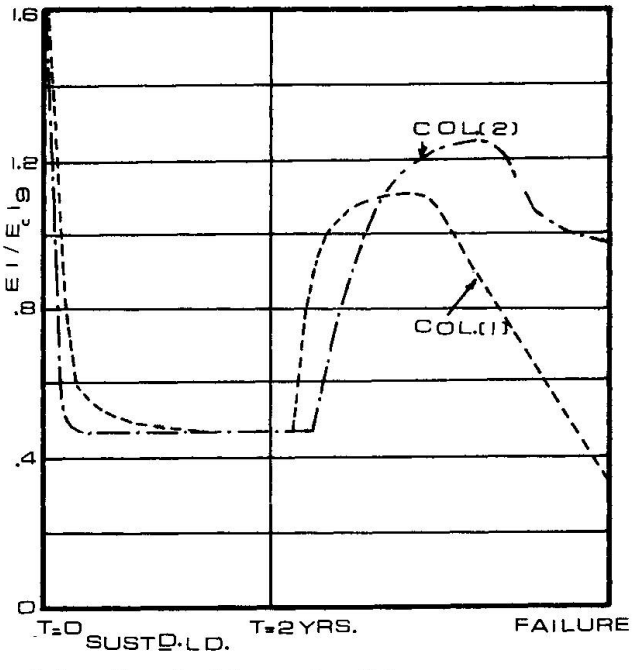

b) Variation in EI

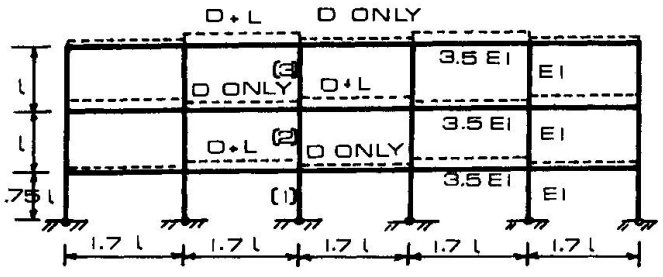

c) Actual Frame

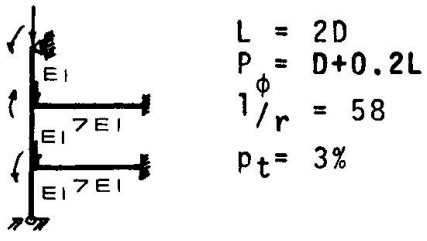

d) Equivalent Frame

Fig. 5. Example of Behaviour of Columns in a Structure

reduction in moment which occurs as the column becomes more flexible.

The axial load and maximum moment on columns 1 and 2 are shown for loads up to failure of column 1. The slight decrease in moment at sustained load indicates that PΔ was more than compensated for by reduced distribution of moment to the columns. The changes in EI during sustained loading and as the loads are increased to failure are also shown.

5. CONCLUSIONS

The fact that slenderness and sustained load decrease column capacity is well documented[2,3,6]. The results of this study indicate that the provisions of ACI 318-71 to account for these effects do not result in consistent safety factors. Using this accepted design method as a basis for comparison, several aspects of the design are identified for consideration.

1. During sustained load the EI values tend to approach $I_s E_s$ for any of the following conditions; high $1/r$, low P_ϕ, large e/h, large p_t, and for more moderate combinations of these such as medium $1/r$ and p_t, or medium P_ϕ and e/h. This behaviour results from the transfer of stress to the steel as the concrete creeps and shrinks. However upon application of short term load to determine failure, the EI values increase. It is suggested that sustained load as a percent of cross section capacity rather than column capacity will provide a more realistic measure of the effects of sustained load.

2. The derivation of the moment magnification formula is based on the concept of including the PΔ effect when calculating the cross section capacity required. However in order to accommodate the possibility of instability failure on the basis of cross section capacity it is necessary to inflate the moment magnification values (increase PΔ) to achieve the appropriate reduction in column strength. Since a common EI is used for both material and instability failure, the added moment (PΔ) for cases with material failure is too large. This study and others[2] show that instability occurs only at small eccentricities and very high $1/r$ values. Very slender columns are rarely found in practice. Also the possibility of instability failure exists only at the slenderness limit specified by ACI. Therefore designers should use the EI which produces the correct deflection rather than an artificial value to accommodate prediction of failure due to instability.

3. The moments applied to columns in structures braced against sidesway are limited to the moments transmitted by the beams or slabs. In many cases the additional moments due to deflection are largely offset by a redistribution of the applied moment as the column deflects. [The stiffness of a flexural member is not affected by deflection and is not affected to the same extent by creep and shrinkage.] Therefore there may be some benefit in using different moment magnifying procedures depending on whether or not the structure is braced against sidesway.

(Notation is defined or corresponds to the Introductory Report.)

REFERENCES

1. ACI Committee 318, "Building Code Requirements for Reinforced Concrete (ACI 318-71)", American Concrete Institute.
2. Cranston, W.B., "Analysis and Design of Reinforced Concrete Columns", Research Report No.20, Cement and Concrete Association, London, 1972.
3. Drysdale, R.G. and Huggins, M.W., "Sustained Biaxial Load on Slender Concrete Columns", Journal Structural Division, ASCE, Vol.97, No.ST5, May 1971, pp.
4. Drysdale, R.G., Mirza, M.S., and McCutcheon, J.O., "Recent Research in Deflection of Concrete Structures", Proc. of the Symposium: Deflections of Structural Concrete, Canadian Capital Chapter of ACI, 1971, pp.161-182.
5. Furlong, R.W., "Column Slenderness and Charts for Design", Proc. American Concrete Inst., Vol.68, Jan. 1971, pp.9-17.
6. MacGregor, J.G., Breen, J.E., and Phrang, E.O., "Design of Slender Concrete Columns", ACI Journal, Proceedings, Vol.67, No.1, January 1970, pp.6-28.
7. Portland Cement Association, "Notes on ACI 318-71 Building Code Requirements with Design Applications", PCA, July 1972.
8. Sallam, S., "Design of Reinforced Concrete Columns", M.Eng. Thesis, McMaster Univ., Hamilton, Ontario, 1974.
9. Tan, K.B., "On Short-Term and Sustained Load Analysis of Concrete Frames", M.Eng. Thesis, McMaster Univ., 1972.

SUMMARY

Individual columns were analysed to determine the PΔ effects for sustained load. The remaining capacity after sustained load compared to the design load using ACI 318-71 gave the actual safety factor. The designs for slender columns and for columns loaded with small eccentricities were quite conservative. Some general comments on column safety are based on results for behaviour of columns in frames.

RESUME

Des colonnes isolées ont été examinées afin de déterminer les effets du PΔ sous l'influence de charges soutenues. La résistance effective après application de charges soutenues divisée par la charge utile selon ACI 318-71 donne le facteur de sécurité. Le dimensionnement de colonnes élancées et colonnes avec de petites excentricités, donne des résultats prudents. Quelques commentaires généraux sur la sécurité sont basés sur les résultats du comportement de colonnes dans des cadres.

ZUSAMMENFASSUNG

Es werden Einzelstützen untersucht hinsichtlich ihres Verhaltens 2. Ordnung unter Dauerlasten. Der Sicherheitsfaktor er-

gibt sich aus der nach Einwirkung der Dauerlast noch verbleibenden Tragkapazität, bezogen auf die Bemessungslast nach der ACI-Norm 318-71. Die Bemessung von schlanken Stützen bzw. Stützen mit kleinen Exzentrizitäten liegt auf der sicheren Seite. Einige allgemeine Bemerkungen zur Sicherheit von Stützen beziehen sich auf das Verhalten von Stützen in Rahmen.

Leere Seite
Blank page
Page vide

Zur einfachen Bemessung schlanker Stahlbetonrahmen

Contribution to a Simple Design of Slender Reinforced Concrete Frames

Vers un dimensionnement simple des cadres élancés en béton armé

Achim IRLE Horst SCHÄFER Horst G. SCHÄFER
Technische Hochschule Darmstadt
Darmstadt, BRD

1. EINLEITUNG

Die Traglast schlanker Stahlbetonrahmen läßt sich heute mit numerischen Berechnungsmethoden wirklichkeitsnah ermitteln, [1] bis [9]. Das nichtlineare Werkstoffverhalten von Beton und Stahl und das Aufreißen des Betons in der Zugzone erfordern jedoch einen großen numerischen Aufwand bei der Berechnung der Traglast. Deshalb benötigt der Ingenieur einfache Näherungsverfahren, die zuverlässige und wirtschaftliche Ergebnisse liefern.

In der Praxis steht der Ingenieur oft vor der Aufgabe, ein gewähltes Tragwerk für vorgegebene Lasten zu dimensionieren. Aufgrund seiner Erfahrung hat er i.a. die Betonquerschnittswerte bereits festgelegt, so daß er nur noch die erforderliche Bewehrung zu ermitteln hat. Nach einer überschläglichen Vorbemessung muß er die Tragfähigkeit am verformten System nachweisen. Viele der hierfür entwickelten Methoden scheiden jedoch oft für eine praktische Anwendung aus, weil entweder die erforderlichen Rechenzeiten und damit die Kosten zu hoch sind oder weil ein entsprechend leistungsfähiger Computer nicht zur Verfügung steht. Aus diesem Grunde enthalten die nationalen Normen in der Regel Näherungsvorschläge, vgl. z.B. [11] und [14].

Nachfolgend soll über zwei Näherungsverfahren berichtet werden, das Ersatzstabverfahren (Effective Length Method) und das Ersatzsteifigkeitsverfahren (Effective Stiffness Method). Die Güte der Übereinstimmung mit einer strengen Traglastberechnung auf der Basis der DIN 1045 [10] soll in Vergleichsrechnungen untersucht werden.

2. DAS ERSATZSTABVERFAHREN

2.1 Grundlage des Verfahrens

Mit dem "Ersatzstabverfahren" versucht man bei der Ermittlung der Schnittkräfte die Berechnung des Gesamtsystems nach Theorie II.

Ordnung zu umgehen, indem man einzelne Stäbe mit definierten Stablängen und Lagerungsbedingungen, die "Ersatzstäbe", herausgreift und diese einer strengen Berechnung unterwirft. In die deutschen Berechnungsvorschriften für Stabilitätsfälle im Stahlbau wurde dies auf Vorschlag von CHWALLA für die Traglastermittlung von Stahlkonstruktionen im Jahre 1952 eingeführt. Als "Ersatzstab" wird ein an beiden Enden gelenkig gelagerter Stab bezeichnet, dessen Länge s_K aus dem Vergleich der EULER-Last des Ersatzstabes mit der Verzweigungslast des idealisierten Gesamtsystems ermittelt wird. Im Prinzip war das Ersatzstabverfahren bereits in der alten deutschen Stahlbetonnorm des Jahres 1942 enthalten. Die Ersatzstäbe wurden damals für ω-fache Lasten nachgewiesen, wobei die ω-Werte in Abhängigkeit von der Schlankheit in Versuchen ermittelt worden waren.

Im folgenden soll kurz das Ersatzstabverfahren beschrieben werden, wie es nach der deutschen Stahlbetonnorm des Jahres 1972, DIN 1045 [10], zugelassen ist. Es basiert weitgehend auf den Empfehlungen von KORDINA [11].

2.2 Das "Ersatzstabverfahren" in der deutschen Stahlbetonnorm

Die deutsche Stahlbetonnorm fordert eine genauere Untersuchung von Stahlbetondruckgliedern mit einer Schlankheit $\lambda = s_K/i > 70$. Dafür werden zwei Verfahren vorgeschlagen:

- Eine Traglastuntersuchung am Gesamtsystem unter 1.75-fachen Gebrauchslasten nach der Theorie II. Ordnung mit wirklichkeitsnahen Steifigkeiten.
- Eine Näherungsberechnung mit Hilfe des "Ersatzstabverfahrens".

Das "Ersatzstabverfahren" erfordert drei Berechnungsschritte:

Im ersten Schritt wird die Länge des Ersatzstabes ermittelt. Sie ergibt sich bei unverschieblichen Systemen als Abstand der Wendepunkte der Knickbiegelinie, bei verschieblichen aus dem Vergleich der zur Verzweigungslast des Gesamtsystems gehörenden Stabnormalkraft mit der EULER-Last des untersuchten Stabes. Dabei wird angenommen, daß die Lasten in den Knoten angreifen und die Stäbe ideal gerade sind. Für deren Steifigkeit können die reinen Betonquerschnittswerte angesetzt und als E-Modul kann der Anfangsmodul des Betons verwendet werden.

Im zweiten Schritt werden die Schnittkräfte nach der Theorie I. Ordnung ermittelt. Dabei wird ebenfalls ein linear-elastisches Verhalten der Struktur vorausgesetzt. Die Exzentrizität der Normalkraft wird in den einzelnen Stäben aus dem größten, im mittleren Drittel der Knickbiegelinie ermittelten Biegemoment berechnet ($e = \max M/N$) und dann für die Ersatzstäbe als konstant angenommen.

Im dritten Schritt wird der Ersatzstab losgelöst vom Gesamtsystem nach der Theorie II. Ordnung berechnet. Dabei wird eine Verformung des Systems oder eine ungewollte Exzentrizität von $e_u = s_K/300$ berücksichtigt. Für die Spannungs-Verzerrungs-Beziehungen werden die auch für die Ermittlung der Bruchschnittgrößen maßgebenden Verläufe entsprechend Abb. 1 vorausgesetzt. Hierdurch wird eine zusätzliche Sicherheit eingebaut, die durch die erhöhte Ausnutzung der Stützen gegenüber der alten Vorschrift angebracht erschien.

Betonzugspannungen werden nicht berücksichtigt. Die Ergebnisse der Berechnung der Ersatzstäbe wurden für die praktische Anwendung in Nomogrammen aufbereitet [11]. Diese gestatten eine schnelle Ermittlung der erforderlichen Bewehrung.

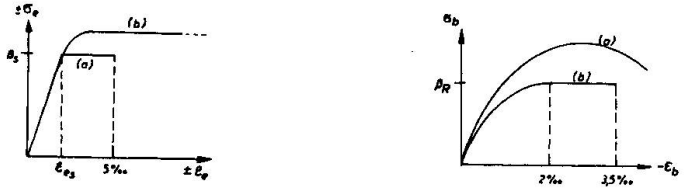

Abb. 1 Werkstoffgesetze für Stahl und Beton

2.3 Systematische Überprüfung der Güte des Ersatzstabverfahrens

2.3.1 Klassische Form des Ersatzstabverfahrens

Zur systematischen Überprüfung der Güte eines Näherungsverfahrens muß die Zahl der Parameter überschaubar bleiben. Es ist deshalb erforderlich, ein möglichst einfaches System zu wählen, an dem jedoch alle Eigenschaften eines komplexen Tragwerks simuliert werden können. Es wurde deshalb ein Einfeldstab gewählt, der an den Enden elastisch gelagert ist und exzentrisch angreifende Normalkräfte aufweist (Abb. 2).

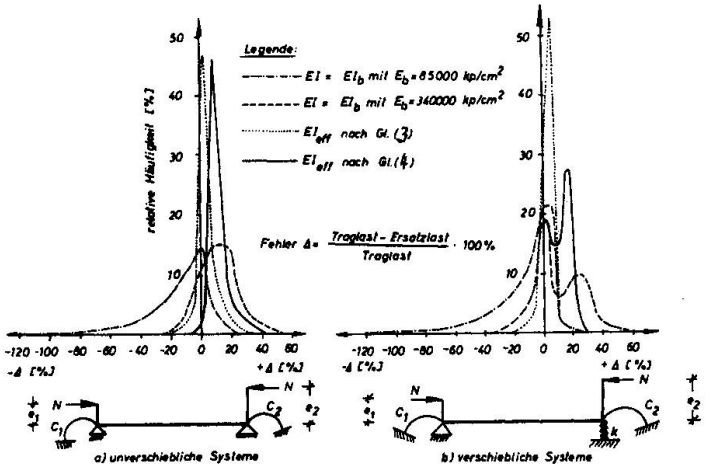

Abb. 2 Fehlercharakteristik des Ersatzstabverfahrens

Für je 1800 verschiebliche und unverschiebliche repräsentative Einfeldstäbe wurden bei systematisch variierten Exzentrizitäten, Bewehrungsverhältnissen ($\mu = \mu' = 0{,}4\% \div 4{,}5\%$) und Federsteifigkeiten ($c = 0 \div \infty$) Traglasten nach dem Ersatzstabverfahren berechnet und mit der strengen Lösung nach einem in [6] beschriebenen Verfahren verglichen. Die relative Häufigkeit der prozentualen Abweichungen der Näherungslösungen von der strengen Lösung ist in Abb. 2 für verschiebliche und unverschiebliche Systeme aufgetragen. Negative Abweichungen zeigen eine zu geringe Sicherheit an.

Für die Steifigkeit EI des Einfeldstabes wurde bei der Ermittlung der Knicklänge und bei der Verteilung des Stabendmomentes auf Stab und Feder zunächst mit linear-elastischen Werten $EI = E_b I_b$ gerechnet, wobei nacheinander für E_b = 85.000/170.000/350.000 kp/cm^2 angesetzt wurde. Wie Abb. 2 zeigt, sind die Fehlercharakteristiken unbefriedigend, weil insbesondere die Abweichungen zur unsicheren Seite hin zu groß sind.

Es war zu vermuten, daß die Hauptfehlerquelle im Ansatz falscher Stabsteifigkeiten liegt. Im folgenden soll daher die Untersuchung auf die Verwendung "effektiver Steifigkeiten" ausgedehnt werden.

2.3.2 Verwendung effektiver Steifigkeiten beim Ersatzstabverfahren

Für die Anwendung "effektiver Steifigkeiten" EI_{eff} gibt es eine Reihe von Vorschlägen, von denen hier genannt seien:

ACI BUILDING CODE [15] (für Kurzzeitlast)

$$EI_{eff} = E_b I_b \left(0.2 + \frac{E_e I_e}{E_b I_b}\right) \qquad (1)$$

KORDINA/QUAST [11]

$$EI_{eff} = E_b I_b \left[0.2 + 15\,(\mu + \mu')\right] \qquad (2)$$

Gl. (2) ist mit Gl. (1) im wesentlichen identisch. Diese wurde als Ergebnis von ca. 100 Vergleichsrechnungen aus Momenten-Krümmungs-Beziehungen gewonnen und an einer Reihe von Beispielen überprüft[14].

JANKÓ [7]

$$EI_{eff} = E_b I_b \left[0.6 - 2\cdot(\bar{n} - 0.5)^2 + (1 - 0.25\cdot\bar{n}^2)\cdot({}_{ges}\bar{\mu} - 0.05)\right] \qquad (3)$$

$$\text{mit } \bar{n} = \frac{N}{b\cdot d\cdot \beta_R}\cdot\frac{1}{(1 + {}_{ges}\bar{\mu})}\;;\quad {}_{ges}\bar{\mu} = \frac{\sum Fe}{b\cdot d}\cdot\frac{\beta_s}{\beta_R}$$

Gl. (3) wurde von JANKÓ an einem beidseits gelenkig gelagerten Stab unter der Wirkung einer exzentrisch wirkenden Normalkraft und eines einseitig angreifenden Bruchmomentes aus der Bedingung gleicher Randverdrehung von Ersatzstab und wirklichem Stab abgeleitet.

IRLE [9]

$$EI_{eff} = E_b I_b \left[a + b\,(\mu + \mu')\right] \qquad (4)$$

IRLE erweitert die Gl. (1) von KORDINA/QUAST, indem er anstelle von konstanten Größen a und b veränderliche einführt. Zu deren Bestimmung wird eine Ersatzsteifigkeit EI_{eff} so festgelegt, daß der Stab mit der konstanten Ersatzsteifigkeit und ein Stahlbetonstab mit konstanter Endausmitte unter der zur Traglast gehörenden Momentenfläche die gleiche Durchbiegung in Feldmitte aufweisen.

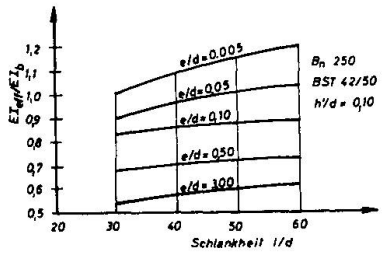

Abb. 3 Ersatzsteifigkeit in Abhängigkeit von Schlankheit und Ausmitte

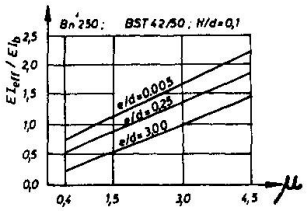

Abb. 4 Ersatzsteifigkeit in Abhängigkeit von Bewehrungsgrad und Ausmitte

Der Einfluß der Schlankheit kann in erster Näherung vernachlässigt werden (Abb. 3). Für eine mittlere Schlankheit e/d = 40 läßt sich stellvertretend für alle Werte e/d die Ersatzsteifigkeit als Geradenschar gemäß Gl. (4) beschreiben (Abb. 4). Die Parameter a und b kann man nun in Abhängigkeit vom Verhältnis h'/d, der Beton- und Stahlgüte ein für alle mal bestimmen. Für Werkstoffe der deutschen Stahlbetonnorm DIN 1045 [10] erhält man z.B. die in der Abb. 5 dargestellten Werte.

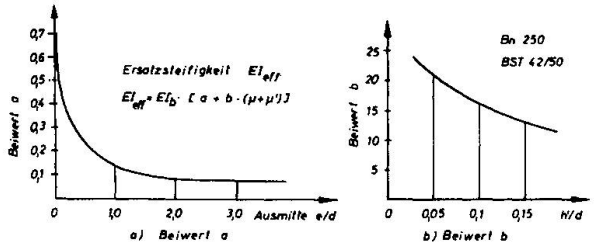

Abb. 5 Beiwerte zur Berechnung der Ersatzsteifigkeit EI_{eff}

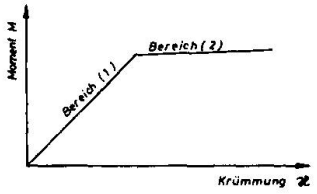

Abb. 6 Momenten-Krümmungs-Zusammenhang für normalkraftfreie Stäbe

Für die normalkraftarmen Rahmenriegel verwendet IRLE [9] nur den nahezu linearen Ast des Biegemomenten-Krümmungs-Zusammenhanges eines normalkraftfreien Stabes (Abb. 6). Linearisiert man den Bereich (1), so erhält man für die Verdrehsteifigkeit den in Abb. 7 angegebenen Zusammenhang für eine häufig vorkommende Werkstoffkombination gemäß DIN 1045 [10].

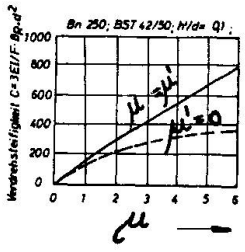

Abb. 7 Verdrehsteifigkeit normalkraftfreier Stäbe

Die Verwendung effektiver Steifigkeiten beim Ersatzstabverfahren führt i.a. zu wesentlich besseren Ergebnissen. Gl. (1) und (2) wurden jedoch nach ca. 50 Tastrechnungen nicht weiter ausgetestet, weil in Grenzfällen Abweichungen von über 100 % aufgetreten waren und sie gegenüber dem Ansatz hoher E_b-Werte keine Verbesserung ergaben. Die Anwendung von Gl. (3) führt - wie Abb. 2 zeigt - im

Mittel zu geringen Abweichungen. Bedenklich ist lediglich, daß die Abweichungen z.T. auf der unsicheren Seite liegen, insbesondere dann, wenn für den Traglastnachweis des Standardstabes auf die Tafeln von KASPAREK/HAILER [12] zurückgegriffen wird, mit denen verschränkte Exzentrizitäten berücksichtigt werden können. Die Verwendung von Gl. (4) führt im Vergleich zu Gl. (3) zu etwas größeren Abweichungen, die jedoch durchweg auf der sicheren Seite liegen; die Übereinstimmung mit der strengen Rechnung wird im Gegensatz zu Gl. (3) durch die Verwendung der Tafeln KASPAREK/HAILER [12] noch besser. In der Abb. 2 sind in beiden Fällen nur die Abweichungen dargestellt, die sich auf der Basis des "klassischen" Standardstabes mit konstanten Exzentrizitäten ergaben.

Zusammenfassend läßt sich sagen, daß das Ersatzstabverfahren bei statisch bestimmten Systemen gute Ergebnisse liefert. Bei statisch unbestimmten Systemen ist es immer dann brauchbar, wenn man die effektiven Stabsteifigkeiten und die Knicklängen gut abschätzt. Die Ermittlung der Knicklängen in komplexeren Systemen ist jedoch i.a. sehr aufwendig; es erhebt sich daher die Frage, ob es nicht sinnvoller ist, in solchen Fällen das Ersatzstabverfahren durch eine direkte Berechnung des Systems nach Theorie II. Ordnung unter Benutzung der bereits genannten "effektiven Steifigkeiten" zu ersetzen.

3. DAS ERSATZSTEIFIGKEITSVERFAHREN

Da die Berechnung von Rahmen mit linear-elastischem Werkstoffgesetz nach der Theorie II. Ordnung auch von mittelgroßen Rechenanlagen gut bewältigt wird, bietet es sich an, mit einer effektiven Ersatzsteifigkeit EI_{eff}, die über die Länge eines ganzen Rahmenstiels konstant ist, in herkömmliche Rechenverfahren einzugehen. Der Rechengang läuft dann nach folgendem Schema ab:

(a) Ermittlung der Schnittkräfte eines Rahmens nach der Theorie II. Ordnung unter Annahme reiner Betonsteifigkeiten EI_b (elastische Rechnung).

(b) Bemessung des Rahmens für die Schnittkräfte nach (a).

(c) Berechnung von wirksamen Steifigkeiten EI_{eff}.

(d) Ermittlung der Schnittkräfte nach der Theorie II. Ordnung unter Annahme wirksamer Stabsteifigkeiten EI_{eff}.

(e) Überprüfung der Bewehrung nach (b); falls erforderlich, iterative Verbesserung nach (d).

Konvergenz ist gegeben, wenn in zwei aufeinanderfolgenden Schritten die Schnittkräfte genügend genau übereinstimmen.

Die systematische Überprüfung der Brauchbarkeit analog zu Abschnitt 2 war zur Zeit der Drucklegung (März 1970) noch nicht abgeschlossen. Alle bisher durchgerechneten Beispiele unter Verwendung von Gl. (4) zeigten jedoch gute Ergebnisse. Es ist zu vermuten, daß dies bei veschieblichen Systemen auch auf Gl. (3) zutrifft.

4. ZAHLENBEISPIEL

4.1 Vergleichsgrundlagen

Um die Güte eines Näherungsverfahrens zu überprüfen, bestehen grundsätzlich mehrere Möglichkeiten:

Man kann z.B. bei vorgegebenen Abmessungen, Bewehrungen und Lasten Schnittkräfte vergleichen. Dies liefert jedoch im Hinblick auf die Sicherheit eines Tragwerkes keine relevante Aussage. Es erscheint aussagekräftiger, mit dem Näherungsverfahren die Schnittkräfte und Bewehrung zu ermitteln und das so bemessene Tragwerk mit einem strengen Verfahren nachzurechnen. Die Güte des Näherungsverfahrens ist dann umso besser und wirtschaftlicher, je weniger der Gesamtsicherheitsbeiwert von dem zu fordernden abweicht. Abweichungen sollten möglichst nur zur "sicheren Seite" hin auftreten.

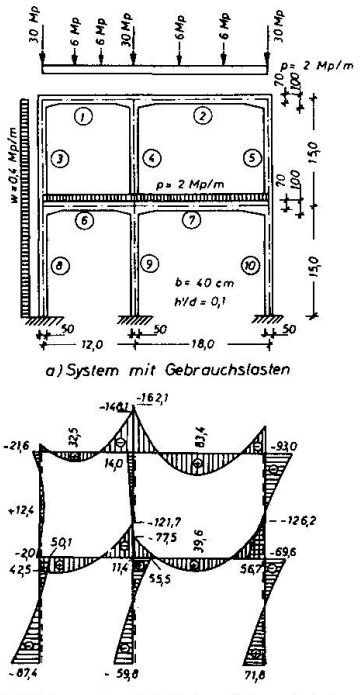

Zahlenwerte

Beton: Bn 250
Stahl: BSt 42/50

Stab	Stelle l = links m = mitte r = rechts	μ [‰]	μ' [‰]	N [Mp] Druck positiv
1	l	0,40	0,40	7,0
	m	0,44	0,40	
	r	0,40	1,15	
2	l	0,40	1,30	9,5
	m	1,40	0,40	
	r	0,40	0,64	
3		0,68	0,68	73,5
4		0,40	0,40	140,4
5		2,75	2,75	90,7
6	l	0,78	0,40	2,3
	m	0,78	0,40	
	r	0,40	0,92	
7	l	0,40	0,56	-0,3
	m	0,58	0,40	
	r	0,40	0,97	
8		2,29	2,29	80,8
9		1,34	1,34	203,8
10		1,66	1,66	124,9

Abb. 8 Zahlenbeispiel zum Ersatzsteifigkeitsverfahren

4.2 Kritische Wertung der Ergebnisse

Im gewählten Zahlenbeispiel (Abb. 8) wurden zunächst die Schnittkräfte unter 1.75-fachen Lasten mit $EI=EI_b$ nach der Theorie II. Ordnung ermittelt. Damit wurde dann eine Bemessung durchgeführt und das Tragwerk mit verschiedenen Ersatzsteifigkeiten neu

berechnet. Nach jedem Schritt wurde die Bewehrung den veränderten Schnittgrößen angepaßt bis diese sich in zwei aufeinanderfolgenden Schritten nicht mehr wesentlich änderten. Dies war bereits im dritten Schritt der Fall.

Die anschließende strenge Traglastrechnung ergab mit EI_{eff} nach Gl. (4) eine Tragwerksicherheit $\nu = 1.82$, die damit nur geringfügig über dem geforderten Wert $\nu = 1.75$ liegt. Das Ersatzstabverfahren lieferte $\nu = 2.05$, im vorliegenden Falle einen auf der sicheren Seite liegenden Wert. Das Ersatzsteifigkeitsverfahren hat sich in allen bisher behandelten Fällen ähnlich gut bewährt.

LITERATUR:

[1] Breen, J.E.: The Restrained Long Concrete Column as a Part of a Rectangular Frame. Diss., Austin, Texas, 1962.

[2] Cranston, W.B.: A Computer Method for Inelastic Analysis of Plane Frames. Techn. Report, Cement and Concrete Association, London, 1965, TRA 402.

[3] Chang, W.F.: Inelastic Buckling and Sidesway of Concrete Frames. ASCE Proceedings, Vol. 193, 4/1967, S. 287-299.

[4] Bubenheim, H.-J.: Ein Beitrag zur Berechnung von Rahmensystemen mit nichtlinear-elastischem Werkstoffgesetz. Diss. D. 17, TH Darmstadt, 1969.

[5] Beck, H., Bubenheim, H.-J.: Ein Verfahren zur optimalen Bemessung ebener Stahlbetonrahmen. DER BAUINGENIEUR, 6/1972, S. 194-200.

[6] Schäfer, H., Irle, A., Hasse, E.: Die Berechnung stabförmiger Stahlbetonbauteile nach dem Reduktionsverfahren mit Berücksichtigung eines wirklichkeitsnahen Werkstoffverhaltens. Beton- und Stahlbetonbau, 7/1972, S. 154-159.

[7] Jankó, B.: Zum Trag- und Verformungsverhalten ebener Stockwerkrahmen aus Stahlbeton. Diss., TU Braunschweig, 1972.

[8] Aas-Jakobsen et al.: CEB, Bulletin d'information, Nr. 93, 1973.

[9] Irle, A.: Zum vereinfachten Stabilitätsnachweis ebener Stahlbetonrahmen. Diss., TH Darmstadt, voraussichtlich 1974.

[10] DIN 1045: Beton- und Stahlbetonbau, Bemessung und Ausführung. Ausgabe Januar 1972, Beuth-Vertrieb GmbH, Berlin und Köln, 1972.

[11] Kordina, K., Quast, U.: Bemessung von schlanken Bauteilen - Knicksicherheitsnachweis. In: Beton-Kalender 1974, Verlag Wilh. Ernst & Sohn, Berlin, 1974, S. 593-708 und in: Bemessung von Beton- und Stahlbetonbauteilen. Deutscher Ausschuß für Stahlbeton, Heft 220, Berlin, 1972.

[12] Kasparek, K-H., Hailer, W.: Nachweis- und Bemessungsverfahren zum Stabilitätsnachweis nach der neuen DIN 1045. Werner-Verlag , Düsseldorf, 1973.

[13] Parme, A.L.: Capacity of Restrained Excentrically Loaded Long Columns. Symposium on Reinforced Concrete Columns, ACI Public. SP-13, Detroit, 1966.

[14] Mac Gregor, J., Breen, J.E., Pfrang, E.O.: Design of Slender Concrete Columns. ACI-Journal, Januar 1970, S.6-28.

[15] ACI-Standard 318-71. Building Code Requirements for Reinforced Concrete. Detroit, Michigan 1971.

ZUSAMMENFASSUNG

Es werden zwei einfache Näherungsverfahren zum Traglastnachweis schlanker Stahlbetonrahmen beschrieben: das "Ersatzstabverfahren" und das "Ersatzsteifigkeitsverfahren". Das Ersatzstabverfahren wird in umfangreichen Serienrechnungen in einigen Varianten ausgetestet. Es ist bei statisch unbestimmten Systemen i.a. nur unter Verwendung "effektiver Steifigkeiten" brauchbar. Beim "Ersatzsteifigkeitsverfahren" wird vorgeschlagen, den Traglastnachweis mit stabweise konstanten "effektiven Steifigkeiten" unter Benutzung herkömmlicher Computer-Programme zu führen.

SUMMARY

Two simple approximation methods for the ultimate limit state analysis of slender reinforced frames are described: the "Effective-Length-Method" (ELM), and the "Effective-Stiffness-Method" (ESM). The ELM is checked in numerous series computations. For statically indetermined systems it is only usable by applying "effective stiffnesses". For the ESM it is suggested to check the ultimate limit state with "effective stiffnesses" using conventional computer programs.

RESUME

On décrit deux méthodes simples d'approximation pour déterminer la charge ultime des cadres élancés en béton armé: le procédé des "barres équivalentes" et le procédé des "rigidités équivalentes". Le procédé des barres équivalentes est contrôlé par de nombreux calculs pour quelques variantes; dans le cas de systèmes hyperstatiques, il n'est utilisable qu'en employant les "rigidités effectives". Pour le procédé des rigidités équivalentes, on propose d'effectuer le calcul de la charge ultime avec des programmes courants d'ordinateur en admettant des "rigidités effectives" constantes pour chaque barre.

Leere Seite
Blank page
Page vide

II

Einfache Methode zur Berechnung der Bruchlast von schlanken Druckgliedern

Simple Method for Determining the Ultimate Load of Slender Compression Members

Méthode simple pour le calcul de la charge ultime de pièces élancées comprimées

C. MENN
Prof. Dr.
ETH Zürich
Zürich, Schweiz

1. Einleitung

Die Bemessung schlanker Druckglieder mit einer Vorschrift über zulässige Spannungen ist deshalb besonders problematisch, weil zu Folge des Spannungsproblems zweiter Ordnung eine zuverlässige Beurteilung der effektiven Sicherheit kaum möglich ist. Die Kommission des SIA für die SIA-Norm Nr. 162 (Norm für die Berechnung, Konstruktion und Ausführung von Bauwerken aus Beton, Stahlbeton und Spannbeton) hat deshalb einer Arbeitsgruppe den Auftrag erteilt, eine einfache, klare Richtlinie für die Bemessung schlanker Druckglieder nach dem Traglastverfahren auszuarbeiten. Nach eingehender Prüfung der bekannten Berechnungsverfahren und umfangreicher Vergleiche und Untersuchungen hat diese Arbeitsgruppe beschlossen, als Grundlage ein neues Berechnungsverfahren anzuwenden, das am Institut für Baustatik und Konstruktion an der ETH Zürich entwickelt wurde. Dieses Verfahren wird im Folgenden kurz dargestellt.

2. Bruchlast schlanker Druckglieder

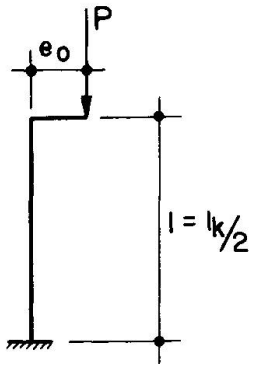

Fig. 1

Die Schwierigkeit der Traglastberechnung für eine einfache Stütze gemäss Fig. 1 besteht vor allem darin, dass bei der Laststeigerung die Querschnittssteifigkeit auf der ganzen Stützenhöhe ständig ändert; d.h. jedem Schnittkraftpaar N und M entspricht eine bestimmte Steifigkeit EI. Diese spezifische Steifigkeit lässt sich im Prinzip aus den Arbeitslinien für Stahl (Fig. 2) und Beton (Fig. 3) berechnen.

Sie beträgt unter Berücksichtigung von

$$y'' = -\frac{M}{EI} \qquad (y = \text{Stützenausbiegung})$$

und $$y'' = \frac{1}{\rho} \qquad (\rho = \text{Krümmungsradius})$$

$$EJ = |M \cdot \rho|$$

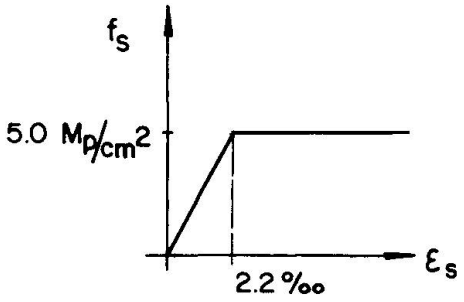

Fig. 2

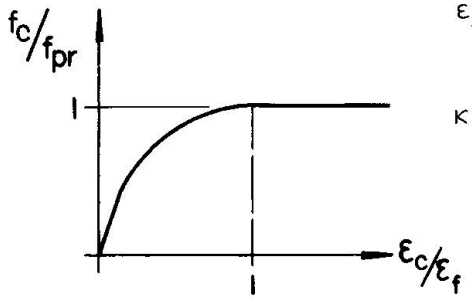

$$\varepsilon_f = \frac{2f_{pr}}{E_c}(1+\kappa\cdot\varphi)$$

$$\kappa = {}^{N}g/N \text{ bzw. } {}^{M}g/M$$

Fig. 3

In Fig. 4 ist das Verhältnis EI/E_cI_c als Funktion der Schnittkräfte N und M für den Querschnitt der Fig. 5 unter Vernachlässigung der Mitwirkung des Betons in der Zugzone aufgetragen.

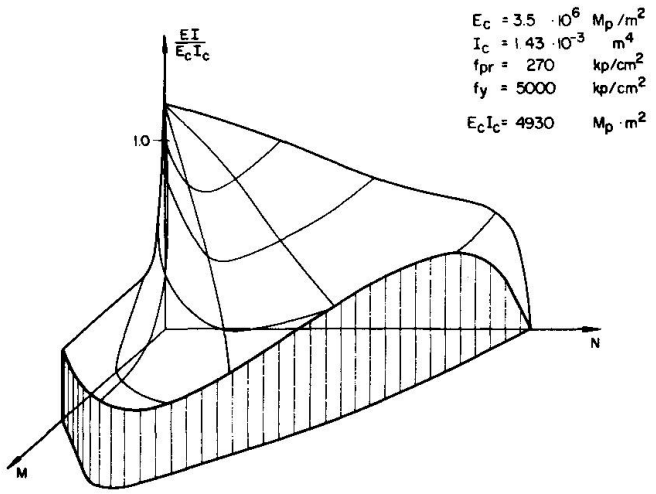

Fig.4 Steifigkeit - Schnittkräfte (N,M)

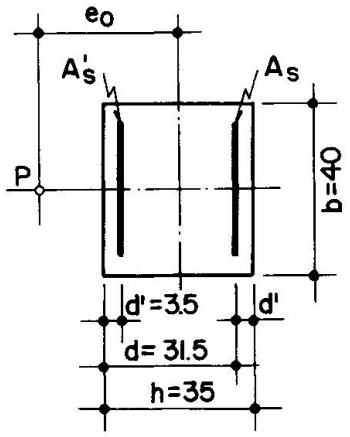

Fig.5 Querschnitt A_c = 35 x 40 cm

$A_s = A'_s = 12$ cm²

Diese relativ komplizierten Verhältnisse lassen sich zwar mit einem Computer-Programm beliebig genau berücksichtigen, eine praktische Berechnung auf dieser Grundlage ist jedoch unverhältnismässig aufwendig. Ein unterer Grenzwert der Traglast lässt sich allenfalls damit bestimmen, dass während der ganzen Laststeigerung (von $P = O$ bis $P = P_{Bruch}$) und auf der ganzen Stützenhöhe mit der Steifigkeit unmittelbar vor dem Erreichen der Bruchlast gerechnet wird. Die Schnittkräfte bei einer Stütze gemäss Fig. 1 sind dabei

$$N = P \qquad M = P \cdot e_o \frac{1}{1-\frac{P}{P_E}} \qquad (P_E = \frac{\pi^2 EI}{l_k^2})$$

Dieses Verfahren ist aber deshalb kompliziert, weil nur eine Iteration zum Ziel führt, oder weil zum mindesten nachgewiesen werden muss, dass die der Berechnung zugrunde gelegte Steifigkeit kleiner ist als die den Bruchschnittkräften N_u und M_u entsprechende Steifigkeit.

3. Moment-Krümmungsdiagramm

Aus einem Moment-Krümmungsdiagramm (h/ρ = bezogene Krümmung), in Fig. 6 für den Querschnitt der Fig. 5 dargestellt, lässt sich die Steifigkeit für bestimmte Kombinationen von N und M ebenfalls herauslesen; sie ist mit

$$EI = M \cdot \rho = \frac{1}{h} \cdot \alpha$$

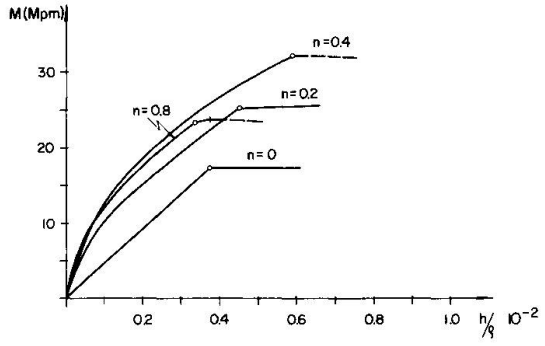

Fig.6 Moment - Krümmung; $A_s = A'_s = 12cm^2$ $(p_t = 1.71\%)$

Kurvenparameter: $n = \frac{N}{bhf_{pr}}$

Dabei ist α die Neigung der Verbindungslinie vom Ursprung ($M = h/\rho = O$) zu einem beliebigen Punkt (N, M) $N = nbhf_{pr}$. Die $M-h/\rho$ - Linien weisen einen deutlichen Knick auf, wenn bei einer bestimmten Normalkraft das Moment Stahlfliessen erzeugt. Diese Knickpunkte sind identisch mit dem Bruchwiderstand des Querschnitts, der bei einem schlanken Druckglied mit dem Stahlfliessen auf der Zug- oder Druckseite praktisch erreicht wird. Der effektive

Querschnittswiderstand ist zwar etwas grösser; es ist aber nicht zweckmässig dies zu berücksichtigen, da nach dem Fliessen des Stahls die Querschnittssteifigkeit rasch absinkt und die Momente zweiter Ordnung um so schneller zunehmen. Nach dem Fliessen des Stahls ist somit die mögliche Laststeigerung bis zum Erreichen des effektiven Bruchwiderstandes sehr klein.

4. Vereinfachung des $M-h/\rho$ - Diagramms

Im Hinblick auf eine einfache, zuverlässige Traglastberechnung werden die beiden folgenden Vereinfachungen gemacht:

- Die Neigung α bzw. die Steifigkeit EI bleibt von $M = 0$ bis zum Knickpunkt $M = M_u$ konstant; dies entspricht einem geradlinigen Verlauf der $M-h/\rho$ - Linie und bedeutet, dass bei konstantem Querschnitt auf der ganzen Stablänge mit der gleichen Steifigkeit gerechnet werden darf.

- Für jede Grösse der Normalkraft wird die Steifigkeit aus der $M-h/\rho$ - Linie für $N = N_F$ bestimmt. N_F ist dabei diejenige Normalkraft, die sich ergibt, wenn Zug- und Druckarmierung gleichzeitig fliessen. Dies bedeutet - zusammen mit der ersten Annahme -, dass die Vergrösserung der Anfangsexzentrizität e_o folgendermassen gerechnet werden darf:

$$e = e_o \frac{1}{1-\frac{P}{P_E}} \qquad P_E = \frac{\pi^2 EI_F}{l_k^2}$$

wobei EI_F die N_F entsprechende Steifigkeit ist; d.h. die Steifigkeit, bei der Zug- und Druckarmierung gleichzeitig fliessen. $EI_F = M_F \cdot \rho_F$ lässt sich besonders einfach bestimmen. Gemäss Fig. 7 gilt z.B. für einen Rechteckquerschnitt

$$M_F = C_c\left(\frac{h}{2} - a\right) + f_y(A_s + A_s')\left(\frac{h}{2} - d'\right)$$

$$\rho_F = \frac{h - 2d'}{2\varepsilon_y}$$

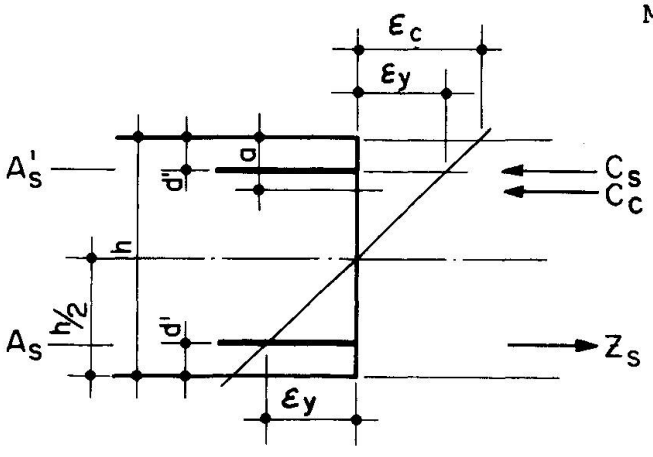

Fig. 7

Während die erstgenannte Vereinfachung bedeutet, dass während der ganzen Laststeigerung bis zum Bruch immer mit der gleichen Steifigkeit gerechnet werden darf, ist die zweite Vereinfachung aus folgenden Erwägungen sinnvoll:

- Bei kleiner Anfangsexzentrizität e_o und kleiner Schlankheit ist $N_u > N_F$; die effektive Steifigkeit ist dann grösser als EI_F; d.h. die berechnete Bruchlast ist auf der sicheren Seite. Erst bei sehr grosser Normalkraft nimmt EI wieder ab. Dann ist aber die Schlankheit so klein, dass nicht nach der Theorie zweiter Ordnung gerechnet werden muss.

- Bei grosser Anfangsexzentrizität und kleiner Schlankheit ist die Bruchlast unter Umständen kleiner als N_F . EI ist aber infolge starker Bewehrung (grosse Momente) nur unwesentlich kleiner als EI_F; zudem spielt in diesem Falle EI keine wesentliche Rolle; der Einfluss der Verformung zweiter Ordnung ist gering.

- Bei kleiner Anfangsexzentrizität und grosser Schlankheit ist die Bruchlast unter Umständen ebenfalls kleiner als N_F; wegen der starken Minimalbewehrung bei grosser Schlankheit ist aber $EI_F \sim EI_{N=O} = EI_{min}$.

- Bei grosser Anfangsexzentrizität und grosser Schlankheit ist die Bruchlast ebenfalls kleiner als N_F; auch in diesem Fall ist aber eine starke Bewehrung erforderlich, so dass $EI_F \sim EI_{N=O} = EI_{min}$ gilt.

5. Berechnungsgang

Für eine Stütze gemäss Fig. 1 mit gegebenen Querschnittswerten und Materialeigenschaften wird zunächst das N-M-Interaktionsdiagramm des Querschnittswiderstandes bestimmt, wobei immer das Fliessen des Stahls auf der Zug- oder auf der Druckseite massgebend ist. Die Berechnung der Steifigkeit $EI_F = M_F \rho_F$ erfolgt nach Abschnitt 4 für $\rho_F = \frac{h-2d'}{2\varepsilon_y}$ (kleinster Krümmungsradius). Damit folgt für die Ausbiegung nach der Theorie zweiter Ordnung:

$$e = e_o \frac{1}{1-\frac{P}{P_E}} \qquad P_E = \frac{\pi^2 EI_F}{l_k^2}$$

mit den massgebenden Schnittkräften

$$N = P \qquad \text{und} \quad M = P \cdot e$$

Die Traglast ist erreicht, wenn die Last-Momenten-Linie das N-M-Interaktionsdiagramm schneidet.

Bei zentrischer Belastung muss immer eine Anfangsexzentrizität $e_{min} \approx \frac{h}{30}$ angenommen werden.

Bei kleinen Anfangsexzentrizitäten $e_o \lesssim \frac{h}{5}$ ist es zur Erzielung einer besseren Genauigkeit zweckmässig, ein $M-{}^{h}/\rho$ - Diagramm gemäss Fig.8 anzunehmen. Mit steigendem Moment sinkt dabei die Steifigkeit linear auf den Wert EI_F ab.

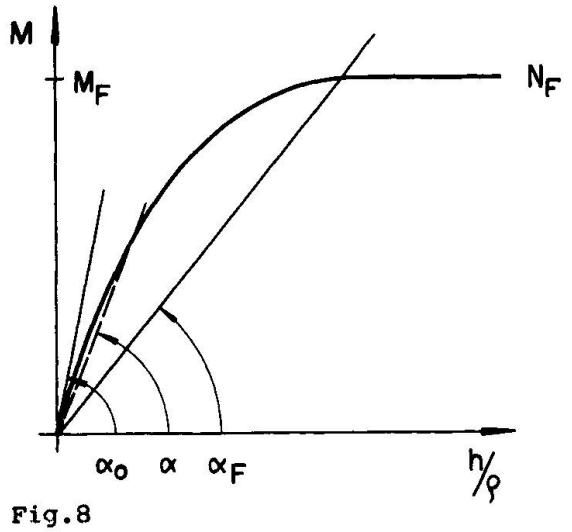

Fig.8

$$EI = M \cdot \rho = h \cdot tg\alpha$$

$$EI = h\left[tg\alpha_o - \frac{M}{M_F}(tg\alpha_o - tg\alpha_F)\right]$$

$$\text{Mit } tg\alpha_o = \frac{1}{h} EI_o$$

$$\text{und } tg\alpha_F = \frac{1}{h} EI_F \text{ wird}$$

$$EI = EI_o - \frac{M}{M_F}(EI_o - EI_F)$$

$$(EI_o = E_c I_c + E_s I_s)$$

In diesem Falle gilt

$$e = e_o \frac{1}{1 - \frac{P}{P_E}} \qquad \text{mit } P_E = \frac{\pi^2 EI}{i_k^2}$$

natürlich nur solange, als $M = P \cdot e$ kleiner ist als das für die Berechnung von EI angenommene Moment M.

Fig.9 zeigt einen Vergleich zwischen der Computer-Rechnung und der vorgeschlagenen Näherungsberechnung für eine Stütze gemäss Fig.1 mit folgenden Abmessungen und Materialwerten:

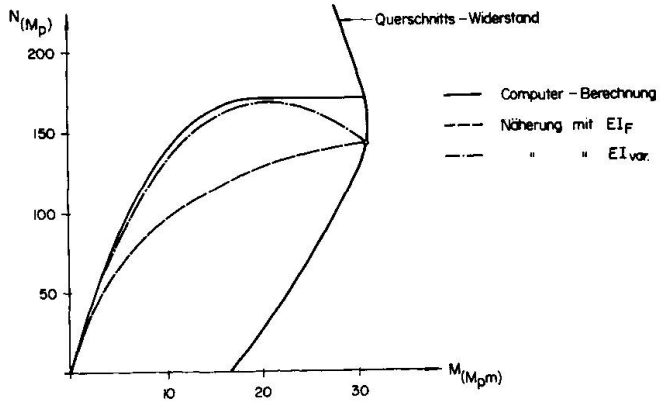

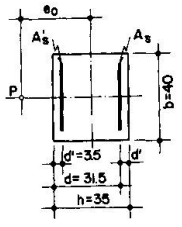

$f_{pr} = 270 \text{ kg/cm}^2$

$f_y = 5000 \text{ kg/cm}^2$

Fig.9 Last-Momenten - Kurve $l_k/h = 28.6$

$p_t = 1.71\%$ $(A_s = A'_s = 12 \text{ cm}^2)$ $e_o/h = 0.143$

6. Traglasten der Standardstütze, die dem Fragebogen zum Vergleich verschiedener Normen zugrunde gelegt wurde

Die Fig. 10 - 12 zeigen einen Vergleich der Traglasten, die einerseits mit dem Computer und anderseits mit dem vorgeschlagenen Näherungsverfahren berechnet wurden. Dabei handelt es sich um jenen Stützentyp, der dem Fragebogen zum Vergleich verschiedener Normen zugrunde gelegt wurde* In der Fig. 13 ist die Streuung aller für diesen Stützentyp berechneten Fälle dargestellt.

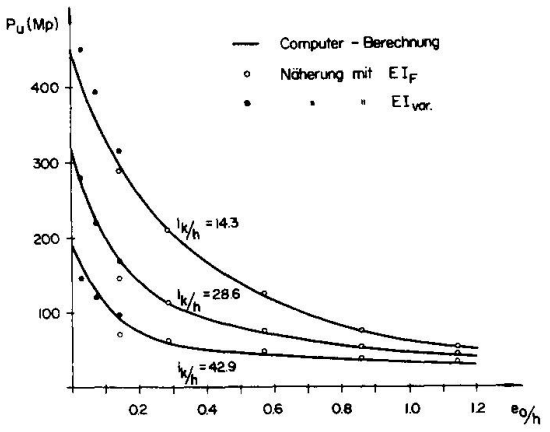

Fig.10 Traglast-Exzentrizität

$A_s = A'_s = 12cm^2$ ($p_t = 1.71\%$)

Kurvenparameter:
Schlankheit $l_{k/h}$

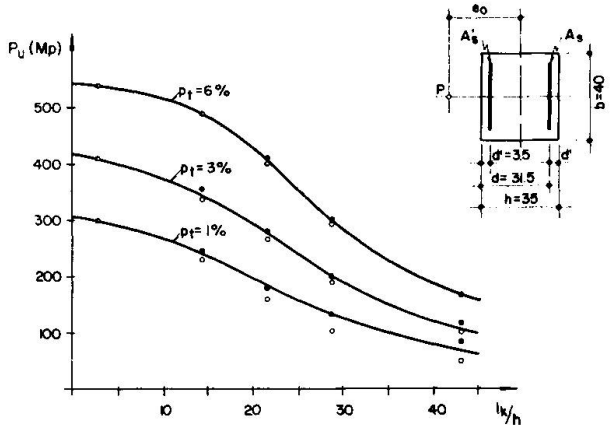

Fig.11 Traglast-Schlankheit

Exzentrizität $e_o = \frac{h}{6} = 5.8$ cm

Kurvenparameter:
Bewehrung p_t ($A_s = A'_s$)

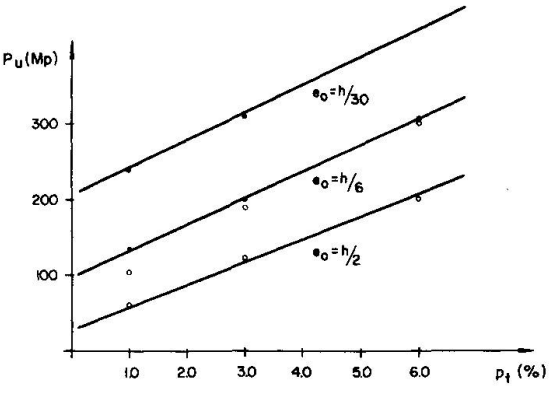

Fig.12 Traglast-Bewehrung

Schlankheit $l_{k/h} = 28.6$

Kurvenparameter:
Exzentrizität e_o

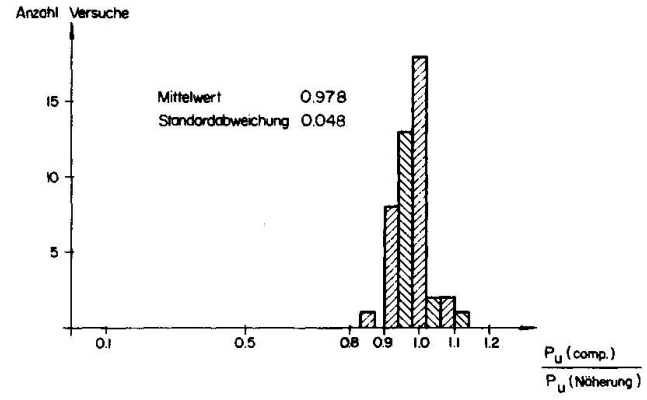

Fig.13 Vergleich der exakten Lösung ($P_{u\ comp}$) mit der Näherungslösung ($P_{u\ Näherung}$)

*vergl. Vorbericht Québec 1974
"Stützen aus Stahlbeton, Vergleich verschiedener Normen"

Bezeichnungen

A_s = Fläche der Zugarmierung
A'_s = Fläche der Druckarmierung
E_s = Elastizitätsmodul des Stahls = 2100 Mp/cm²
J_s = Trägheitsmoment des Stahlquerschnitts
f_s = Stahlspannung
f_y = Fliess-Spannung des Stahls
ε_s = Stahldehnung
ε_y = Fliess-Dehnung des Stahls
A_c = Betonfläche
E_c = Elastizitätsmodul des Betons
J_c = Trägheitsmoment des homogenen Betonquerschnitts
f_c = Betonspannungen
f_{pr} = Prismenfestigkeit des Betons
ε_c = Betonstauchung
ε_u = maximale Betonstauchung = 0.003
φ = Kriechzahl
N_g, M_g = Beanspruchung infolge Dauerlasten
p_t = Armierungsgehalt ($^{\text{Stahlfläche}}/_{\text{Betonfläche}}$)

144

$$EI_F = M_F \cdot \rho_F .$$

ZUSAMMENFASSUNG

Das vorgeschlagene Verfahren für eine einfache Berechnung der Traglast von Stützen beruht darauf, dass die Ausbiegung zweiter Ordnung mit einer konstanten, ideellen Steifigkeit berechnet wird. Diese Steifigkeit wird am gerissenen Querschnitt bestimmt, wobei angenommen wird, dass die Bewehrung auf der Zug- und Druckseite gleichzeitig fliesst.

SUMMARY

The proposed method for a simple calculation of the ultimate load of columns is based on calculating the 2nd-order deflection with a constant virtual stiffness. This stiffness is determined from the fractured cross-section, assuming that the reinforcement on the tension and compression sides flows simultaneously.

RESUME

On propose, pour le calcul de la charge ultime des colonnes, un procédé basé sur un calcul de déformation du second ordre avec une rigidité fictive constante. Cette rigidité est déterminée pour la section fissurée en admettant que les armatures dans les zones tendues et comprimées travaillent à la limite apparente d'élasticité.

Ein halbgraphisches Verfahren zur Bemessung von beliebig belasteten Stahlbetondruckstäben

A Semi-Graphical Procedure for the Design of Arbitrarily Loaded Reinforced Concrete Struts

Une méthode semi-graphique permettant le dimensionnement des barres en béton armé comprimées sous l'effet d'une charge quelconque

L. SPAROWITZ
Dipl. Ing.
Institut für Stahlbeton- und Massivbau
Technische Hochschule Graz
Graz, Oesterreich

1. MOEGLICHKEITEN DER DARSTELLUNG DES MOMENTEN-NORMALKRAFT-KRUEMMUNGS-ZUSAMMENHANGES EINES STAHLBETONQUERSCHNITTES

1.1 Die Ermittlung des M-N-K-Zusammenhanges mit Hilfe nomographischer Diagramme

Durch Trennung der Tragwirkung von Stahl und Beton in die vier Teilgrössen

$\bar{N}_c = N_c/\beta_c bh$ (Anteil des Betons a.d. bezogenen inneren Normalkraft)

$\bar{M}_c = M_c/\beta_c bh^2$ (Anteil des Betons am bezogenen inneren Biegemoment)

$\bar{N}_s = N_s/\beta_c bh$ (Anteil des Stahls a.d. bezogenen inneren Normalkraft)

$\bar{M}_s = M_s/\beta_c bh^2$ (Anteil des Stahls am bezogenen inneren Biegemoment)

gelingt eine graphische Darstellung des M-N-K-Zusammenhanges als Funktion der beiden Veränderlichen ε_1 und $\bar{K}=K\cdot h$. Das Bild 1 stellt den Verlauf der inneren Schnittlastenanteile für einen symmetrisch bewehrten Rechteckquerschnitt ($h'/h=0.1$) und die σ-ε-Diagramme nach Bild 2 (Linien a) dar.

Die beiden linken Kurvenscharen (Bild 1a) zeigen die inneren Normalkraftanteile, die beiden rechten (Bild 1b) die inneren Momentenanteile, die oberen Kurvenscharen enthalten jeweils die Betonanteile, die beiden unteren die durch den bezogenen Bewehrungsgrad

$$\bar{\mu} = \frac{A_s+A_s'}{2A_c}\quad\frac{\beta_{300}}{\beta_c} \qquad (1)$$

geteilten Stahlanteile an den inneren Schnittgrössen. Die Multiplikation der Ordinaten der unteren Kurvenscharen mit dem bezogenen Bewehrungsgrad (1) erfolgt mit Hilfe projektiver nomographischer Leitern (L1, L2, L3). Die beiden Teilschnittgrössen werden mit parallelen linearen Nomogrammleitern (L2, L4, L5) addiert. Für vorgegebene Werte $\bar{K}$ und ε_1 lassen sich die bezogenen Schnittlasten $\bar{N}_r=\bar{N}_c+\bar{N}_s$ und $\bar{M}_r=\bar{M}_c+\bar{M}_s$ nach Bild 1 (strichlierte Geraden) bestimmen. Will man Mo-

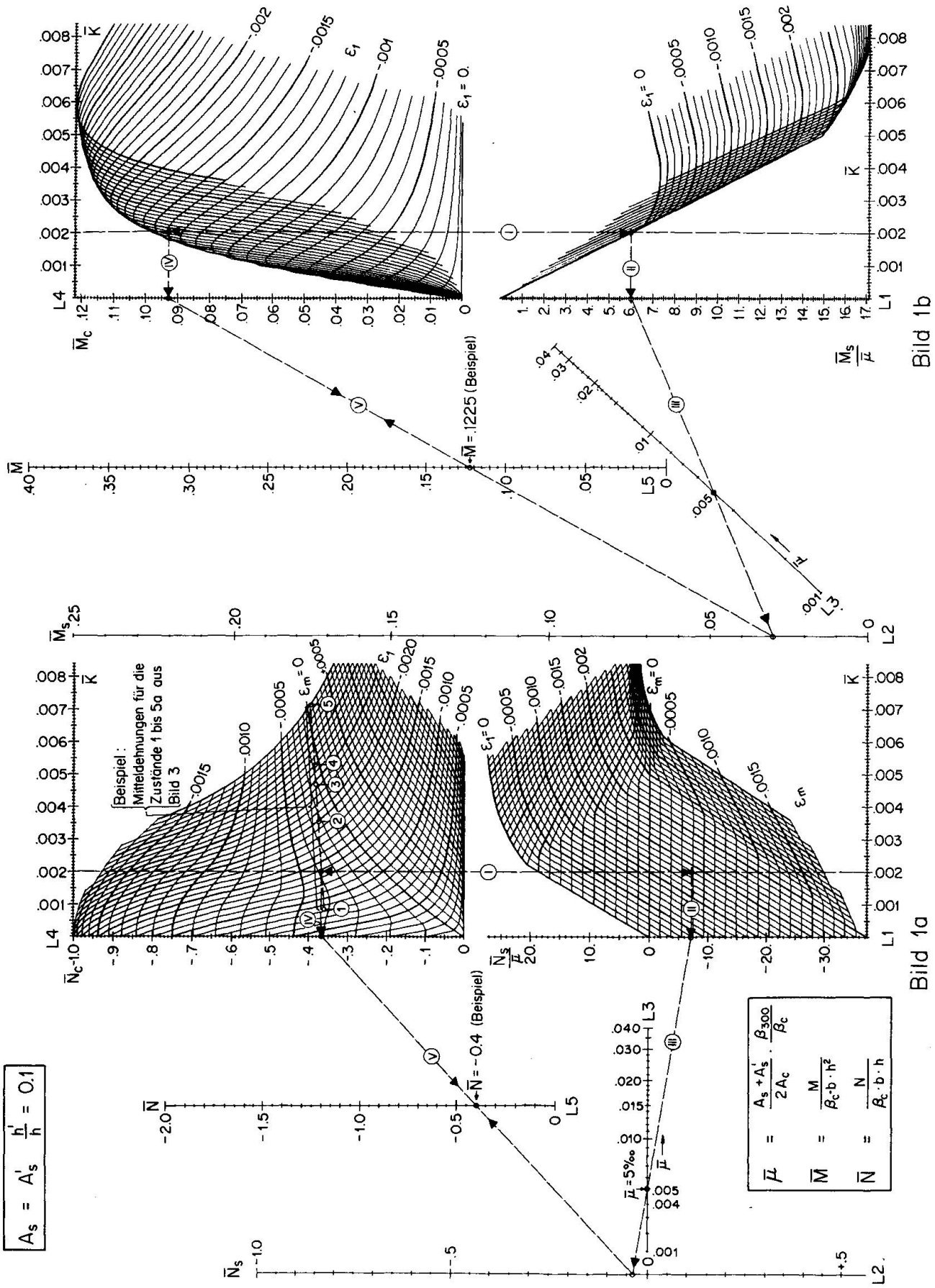

Bild 1 : Nomographisches Krümmungsdiagramm

mentenkrümmungslinien zeichnen, so ist neben $\bar{K}$ die Normalkraft $\bar{N}_r$ vorgegeben und $\bar{M}_r$ gesucht. Dann muss ε_1 im Bild 1a variiert werden, bis die Gerade Ⓥ die $\bar{N}$-Leiter im vorgegebenen Wert $\bar{N}_r$ schneidet. Eine weitere Kurvenschar mit der Mitteldehnung ε_m als Parameter erleichtert diesen Vorgang. Erhält man beim ersten Versuch $\bar{N}_r$ zu klein, so ist für den nächsten ε_1 bzw. ε_m grösser zu wählen. Wenn ε_1 gefunden ist, kann das zugehörige bezogene Moment für ε_1 und $\bar{K}$ dem Bild 1b entnommen werden.

Das Diagramm gilt für beliebige Betongüten und Bewehrungsgrade. Es lassen sich entsprechende Kurventafeln für alle praktisch üblichen Querschnittsformen, Stahlüberdeckungen, Stahlsorten und Bewehrungsverhältnisse A'_s/A_s erstellen. Der Einfluss der Zugtragwirkung des Betons könnte näherungsweise in den oberen Kurvenscharen erfasst werden. Eine Berücksichtigung von Kriechverformungen ist im Abschnitt 4 beschrieben.

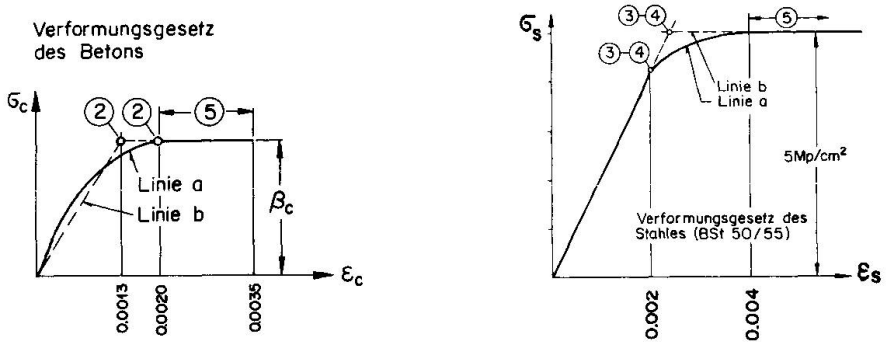

Bild 2

1.2 Die polygonale Darstellung des M-N-K-Zusammenhanges

Mit nomographischen Diagrammen nach Bild 1 kann man den Berechnungsgrundlagen entsprechend genaue Kurvenverläufe zeichnen. Meistens liefert eine polygonale Annäherung der M-N-K-Kurven bereits genügend genaue Ergebnisse.

Jede M-K-Linie enthält Punkte, die einen Uebergang zwischen Kurvenästen mit verschiedener Verformungscharakteristik darstellen (Bilder 2 und 4). Solche Uebergangszustände sind:

① Betonzugzone beginnt zu versagen
② Betondruckzone beginnt zu fliessen
③ Stahldruckbewehrung beginnt zu plastifizieren
④ Stahlzugbewehrung beginnt zu plastifizieren

Der Endpunkt ⑤ der M-K-Kurve wird normalerweise durch die Grenzdehnung des Betons (5a) festgelegt. Ist auch eine Stahlgrenzdehnung vorgeschrieben, so kann diese bei geringer Normalkraftbeanspruchung den Punkt ⑤ bestimmen (5b).

Für jeden der Zustände ① bis ⑤ lassen sich in Abhängigkeit vom bezogenen Bewehrungsgrad M-K-N-Interaktionsdiagramme konstruieren, die im Bild 3 zusammengefasst dargestellt sind. Aus diesem erhält man für vorgegebene Werte $\bar{N}$ und μ die Grössen $\bar{M}$ und $\bar{K}$ (Beispiel Bild 3: strichlierte Geraden) aller jener Zustände ① bis ⑤, die im betrachteten M-K-Zusammenhang vorkommen (Bild 4). Verbindet man diese Punkte durch Gerade, so erhält man eine sehnenpolygonale Annähe-

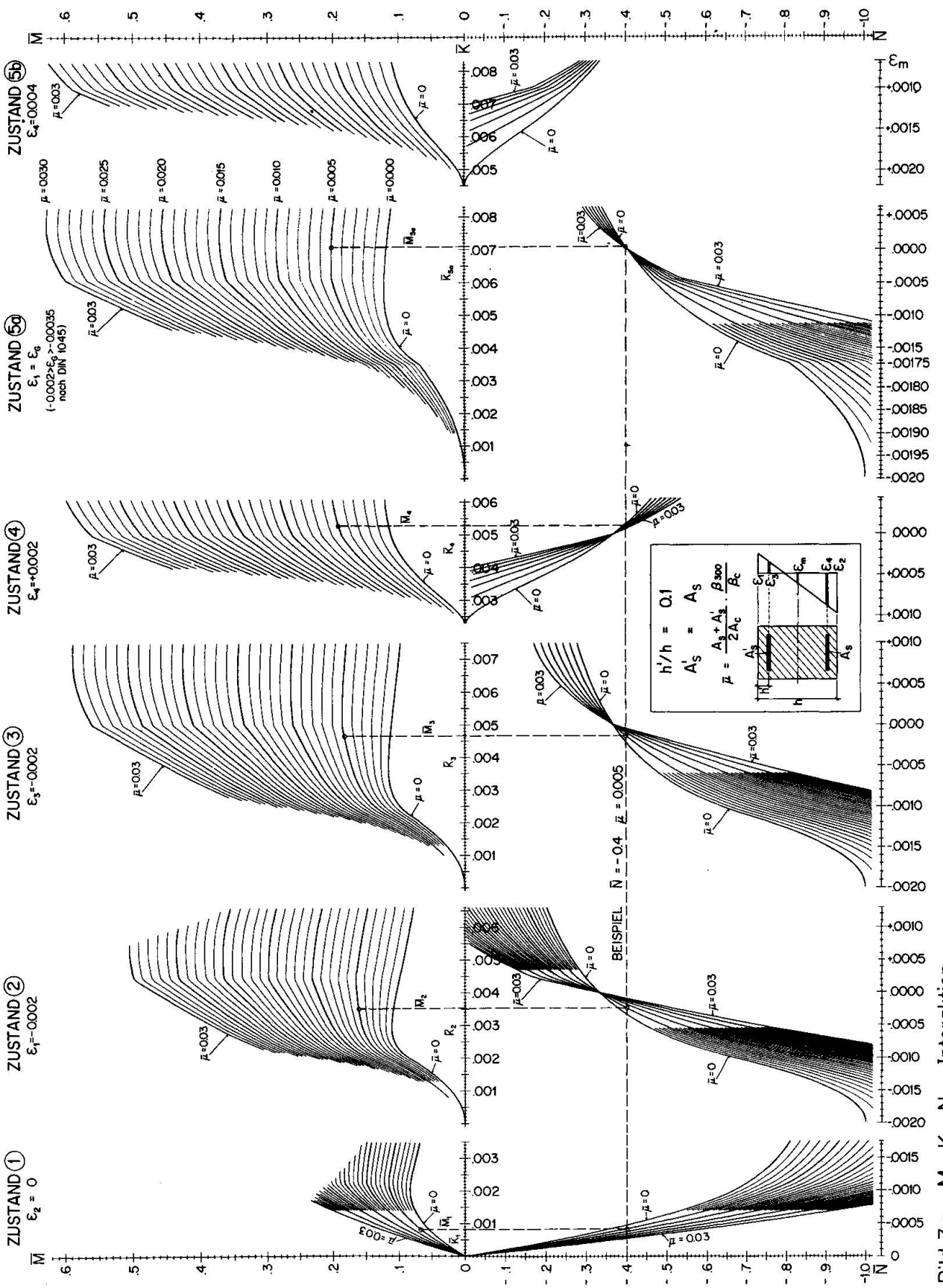

Bild 3: M – K – N – Interaktion

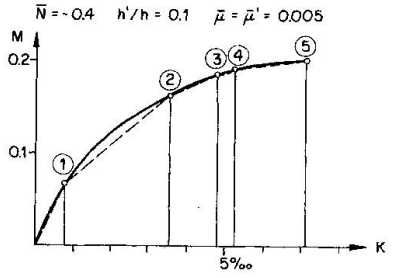

Bild 4

rung des Momenten-Krümmungs-Zusammenhanges. Wählt man anstelle der gekrümmten σ-ε-Diagramme (Bild 2, Linien a) bi-lineare (Linien b) als Berechnungsgrundlage, so besteht eine noch bessere Uebereinstimmung zwischen dem genauen Kurvenverlauf und der polygonalen Annäherung.

Dem Bild 3 können auch die Mitteldehnungen $\varepsilon_m = f(\bar{K})$ entnommen werden. Wenn man diese im Bild 1a einträgt und miteinander verbindet, erhält man sehr gute Ausgangswerte ε_1 zur Bestimmung weiterer Zwischenpunkte.

Quast [1] nähert die M-N-K-Beziehung durch eine Ersatzgerade an.

2. ZUR BEMESSUNG VON STAHLBETONDRUCKSTAEBEN

2.1 Die allgemein gültige halbgraphische Bemessung

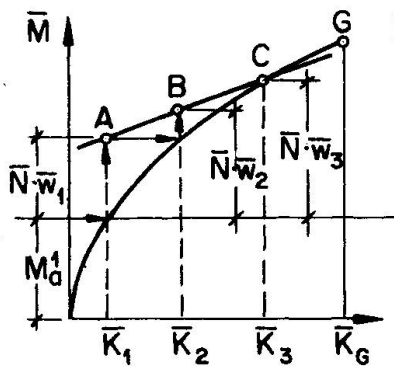

Bild 5

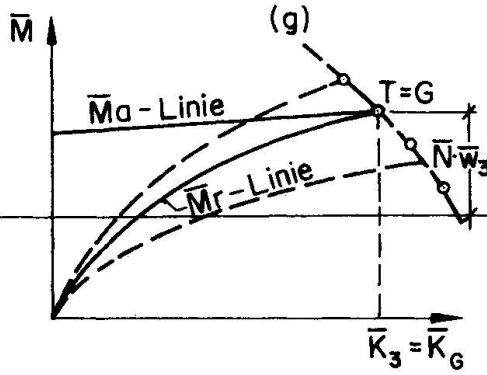

Bild 6

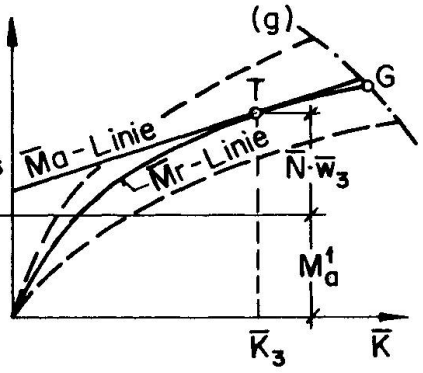

Bild 7

Man kann die Linie der äusseren Momente im massgebenden Querschnitt mit genügender Genauigkeit wie folgt ansetzen:

$$\bar{M}_a = \bar{M}_a^1 + \bar{N}\cdot\bar{w} = C_1\cdot\bar{N}\cdot\bar{\ell}^2\cdot\bar{K} + C_2\cdot\bar{N}\cdot\bar{\ell}^2 = \bar{C}_1\cdot\bar{K} + \bar{C}_2 \qquad (\bar{\ell} = \ell/h) \qquad (2)$$

Die Werte C_1 und C_2 sind von der Krümmungsverteilung in Stablängsrichtung abhängig, die normalerweise nur geringfügig mit der Grösse von $\bar{K}$ veränderlich ist. $\bar{M}_a$ kann somit näherungsweise als lineare Funktion von $\bar{K}$ angesehen werden; die Linie der inneren Momente ist nach Abschnitt 1 bestimmbar. Wenn der Querschnitt und/oder Bewehrungsgrad in Stablängsrichtung veränderlich ist, müssen mehrere M-K-Linien gezeichnet werden. Für die aktiven Momente $\bar{M}_a = \bar{M}_a^1$ erhält man mit $\bar{w}'' = \bar{K}(\bar{M}_a)$ die Stabausbiegung $\bar{w}_1$, die den Punkt A bestimmt und für $\bar{M}_a = \bar{M}_a^1 + \bar{N}\cdot w_1$ die Auslenkung w_2, durch die der Punkt B und damit die $\bar{M}_a$-Gerade festgelegt ist (Bild 5). Durch Zeichnen von auf max. w=1 reduzierten Biegelinien lässt sich die Biegelinienform kontrollieren. Bestehen zwischen den beiden reduzierten Biegelinien A und B grosse Unterschiede, so kann die Lage der M_a-Geraden durch eine

weitere Biegelinienberechnung für $\bar{M}_a=\bar{M}_a^1+\bar{N}\cdot\bar{w}_3$ korrigiert werden. Die Rechnung wird schematisiert in Tabellenform durchgeführt. Schneidet die M_a-Gerade die M_r-Linie bei $\bar{K}_3<\bar{K}_G$, so kann der Beton- und/oder Stahlquerschnitt verringert werden, bis entweder das Stabilitätskriterium $d\bar{M}_a/d\bar{K}=d\bar{M}_r/d\bar{K}$ erfüllt ist oder die M_a-Gerade die M_r-Linie im Punkt G (Grenzdehnungszustand) schneidet. Da sich die Biegelinienform bei geringfügigem Variieren der Querschnitte kaum ändert, kann die Lage der M_a-Geraden näherungsweise beibehalten werden.

Die Wahl des erforderlichen Beton- und/oder Stahlquerschnittes lässt sich durch Zeichnen der Grenzlinie g (Bilder 6 und 7) vereinfachen, die man bei Variation des Bewehrungsgrades aus Interaktionsdiagrammen für den Grenzdehnungszustand entnehmen kann (Bild 3). Die Grenzlinie schneidet die $\bar{M}_a$-Gerade bei einem bestimmten Bewehrungsgrad im Punkt G. Die Interaktionsdiagramme können als weitere Kurvenschar den Anstieg der M_r-Kurve im Grenzdehnungszustand enthalten. Ist er grösser als der Anstieg der M_a-Geraden, so hat man es mit einem Spannungsfall 2. Ordnung zu tun (Bild 6). Andernfalls kann z.B. der Bewehrungsgrad weiter abgemindert werden, bis die M_r-Linie die M_a-Gerade tangiert. Je kleiner man die Grenzdehnungen festsetzt, desto seltener tritt der Instabilitätsfall (Bild 7) auf.

2.2 Die Bemessung bei Vereinfachung der Verformungsberechnung

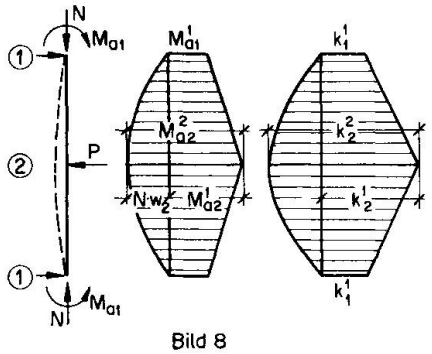

Bild 8

Besonders einfach wird das Verfahren, wenn man die Form des Krümmungsverlaufes in Stablängsrichtung vorgeben kann, da man in diesem Fall die $\bar{M}_a$-Gerade ohne Biegelinienberechnung erhält [2].

Eine gute Näherung erreicht man, wenn man den Krümmungsverlauf infolge der Biegemomente nach Theorie 1. Ordnung affin zu diesen und den Krümmungszuwachs infolge der Stabverformungen parabelförmig verteilt annimmt [1,3]. Für das im Bild 8 dargestellte Beispiel erhält man die Grössen C_1 und C_2 in (2) zu:

$$C_1=5/48 \qquad C_2=(2\bar{K}_1^1-\bar{K}_2^1)/48$$

3. EINE NAEHERUNGSWEISE ERFASSUNG DER KRIECHEINFLUESSE

Der Traglastabfall infolge Kriechen wächst mit der Stabschlankheit und mit abnehmender Lastexzentrizität und/oder Bewehrung. Ausser in Extremfällen erreicht man, beim üblichen Verhältnis der Gebrauchsspannungen (unter Dauerlast) zu den Grenzspannungen, mit folgenden Vereinfachungen brauchbare Ergebnisse:

Während des Kriechvorganges werden die kriecherzeugenden Spannungen zeitlich konstant angenommen,und die Auswirkungen der Nullinienverschiebung auf die Kriechumlagerung bleibt unberücksichtigt. Die Kriechdehnungen ε_ϕ (Bild 9) und damit die Langzeit-Betonanteile an den reaktiven Schnittlasten ergeben sich dadurch zu:

$$\varepsilon_\phi = \varepsilon_{1L} \cdot \frac{\phi}{1+\phi} \qquad {}^{t}N_c = \bar{N}_c \cdot \frac{1}{1+\phi} \qquad {}^{t}\bar{M}_c = \bar{M}_c \cdot \frac{1}{1+\phi} \qquad (3)$$

Diagramme entsprechend Abschnitt 1.1 (für lineares Verformungsverhalten des Betons), in denen die Kurzzeit-Betonanteile nach (3) mittels projektiver Leitern um den Faktor $1/(1+\phi)$ reduziert werden, ermöglichen die Darstellung von Langzeit-M-N-K-Linien (Bild 10, Linie a). Bei der Ermittlung der abschliessenden Kurzzeit-M-N-K-Linie b werden die Werte ε_1 und $\bar{K}$ in den oberen Kurvenscharen des Bildes 1 (Betonanteile) um die für den Schnittpunkt L (Bild 10) geltenden Grössen ε_ϕ und α (Bild 9) verringert. Dadurch wird die Spannungsumlagerung vom Beton auf die Bewehrung näherungsweise erfasst.

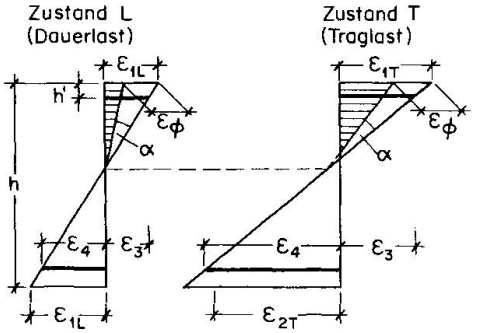

Bild 9

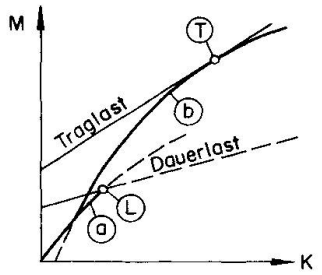

Bild 10

Wenn man an Stelle von ϕ in (3) die Grösse $\rho \cdot \phi$ einführt, kann man die Genauigkeit steigern. ρ berücksichtigt die zeitliche Aenderung der kriecherzeugenden Betonspannungen in Abhängigkeit von der Lastexzentrizität, dem Bewehrungsgrad, der Stabschlankheit und der Grösse der Dauerlast.

Bezeichnungen

Der Querstrich über den Bezeichnungen bedeutet, dass es sich um eine dimensionslose Grösse handelt. Der Kopfzeiger 1 (bzw. 2) bedeutet Theorie 1. (bzw. 2.) Ordnung.

M_a	aktives (äusseres) Moment
M_r	reaktives (inneres) Moment $\bar{M}_r = M_r/(\beta_c b h^2)$
N_a	aktive (äussere) Normalkraft
N_r	reaktive (innere) Normalkraft $\bar{N}_r = N_r/(\beta_c b h)$
M_c	Betonanteil am reaktiven Biegemoment
N_c	Betonanteil an der reaktiven Normalkraft
M_s	Stahlanteil am reaktiven Biegemoment
N_s	Stahlanteil an der reaktiven Normalkraft
β_c	rechnungsmässige Prismenfestigkeit des Betons
β_{300}	Bezugsgrösse: rechnungsmässige Prismenfestigkeit eines Betons, dessen mittlere 28 Tage Würfelfestigkeit 300 kp/cm² beträgt (β_{300} = 225 kp/cm²)
b	Querschnittsbreite
h	Querschnittshöhe
h'	Randabstand der Bewehrung
μ	Bewehrungsgrad $\bar{\mu} = \mu \cdot \frac{\beta_{300}}{\beta_c}$

ε_1 gesamte Dehnung am Druckrand
ε_2 gesamte Dehnung am Zugrand
ε_3 Dehnung der Druckbewehrung
ε_4 Dehnung der Zugbewehrung
ε_ϕ Kriechstauchung am Druckrand
A_s Querschnittsfläche der Zugbewehrung $A_s = \mu \cdot A_c$
A'_s Querschnittsfläche der Druckbewehrung $A'_s = \mu' \cdot A_c$
A_c Betonquerschnittsfläche
K Krümmung $\bar{K} = K \cdot h$
ℓ Stablänge $\bar{\ell} = \ell / h$
w Stabausbiegungen $\bar{w} = w/h$
ϕ Kriechzahl

Literaturverzeichnis

[1] Kordina K., Quast U.
Bemessung von schlanken Bauteilen - Knicksicherheitsnachweis. Betonkalender 1974 (1. Teil).

[2] Kupfer H., Bemessungsverfahren für knickgefährdete Stahlbetonstützen (unveröffentlichte Arbeit), 1965.

[3] Aas-Jakobsen A., "Rapport préliminaire à la session plénière de Lausanne - 1968".

ZUSAMMENFASSUNG

Das komplexe Problem der Bemessung beliebig belasteter Stahlbetondruckstäbe lässt sich graphisch anschaulich darstellen, indem man das Trag- und Verformungsverhalten des gesamten Stabes auf eine Betrachtung des Momenten-Normalkraft-Krümmungs-Zusammenhanges im "massgebenden Querschnitt" reduziert. Es werden Diagramme zur Ermittlung der M-N-K-Linien beschrieben, die auch die näherungsweise Berücksichtigung des Betonkriechens gestatten.

SUMMARY

The rather difficult design of arbitrarly loaded reinforced concrete compression members can be done graphically if the load carrying capacity and the deformation behavior of the compression member can be represented by the moment-load-curvature-behavior of a specified cross-section. Diagrams for the computation of the M-N-K-relations are given. An approximative consideration of the concrete creep is possible.

RESUME

Le problème complexe du dimensionnement des pièces comprimées en béton armé sous l'effet d'une charge quelconque peut être traité graphiquement de façon claire en remplaçant le comportement charge-déformation de l'ensemble de la colonne par l'étude du rapport moment de flexion (M) - effort normal (N) - courbure (K) dans la "section déterminante". On présente, pour la construction des courbures M-N-K, des diagrammes qui permettent également de tenir compte approximativement du fluage du béton.

II

Simplified Calculation Method for Flexural and Shear Strength and Deformation of Reinforced Concrete Columns under Constant Axial Loads

Une méthode de calcul simplifié de la résistance et de la déformation à la flexion et au cisaillement des colonnes en béton armé soumises à une charge axiale constante

Vereinfachte Methode für die Berechnung der Biege- und Schubfestigkeit sowie der Verformung von Stahlbetonstützen unter konstanter Normalkraft

Minoru YAMADA Prof. Dr.-Ing.
Hiroshi KAWAMURA Ass. Dipl.-Ing.
Kobe University
Kobe, Japan

1. INTRODUCTION

The importance of the shear resistance and shear deformation of reinforced concrete restrained short columns for the aseismic design of reinforced concrete structures was already discussed and emphasized by the author [1].

In order to establish a design method of reinforced concrete columns which play an important role as one of earthquake-resisting elements [5], it is necessary to develope a simplified calculation method for the lateral sway behaviors of them under the combined action of bending moment, shear force and constant axial load. In this paper, a simplified calculation method, which is based on the superposition of flexural and shear deformations of reinforced concrete columns(see Fig.1), is presented and verified by experimental results.

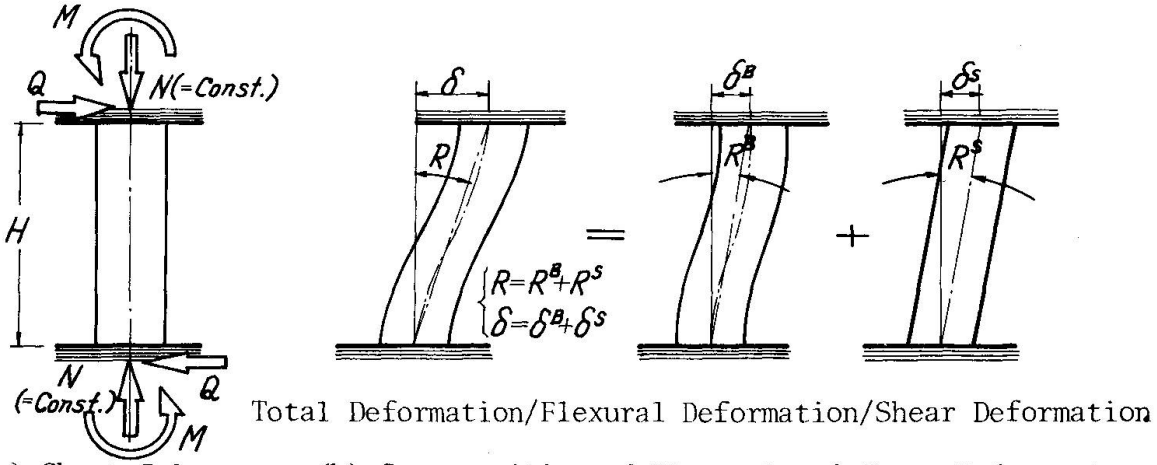

Total Deformation/Flexural Deformation/Shear Deformation

(a) Short Column (b) Superposition of Flexural and Shear Deformation under Combined Forces

Fig.1 Short Column with Double Curvature

2. FLEXURAL STRENGTH AND DEFORMATION

2-1. Assumptions

In order to calculate the flexural component of the strength and deformation of reinforced concrete columns under the combined action of bending moment, shear force and constant axial load, the "CRITICAL STRAIN POINT METHOD" of the authors [2,3] was applied, which is based on the following assumptions and idealizations.

(1) A reinforced concrete cross section may be assumed to be composed of three lumped points of concrete and two of longitudinal reinforcing steel such as shown in Fig.2(a).

(2) The strain and stress of this section are defined only on the position of these points such as shown in Fig.2(b)(c), where the strain distribution is remained linear after bending.

(3) The normal stress-strain relationships of concrete and reinforcing steel are assumed as shown in Fig.3(a)(b). As for concrete, B, Y' and B' show the points of tensile fracture, compressive yielding and compressive fracture, respectively. Y and Y' in the stress-strain relationship of reinforcing steel show tensile and compressive yielding points.

The concept of "CRITICAL STRAIN POINT" is illustrated on the two-dimensional plane such as shown in Fig.4. The simbols C and S in this figure correspond to the concrete and reinforcing steel on the tension side, and the dash (') and the suffix (n) show the ones at the compressive and the centroidal positions. The meaning of B,B',Y and Y' is already explained in Fig.3(a)(b).

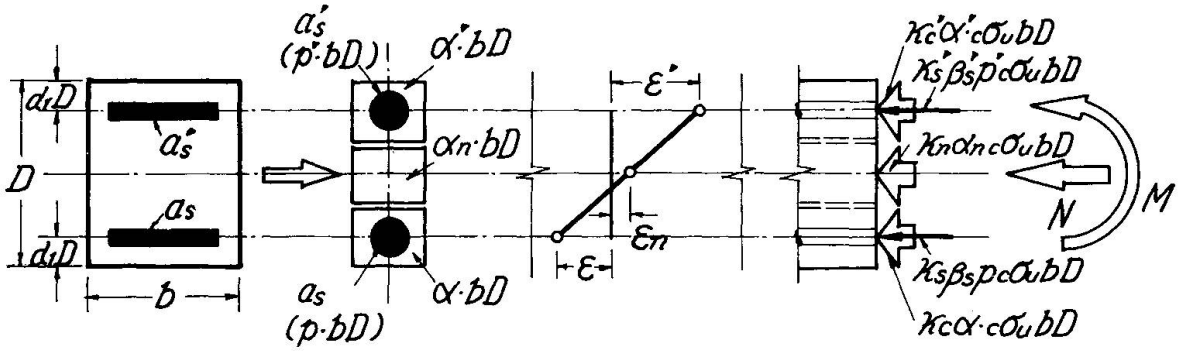

(a) Idealized Cross Section (b) Strain Distribution (c) Stress Distribution

Fig.2 Cross Section, Strain and Stress

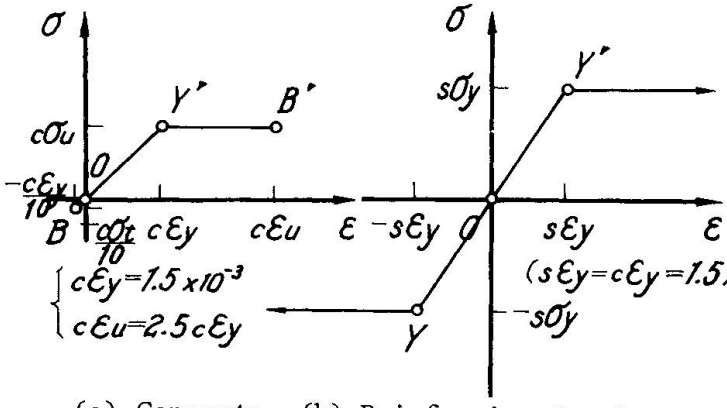

(a) Concrete (b) Reinforcing Steel

Fig.3 Stress - Strain Relationships

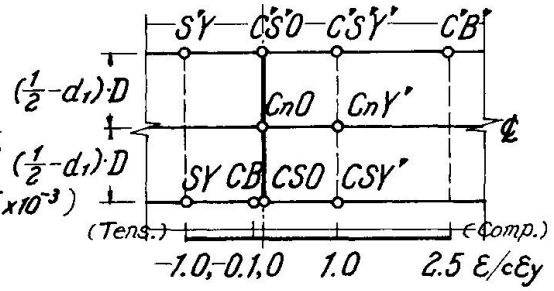

Fig.4 Critical Strain Points

2-2. Bending Moment - Axial Force - Curvature Relationships

From the stress and strain distributions of an idealized reinforced concrete cross section and the stress-strain relationships of concrete and reinforcing steel, the bending moment (m), axial force (n) and curvature (ϕ) are expressed by the following equations:

$$m = M/(1/2-d_1)_c\sigma_u bD^2 = \kappa_c'\alpha' - \kappa_c\alpha + \kappa_s'\beta_s'p' - \kappa_s\beta_s p \ , \qquad (1)$$

$$n = N/_c\sigma_u bD = \kappa_c'\alpha' + \kappa_{cn}\alpha_n + \kappa_c\alpha + \kappa_s'\beta_s'p' + \kappa_s\beta_s p \ , \qquad (2)$$

$$\phi = \Phi/(1-2d_1)D_c\varepsilon_y = \varepsilon'/_c\varepsilon_y - \varepsilon/_c\varepsilon_y \ , \qquad (3)$$

where κ is the stress level ratio of existing stress to yielding stress, $\beta_s p$(= $\beta_s'p' = {}_s\sigma_y/{}_c\sigma_u \cdot a_s/bD$) is the reinforcement index, and dash ('), suffixes (n),(s), (c) indicate the same such as mentioned above.

When a linear strain distribution rotates, passing through a certain "CRITICAL STRAIN POINT" as the rotation center, m, n, and ϕ are able to be calculated easily and illustrated in the three-dimentional space with the Cartesian coordinates corresponding to m, n and ϕ.

As an example, Fig.5 shows the m-n-ϕ relationships of reinforced concrete cross section in which the names of lines represent those of the "CRITICAL STRAIN POINT". The dotted lines CB shows the occurrence of tensile cracking of the tensile concrete point, which is computed under the condition of the existence of the tensile resistance of concrete. When axial load is constant, bending moment (m) - curvature (ϕ) relationship is able to be easily illustrated such as shown in Fig.6.

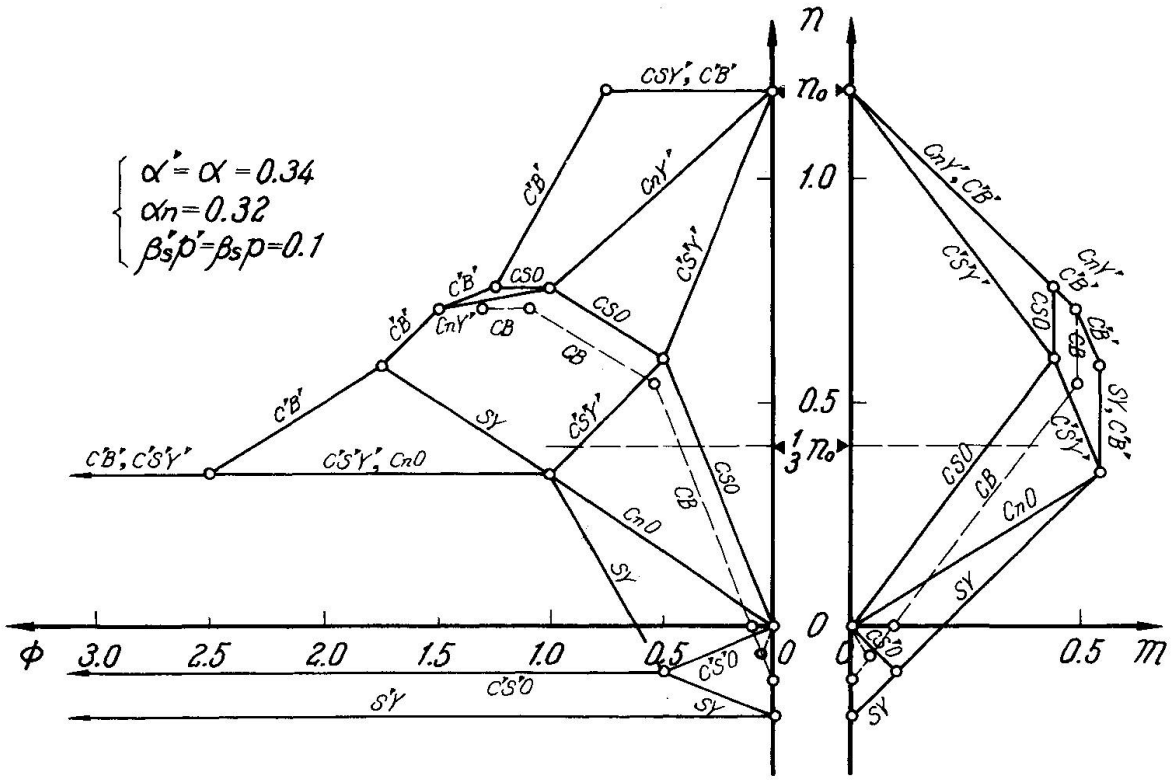

Fig.5 Bending Moment(m) - Axial Force(n) - Curvature(ϕ) Relationships

As an example, it is shown in Fig.6 under the condition of the axial load level ratio (X=1/3) which indicates the ratio of constant axial load (N) to the maximum axial strength (N_0) of columns. The "CRITICAL STRAIN POINTS" in this figure shows the points through which a linear strain distribution passes.

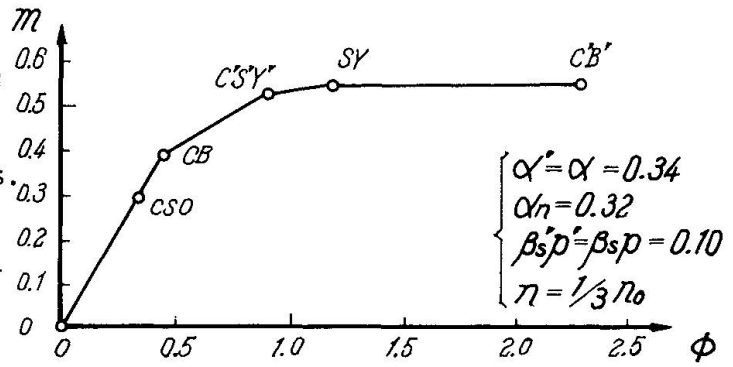

Fig.6 Bending Moment(m) - Curvature(ϕ) Relationship

2-3. Shear Force - Flexural Lateral Displacement Angle Relationships

When a moment - curvature relationship of a reinforced concrete cross section is given, and if the P-δ effect is able to be neglected in the case of relatively short columns, a shear force (Q)- flexural lateral displacement angle (R^B) relationship may be calculated by integrating the curvature distribution given along the longitudinal axis or by means of Mohr's theory.

Using the "CRITICAL STRAIN POINT METHOD", even in Q - R^B relationships, the physical meanings, namely, the stress and strain distribution states at the end cross section of columns are able to be shown clearly.

The plastic displacement angle increment ΔR^B may be computed by the follwing equation:

$$\Delta R^B = L_p \Delta \Phi \ , \qquad (4)$$

where L_p is the longitudinal length of plastic hinge region at the end of columns assumed to be D in this report and $\Delta\Phi$ is the plastic curvature increment in M - Φ relationship, which is based on the assumption that the lateral displacement angle of columns in the plastic range occurs only due to the rotation of the plastic hinge.

3. SHEAR STRENGTH AND DEFORMATION

3-1. Assumptions

In order to calculate approximately the shear component of the strength and deformation of reinforced concrete columns under the combined action of bending moment, shear force and constant axial load, the following assumptions are applied:

(1) Considering the condition of double-curvature deformation, the inflexion point of columns may be regarded as the critical section that determines the shear strength and deformation of short columns.

(2) The critical section mentioned above is assumed to have the area, $\frac{7}{8}(1-d_1)bD$ and the shear stress and strain distributions are assumed to be uniform over the area.

(3) The shear stress - strain relationship of concrete is assumed as shown in Fig.7, where the two dotted lines show the extreme cases, in one of which concrete shows sufficient shear ductility (with web reiforcement ratio, $\eta \geqq 1\%$), and in the other of which poor shear ductility ($\eta \fallingdotseq 0\%$). In this paper, the calculations are concerning only with the latter case.

(4) The shear yielding stress τ_y is determined from the fracture criterion of concrete under combined shear and normal stresses which is shown in Fig.8 [4]. As the abscissa of Fig.8 the constant axial load level ratio X of columns is adopt-

ed here, so τ_y is expressed by the following equation:

$$\tau_y / {}_c\sigma_u = \sqrt{-0.10X^2 + 0.09X + 0.01} \ . \qquad (5)$$

3-2. Shear Force - Shear Lateral Displacement Angle Relationships

Based on the assumptions mentioned above, shear force (Q) - shear lateral displacement angle (R^S) relationships of reinforced concrete columns may be easily computed, and of course, they are analogous to the shear stress-strain relationship (see Fig.7). Finally, Q-R^S relationship until shear explosion is able to be expressed by the following equation:

$$R^S = [Q/(7/8)(1-d_1)bD]/(\tau_y / {}_c\gamma_y) \ . \qquad (6)$$

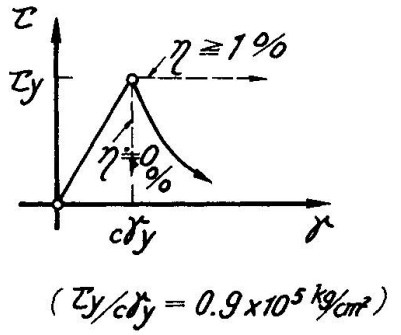

Fig.7 Shear Stress - Strain Relationships of Concrete

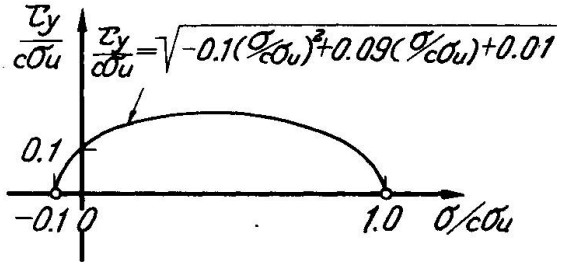

Fig.8 Fracture Criterion of Concrete

4. TOTAL STRENGTH AND DEFORMATION

4-1. Shear Force - Total Lateral Displacement Angle Relationships

By means of the superposition of the flexural and shear deformation components on the same shear force level, shear force (Q) - total lateral displacement angle ($R = R^B + R^S$) relationships of reinforced concrete columns under combined bending moment, shear force and constant axial load are able to be calculated. The processes are shown in Fig.9(a)(b) schematically. Fig.9(a) shows the shear explosion type and Fig.9(b) flexural fracture type. The fracture type is determined by the relative quantity relationship between Q^B_y (yielding shear force of Q-R^B relation) and Q^S_y (explosing shear force of Q-R^S relation), so mainly by the story height to depth ratio (H/D or shear span ratio) of columns.

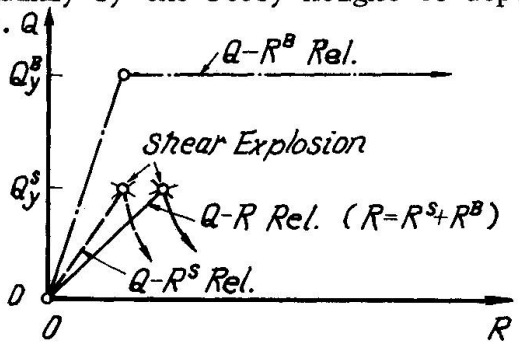

(a) Shear Explosion Type

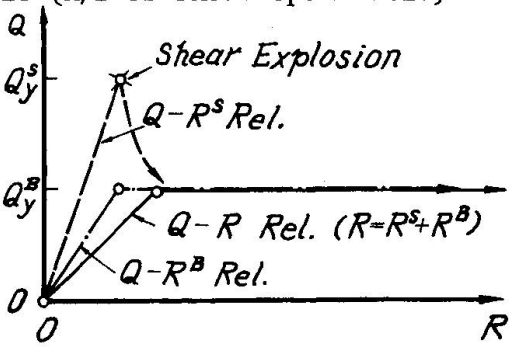

(b) Flexural Fracture Type

Fig.9 Graphical Procedure of Superposition of Flexural and Shear Deformation

4-2. Comparison between Caluculated and Tested Results

The calculated Q-R relationships of reinforced concrete columns are compared with tested results. Test specimens with a $16_{cm}X16_{cm}$ cross section are reinforced with the same tensile and compressive longitudinal reinforcement ratios of p=p'=1.0%, and without web reinforcement. The axial load level ratios (X) are 1,2,3 and 4. A test specimen and the loading system are shown in Fig. 10. The more detailed descriptions on these tests were reported in the reference [1]. The experimental results are shown by solid lines in Fig.11(a)(b)(c)(d) in the case of H/D=1,2,3 and 4, where TC, SC and SE(X) show the points of the occurrence of tensile crack on the tensile concrete fiber, shear crack in the shear span and shear explosion, respectively. The dotted lines show the computed results corresponding to the experimental results. The symbols in parentheses on them mean the "CRITICAL STRAIN POINT", and the special symbol "SE" shows the point of shear explosion.

The coincidence between computed and experimental results is good enough except the case that X=0 and H/D=1,2, where the dowel action of longitudinal reinforcing steel seems to have considerable effects on the shear resistance.

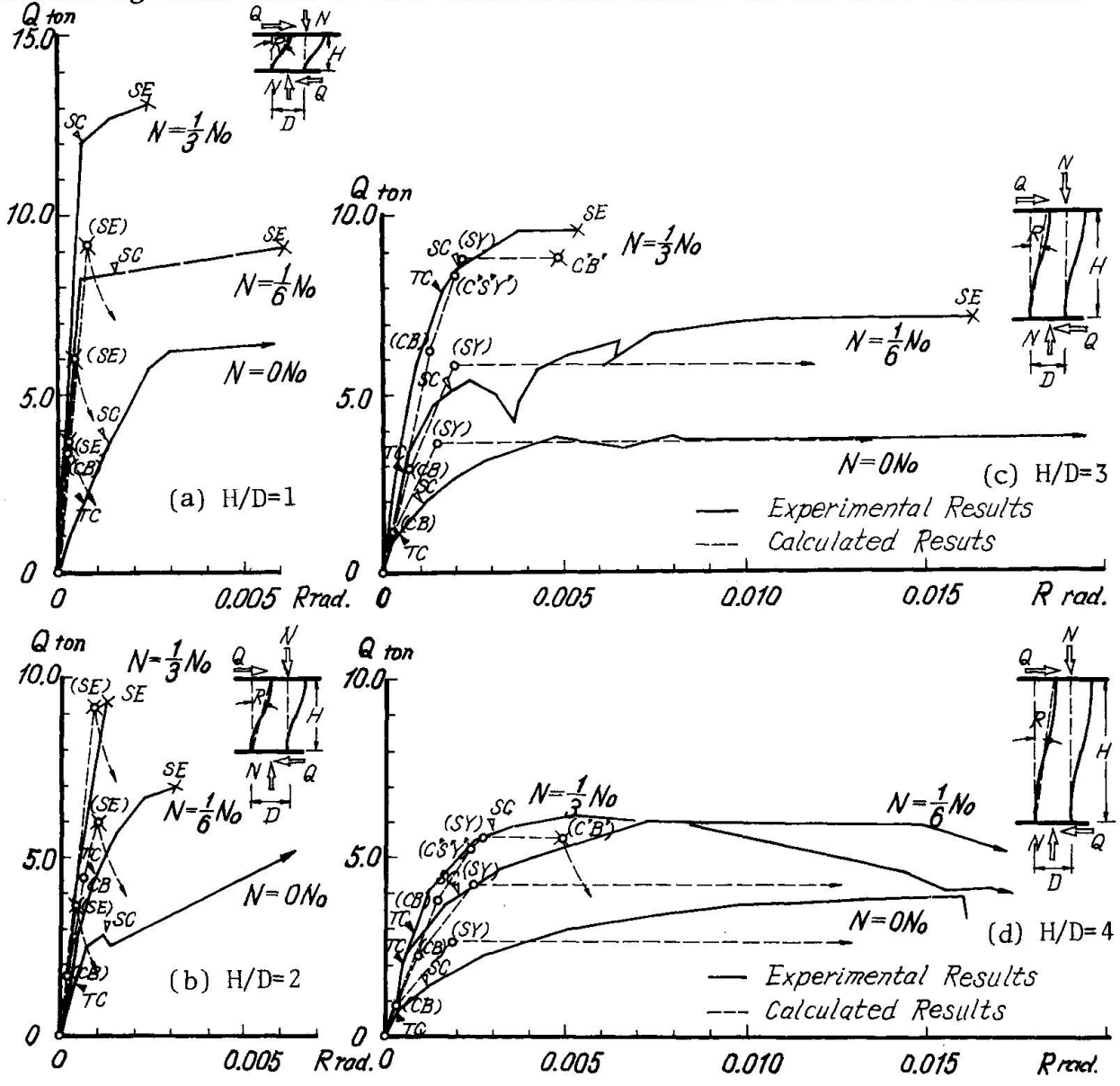

Fig. 11 Shear Force (Q) - Lateral Displacement Angle (R) Relationships

5. DISCUSSION

5-1. Maximum M-N-Q Interaction

Judging from the good coincidence between computed and experimental results, the simplified assumptions and calculation methods proposed here may be reasonable. Based on these idealizations, the interaction of the maximum M,N and Q is able to be illustrated as shown in Fig.12. A section parallel to the M-N plane of this figure shows a M-N interaction which is analogous to the Fig.5, and a section parallel to the Q-N plane shows a Q-N interaction analogous to the Fig.8. A section parallel to the M-Q plane shows a M-Q interaction in case of constant axial load, which is shown in Fig.13. In reality, however, M-Q interaction may be pseudo-elliptic such as shown by dotted line. The more precise analysis is now under consideration in the authors' laboratory.

5-2. Critical Hight to Depth Ratio

When Q_y^S is equal to Q_y^β in Fig.9, H/D means the critical height to depth ratio ($(H/D)_{cr}$ or the critical shear span ratio) that distinguishes the fracture modes of reinforced concrete columns into the shear explosion and the flexural fracture [6]. It is given by the slope of the line OC in Fig.13, too.

Finally, $(H/D)_{cr}$ is given as follows:

$$\text{if } \frac{\alpha}{1+2\beta_s p} \leqq X \leqq \frac{\alpha+(3/4)\alpha_n}{1+2\beta_s p}, \quad (H/D)_{cr} = \frac{2(\alpha+2\beta_s p)(1/2-d_1)}{(7/8)(1-d_1)\sqrt{-0.10X^2+0.09X+0.01}}, \tag{7-1}$$

$$\text{if } 0 \leqq X \leqq \frac{\alpha}{1+2\beta_s p}, \quad (H/D)_{cr} = \frac{2[X+2(1+X)\beta_s p](1/2-d_1)}{(7/8)(1-d_1)\sqrt{-0.10X^2+0.09X+0.01}}. \tag{7-2}$$

As an example, $(H/D)_{cr}$ is shown in H/D-$\beta_s p$ coodinates in Fig.14 with X as paramete. In the upper region than $(H/D)_{cr}$ lines, reinforced concrete columns show the flexural fracture, and in the lower region they show the shear explosion. If $X \geqq [\alpha+(\frac{3}{4})\alpha_n]/(1+2\beta_s p)$, columns show compressive flexural fracture mode, then such a case may be omitted. The condition that X=1/3, and $\beta_s p \geqq 0.25$ in Fig.14 belongs to such a case.

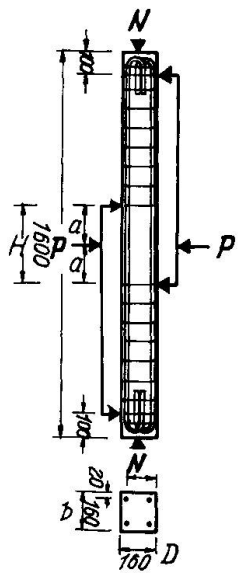

Fig.10 Test Specimen and Loading System

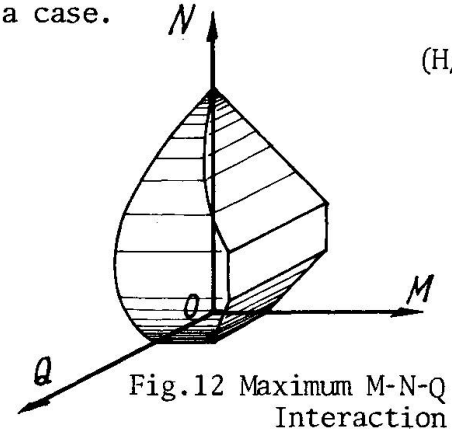

Fig.12 Maximum M-N-Q Interaction

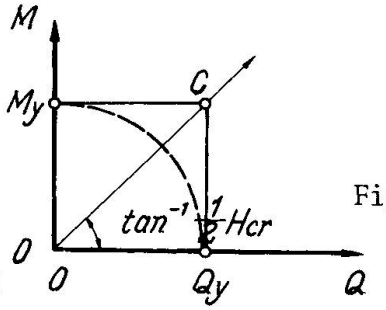

Fig.13 Maximum M-Q Interaction

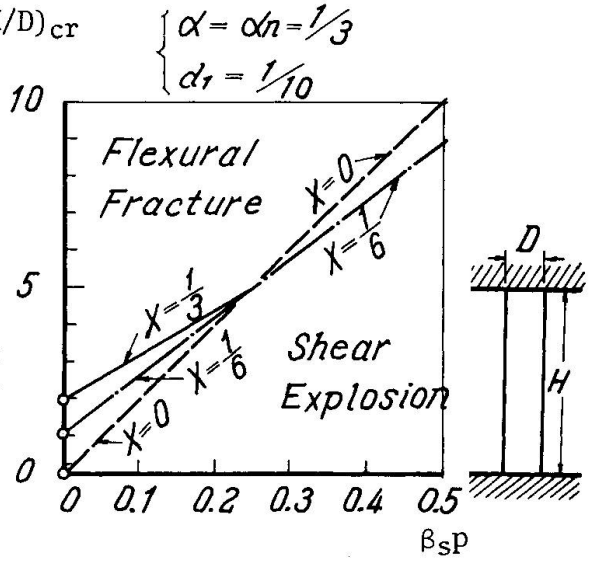

Fig.14 Critical Height to Depth Ratio $(H/D)_{cr}$- $\beta_s p$ Relationships

6. CONCLUSION

A simplified method of the calculation for the strength and deformation of reinforced concrete columns under the combined action of bending moment, shear force and constant axial load is presented. It is based on the superposition of the flexural and shear deformations (see Fig.1). The former is calculated by means of the "CRITICAL STRAIN POINT METHOD" of the authors (see Figs.2,3,4,5, 6), the latter is derived from the combined normal and shear stress characteristics at the cross section of the inflection point of reinforced concrete columns (see Fig. 7,8). The reasonable coincidence between the computed values and experimental results (see Fig.11) show the fact that these simplified calculation procedures are good enough to predict the lateral sway behaviors of reinforced concrete short columns.

7. REFERENCES

[1] Yamada,M., Furui,S.:Shear Resistance and Explosive Cleavage Failure of Reinforced Concrete Members Subjected to Axial Loads, Final Rep. 8th Congress of IABSE, New York, Sep. 1968, Zürich, pp. 1091/1102.
[2] Yamada,M., Kawamura,H.:Elasto-plastische Biegeformänderungen der Stahlbetonsäulen und -balken (Einseitige Biegung unter Axial Last), Abh., IVBH, Bd. 28/I, 1968, Zürich, pp.193/220.
[3] Yamada,M., Kawamura,H.,Kondoh,K.:Elasto-plastic Cyclic Horizontal Sway Behaviors of Reinforced Concrete Unit Rigid Frames Subjected to Constant Vertical Loads, Prel. Rep., IABSE (Rep., WC. Vol.13), Symp., Lisboa, Sep. 1973, pp. 199/204.
[4] Yamada,M., Tada,K.:Experimental Investigation on the Fracture Criteria of Concrete under Combined Stresses, RILEM, Symp., Cannes, Oct. 1972, Vol.1, Paris, pp. 245/255.
[5] Yamada,M., Kawamura,H.:Fundamental New Aseismic Design of Reinforced Concrete Buildings, Session 3A, No.102, 5WCEE, Jun. Rome, 1973.
[6] Yamada,M.:Shear Strength, Deformation and Explosion of Reinforced Concrete Short Columns, ACI Shear Symposium, ACI Special Publication, 1974.

SUMMARY

Based on the superposition of shear and flexural deformations, a simplified calculation method for the lateral sway deflections of reinforced concrete short columns under the combined action of bending moment, shear force and constant axial load is presented. The coincidence between the computed values (dotted) and the experimental results (solid lines in Fig. 11) is reasonable.

RESUME

En se basant sur la superposition des déformations à la flexion et au cisaillement, on présente une méthode de calcul simplifiée des déformations latérales des colonnes courtes en béton armé soumises à l'action combinée d'un moment de flexion, d'un effort tranchant, et d'un effort axial constant. La correspondance entre les valeurs calculées (pointillés) et les résultats expérimentaux (courbes pleines, Fig. 11) est raisonnable.

ZUSAMMENFASSUNG

Gestützt auf die Ueberlagerung von Schub- und Biegeverformungen wird eine einfache Berechnungsmethode für die seitliche Auslenkung kurzer Stahlbetonstützen unter der kombinierten Wirkung von Biegemoment, Querkraft und konstanter Normalkraft vorgelegt. Die Uebereinstimmung zwischen den berechneten Werten (gepunktete Linie) und experimentellen Ergebnissen (ausgezogene Linien in Fig. 11) ist vernünftig.

II

Strength of Reinforced or Prestressed Concrete Slender Columns under Biaxial Load

Résistance des poteaux élancés en béton armé ou précontraint en flexion déviée

Tragfähigkeit von schlanken Säulen aus Stahlbeton oder Spannbeton bei schiefer Biegung

Marco MENEGOTTO Paolo E. PINTO
(computer program: Giuseppe BACIGALUPI)
Istituto di Scienza e Tecnica delle Costruzioni
University of Rome
Rome, Italy

INTRODUCTION. Theoretical research aiming to "exact" solutions for reinforced and prestressed concrete structures in non-linear range has been very active in recent times, improving the accuracy of results for basic problems and engaging gradually with more complex cases of structural behavior.

A problem which has received up to now only limited solutions (see ref.|1|,|7|,|8|,|9|) is that of slender structures acted by normal force and biaxial bending. For problems like those of columns of buildings having typical cross sections and restraint, solutions are available in the form of tables, graphs or approximate formulae (|3|,|4|), and this is certainly sufficient for design needs. More variable conditions of shape and loading occur frequently: an important example is offered by tall bridge piers. A realistic analysis of these structures requires both geometrical and mechanical non-linearities to be considered, and neither the hollow shaped sections, variable together with reinforcement along the height, nor the complex loading patterns allow for the use of any simplified formula.

The method presented here, and the corresponding computer program, are based on a quite comprehensive analytical model, as described in the following; the result is a convenient tool for a complete analysis of that kind of structural problems.

DESCRIPTION OF THE MODEL.

Geometry. The model (Fig. 1) consists of a cantilever column, discretized by a sufficiently large number of cross-sections. These are contained in parallel planes, and their geometry is defined in a fixed coordinate system x, y, z. The shape of the sections is poly-

gonal -eventually with poligonal voids- being described as a sum of positive and negative triangular areas (Fig. 2). The shape may vary along the vertical axis z.

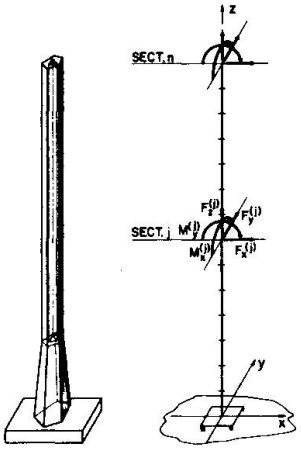

Fig.1 Idealization of the structure

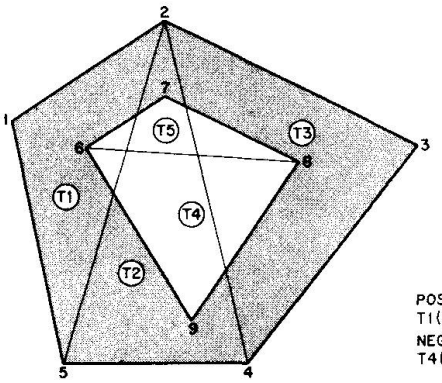

Fig.2 Description of a section by triangles

External loads. External loads are applied to every cross-section by two vectors of five components: $\{F_x, F_y, F_z, M_x, M_y\}^j$ for the dead load and the live load respectively (Fig. 1). Prestressing is introduced giving tendons areas and pretensioning strains along the sections.

Materials. Three separate constitutive laws can be assigned to concrete, reinforcing and prestressing steels. Figure 3 illustrates the "non-linear elastic" types presently adopted. The law for steels can describe, by varying its coefficients, the behavior of ordinary and high strength prestressing reinforcement.

The laws are assumed independent of time. Perfect bond is assumed between concrete and ordinary reinforcement; prestressing steel is considered free during the application of dead load, and bonded under the effect of live load. The deformations in the model are entirely attributed to axial and bending forces, shear and torsional effects being neglected.

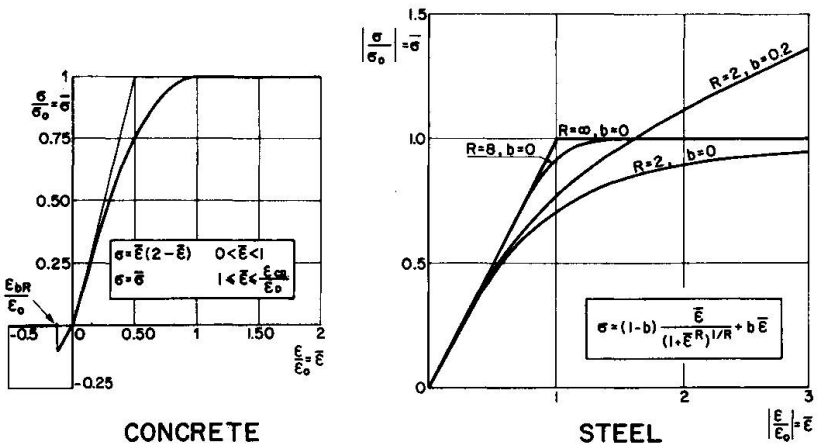

Fig.3 Constitutive laws adopted for the three materials

DESCRIPTION OF THE METHOD. The procedure calculates the stress and strain state of the structure for a given set of loads.

The second-order solution is pursuited through the following iterative scheme ("general" iteration):

- for every section, normal force and bending moments are calculated according to the deformed shape of the axis previously obtained.
- each section is then analized, in order to calculate the axial deformation ε_c, referred to the point C (appertaining to the conventional axis of the structure), and the curvatures K_x and K_y.
- by numerical integration of the curvatures a new deflected shape is obtained, which is used for starting a new "general" cycle.

Analysis of the section. The analysis is performed by means of an iterative procedure ("internal" iteration), which arrives at the determination of the neutral axis n and of the curvature K about it, for a given set of applied forces N, M_x, M_y.

Numerical analysis requires a discretization of the section. For each cycle, the concrete part is automatically discretized into strips parallel to the last neutral axis n, triangle by triangle.(The m axis is defined as orthogonal to n and passing through point C). The technique of subdivision is illustrated in Fig. 4. Each triangle is first divided into two sub-triangles by a line parallel to n. Then each one is discretized into strips of equal thickness (an upper bound is assigned for the structure). If the tensile strength axis ($\varepsilon = \varepsilon_{br}$)cuts a triangle, the cracked zone is cut off the discretization. The areas of ordinary and pretensioned steel are treated individually.

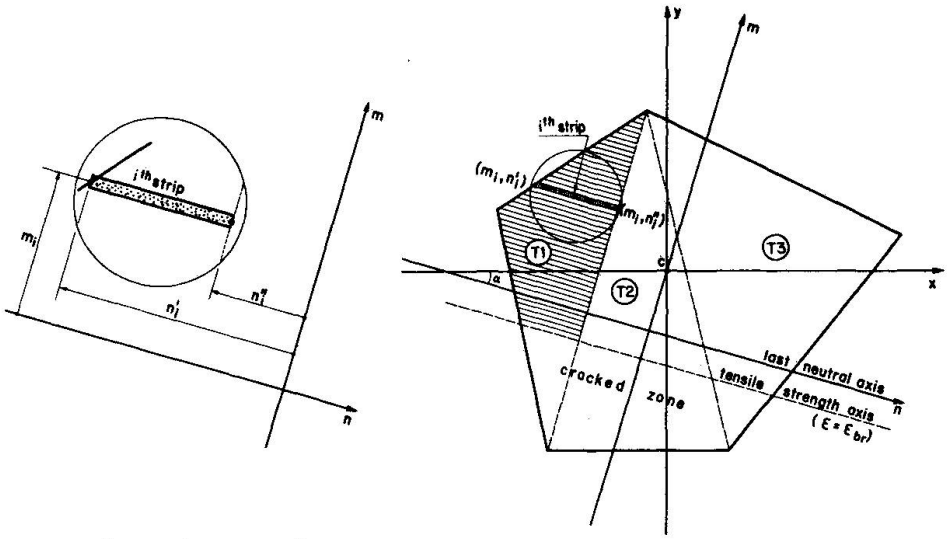

Fig.4 Automatic discretization of the concrete area in each step

i^{th} If the actual values of n and K were known, the strain ε_i of the concrete or ordinary steel area would be given by the expression:

$$\varepsilon_i = K \cdot m_i \qquad (1)$$

m_i being the distance from n.

The actual secant modulus of the i^{th} area would be defined thus:

$$E_i = \frac{\sigma_i(\varepsilon_i)}{\varepsilon_i} \qquad (2)$$

being σ_i the stress corresponding to ε_i according to the constitutive law of the material. By the use of E_i the section can be treated as if composed of linear elastic parts with varied moduli (Ref. [10]). To the homogenized section can then be applied the elastic relationships between external forces and internal stresses. The following quantities must be first calculated:

$$\begin{aligned} A &= \Sigma_i(B_i E_i) + \Sigma_\ell(A_\ell \cdot E_\ell) \\ S_n &= \Sigma_i(B_i E_i m_i) + \Sigma_\ell(A_\ell E_\ell \cdot m_\ell) \qquad (B_i = (n_i'' - n_i') \cdot s) \\ S_m &= \Sigma_i\left(B_i E_i \frac{n_i'' + n_i'}{2}\right) + \Sigma_\ell(A_\ell E_\ell n_\ell) \qquad (A_\ell = \text{individual steel area}) \end{aligned} \tag{3}$$

The coordinates of the homogenized centroid 0 of the section, referred to the system n, m, are:

$$n_o = S_m/A \quad ; \quad m_o = S_n/A \tag{4}$$

The homogenized moments of inertia, referred to the central coordinate system n_o, m_o, parallel to n, m (Fig. 5)are:

$$\begin{aligned} J_{n_o} &= \Sigma_i \left| B_i E_i (m_i^2 + s^2/12) \right| + \Sigma_\ell (A_\ell E_\ell m_\ell^2) - A \cdot m_o^2 \\ J_{m_o} &= \Sigma_i \left| E_i |(n_i'')^3 - (n_i')^3| \cdot s/3 \right| + \Sigma_\ell (A_\ell E_\ell n_\ell^2) - A \cdot n_o^2 \\ J_{n_o m_o} &= \Sigma_i \left| A_i E_i m_i (n_i'' + n_i')/2 \right| + \Sigma_\ell (A_\ell E_\ell m_\ell n_\ell) - A \cdot m_o \cdot n_o \end{aligned} \tag{5}$$

The Culmann ellipse, modified with the introduction of the varied E_i, has center in 0 , and is defined by its axes and by the angle α_o between its major axis ξ and the neutral axis n (Fig. 5).

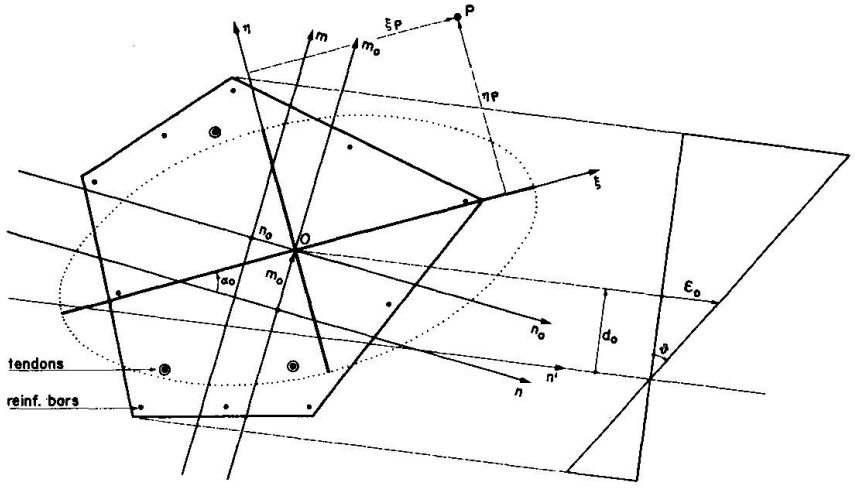

Fig.5 Homogenized cross-section

The homogenized principal moments of inertia of the section are:

$$J_{\xi,\eta} = \frac{J_{n_o} + J_{m_o}}{2} \pm \sqrt{\left(\frac{J_{n_o} - J_{m_o}}{2}\right)^2 + J_{n_o m_o}^2} \tag{6}$$

and the angle α_o :

$$\alpha_o = -\frac{1}{2}\, arctg\, \frac{2\, J_{no mo}}{J_{n_o} - J_{m_o}}\, (+\frac{\pi}{2}) \qquad (7)$$

The neutral axis obeys the antipolarity relationship with the center of application of the external forces, P.

As the neutral axis is being researched through an iterative procedure, the antipolarity is employed to find a new approximate position n' of it (Fig. 5). The equation of the n' axis, referred to the coordinate system ξ, η, is:

$$(\frac{\xi_p}{J_\eta})\, \xi + (\frac{\eta_p}{J_\xi})\, \eta + \frac{1}{A} = 0 \qquad (8)$$

in which ξ_p and η_p are the coordinates of the point P.

Repeated discretization of the section and use of the expressions (1) to (8) end up with coincidental n and n'.

Finally, being $\varepsilon_o = \frac{N}{A}$ the strain on the homogenized centroid O, the curvature K of the section is given by (see Fig. 5):

$$K = \frac{\varepsilon_o}{d_o} \qquad (9)$$

Cases of sections subjected to pure compression or pure bending are dealt with analogous homogenization and expressions derived from the elastic theory.

Analysis of the structure. Given the different positions of the neutral axes in each section and the associated curvatures K^j, the curvatures K_x^j K_y^j about the fixed axes x, y and the vertical deformations ε_c^j for all the sections of the column are:

$$K_x^j = K^j \cdot cos\, \alpha^j \qquad K_y^j = K^j \cdot sin\, \alpha^j \qquad \varepsilon_c^j = K^j \cdot d_c^j \qquad (10)$$

Numerical integration of these quantities gives the deflected shape of the column axis, with five components of displacement for each section j :

$$\{S_x,\ S_y,\ S_z,\ \phi_x,\ \phi_y\}^j \qquad (11)$$

The "general" iteration terminates when convergence on the deflected shape is reached.

Test for convergence. In the procedure outlined, the iterative solutions are in a monotonic progression from below (constitutive laws are monotonic, and only "small" displacements are considered). This requires checking both increments size and rate of convergence. A test wich has some theoretical bases, and proved to be effective is:

$$\frac{\Delta S_x{}^j}{\bar{S}} < \gamma \cdot \left(1 - \left| \frac{\Delta S_x{}^j}{\Delta S_x'^j} \right| \right) \qquad (j = 1,2,\ldots,n) \qquad (12)$$

and analogous for direction y. In the (12) $\Delta S_x{}^j$ and $\Delta S_x'^j$ are the last and the penultimate increments of S_x^j, $\bar{S}$ is an averaged displacement and γ is the assigned tolerance (the value adopted is 0,01).

When the second-order effects become important, the iteration converges very slowly. Therefore, an extrapolation formula is applied to the solution (after a certain number of cycles). This formula derives from the hypothesis that the successive solutions form a geometrical series, and makes use of the last three calculated solutions to extrapolate a tentative one, as the limit of the series. The factor to be applied at the last solution S_x results:

$$r = \frac{1}{S_x} \cdot \frac{S''_x \frac{\Delta S_x}{\Delta S'_x} - S'_x \frac{\Delta S'_x}{\Delta S''_x}}{\frac{\Delta S_x}{\Delta S'_x} - \frac{\Delta S'_x}{\Delta S''_x}} \qquad (13)$$

Prestressing. With the steel strains initially assigned, the forces in the tendons are calculated, for each section, and hence their contribution to the external normal force and bending moments.

The stress and strain variations in the prestressing steel after the bonding, due to the application of live loads, are calculated in this way: a preliminary analysis is made, in which only the dead load and prestressing (as external action) are applied. This analysis yields the concrete strains at all the points where tendons are located. In the subsequent iterative analysis, in which both dead and live loads are applied, the strain variations in the steel due to live loads are obtained as:

$$\Delta\varepsilon_i = (\varepsilon_i - \hat{\varepsilon}_i)$$

($\hat{\varepsilon}_i \equiv$ concrete strain from the preliminary analysis)

The corresponding stress variations produce $\overline{\Delta N}$, $\overline{\Delta M}_x$ and $\overline{\Delta M}_y$: these are added to external forces, and the cycle proceeds to the analysis of the section as for the ordinary case.

Ultimate conditions. After the solution for the given loading has been found, the program can automatically increase the set of live loads by a multiplier λ. It is thus possible to draw load-displacement curves, from the service load conditions up to collapse. For better approximation, the increments of λ are automatically reduced when the collapse value is reached.

APPLICATION.

The results obtainable by the method are illustrated with reference to a simplified scheme of a bridge pier.

Geometry of cross-sections details of reinforcement and material characteristics are shown in Fig. 6a.

The pier is 100 m high: eleven equidistant sections have been considered in the analysis.

The Table 1 contains the loading conditions examined. The dead load consists of the weight of the pier and of the bridge deck. A first live load ("X") consists of horizontal forces parallel to x

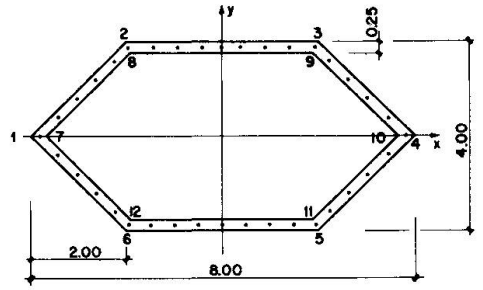

CONCRETE f_c = 300 Kg/cm²
E_{in} = 300,000 Kg/cm²

STEEL f_y = 4,000 Kg/cm²
E_s = 2,100,000 Kg/cm²

THICKN. OF CONC. STRIPS : 5 cm
NUMBER OF STEEL AREAS : 42 x 20 cm²
SUBDIVISION IN TRIANGLES :
4 positive,, 4 negative

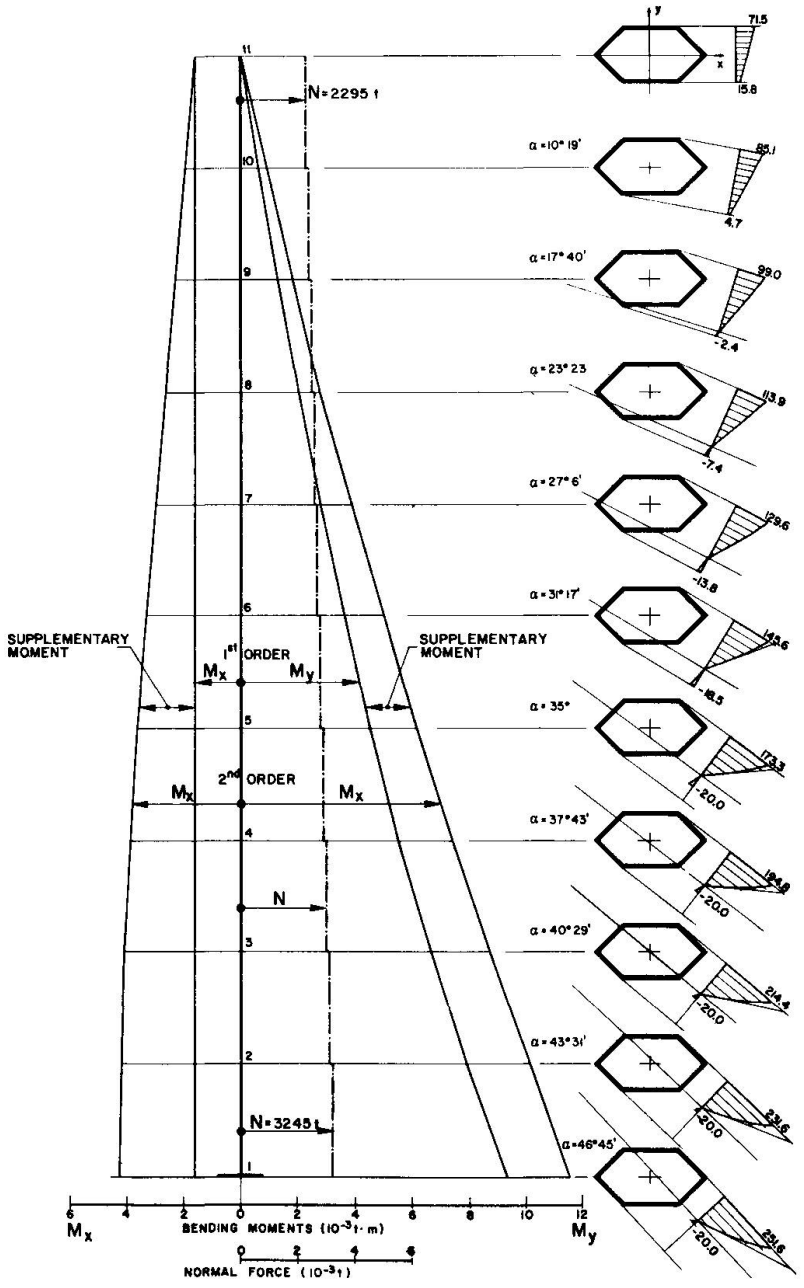

LOADING CONDITIONS OF THE PIER

SECTION	Z(m)	DEAD LOAD F_z (t)	LIVE LOADS "X" F_x (t)	LIVE LOADS "Y" F_z (t)	LIVE LOADS "Y" M_R (t·m)
1	0.	- 50.	-	-	-
2	10.	- 100.	8.	-	-
3	20.	- 100.	8.	-	-
4	30.	- 100.	8.	-	-
5	40.	- 100.	8.	-	-
6	50.	- 100.	3.	-	-
7	60.	- 100.	3.	-	-
8	70.	- 100.	3.	-	-
9	80.	- 100.	3.	-	-
10	90.	- 100.	3.	-	-
11	100.	- 1500.	40.	-500.	1000.

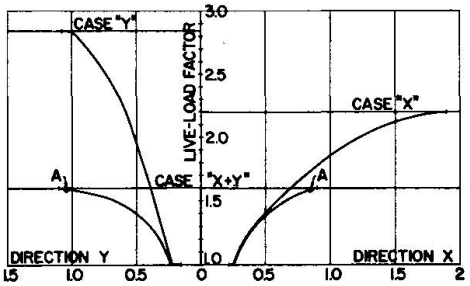

Fig.6 : a) cross section and reinforcement
b) stress-state of the pier in near-collapse stage
c) load-deflections curves of the top section

axis distributed along the column; the second live load ("Y") comprises a vertical load and a couple M_x applied to the top section.

Both "X" and "Y" loading conditions were increased up to collapse; in a third case, "X" and "Y" were applied together.

The load-displacement curves appear in Fig.6c. The "X + Y" condition produces biaxial bending; as can be seen, the live load factor at collapse is noticeably less than for the separate cases. The onset of collapse is due to instability in the y direction. The Δy displacement under service loads (load factor = 1) is less than for x direction: under the proportional increase of live loads Δy overpasses Δx and tends to horizontal tangent. The stress state on the pier at a near-collapse condition (point A in Fig.6c, $\lambda = 1.59$; collapse value: $1.59 < \lambda < 1.60$) is illustrated in Fig. 6b.

Diagrams show the shifting and rotating of neutral axis from the base to the top. It can be noted that limit stresses have not been attained yet in any point of the structure (only concrete stresses are plotted beside the sections). In fact, this case of collapse is due to instability appearing almost in the "elastic" range.

The slenderness of the pier is confirmed by the bending moment M_x which is at the base more than 2,5 times the corresponding first order value (Fig.6b).

B I B L I O G R A P H Y

| 1 | AAS-JAKOBSEN, A. - "C.E.B. - BULLETIN D'INFORMATION - N.76 & N.77".

| 2 | ARONI, S. - "Slender Prestressed Concrete Columns" Jnl. of Str. Div., ASCE Vol.94, Apr. 1968.

| 3 | C.E.B. - "BULLETIN D'INFORMATION N. 93" - Manuel de Calcul "Flambement - Instabilite", Juillet 1973.

| 4 | DIN 1045 German Code for the Design of Reinforced Concrete Structures.

| 5 | DRYSDALE, R.G., HUGGINS, M.W. - "Sustained Biaxial Load on Slender Prestressed Columns". Jnl. of Str. Div., ASCE Vol. 97, May 1971.

| 6 | GESUND, H., VANDEVERLDE, C.E. - "Stifness of Reinforced Concrete Columns in Biaxial Bending". - Proc.Int.Conf. on Planning and Design of Tall Buildings - Lehigh Univ., 1972 - Tech. Comm. N.22.

| 7 | KORDINA, K., RAFLA, K., HJORTH, O. - "Traglast von Stahlbetondruckgliedern unter schiefer Biegung mit Achsdruck" - Techn. Univ. Braunschweig, Juli 1973.

| 8 | Mac GREGOR, J.C. - "Simple Design Procedures for Concrete Columns" Introd.Rep., Theme II, IABSE Symp., Quebec 1974.

| 9 | MARTIN, I. - State of Art Report, N.5 - "Reinforced Concrete Columns" Proc.Int.Conf. on Planning and Design of Tall Buildings-Lehigh Univ., 1972 - Tech.Comm.N.22.

|10 | MENEGOTTO, M., PINTO, P.E. - "Method of Analysis for Cyclically Loaded R.C. Plane Frames Including Changes in Geometry and

Non-Elastic Behavior of Elements under Combined Normal Force and Bending" Prel.Rep. IABSE Symposium, Lisbon, 1973. IABSE Vol. 13.

|11| PARME, A.L., NIEVES, J.M., GOUWENS, A. - "Capacity of Reinforced Rectangular Columns Subjected to Biaxial Bending". Jnl. A.C.I. Vol.63, Sept. 1966.

|12| WARNER, R.F. - "Biaxial Moment Thrust Curvature Relations" Jnl. of Str. Div., ASCE Vol. 95, May 1969. Introd.Rep., Theme I, IABSE Symposium, Quebec 1974.

|13| ZIA, P., MOREADITH, F.L. - "Ultimate Load Capacity of Prestressed Concrete Columns" Jnl. A.C.I., Vol. 63, July 1966.

SUMMARY

A procedure is presented for the analysis of slender columns in biaxial bending, for general loading conditions and cross sections variable in shape and reinforcement. The behavior of the three materials is described by different non-linear laws. Discretization of the sections and numerical integration of the actual strains yield the deformed shape of the column for any given set of loads. Ultimate conditions can be found by automatic incrementing of part of the loads.

RESUME

On décrit une méthode pour l'analyse des poteaux élancés en béton armé ou précontraint soumis à flexion biaxiale. Les charges dans les deux plans ont des distributions quelconques: la forme et les armatures des sections sont variables. Trois lois constitutives non-linéaires décrivent le comportement des trois matériaux. L'étude des sections est réalisée au moyen d'une discrétisation, et la ligne déformée du poteau s'obtient en intégrant les déformations de chaque section. La condition d'équilibre limite est atteinte en accroissant automatiquement l'intensité d'une partie ou de la totalité des charges.

ZUSAMMENFASSUNG

Es wird eine Methode vorgestellt für die Berechnung von schlanken Säulen unter schiefer Biegung, für allgemeine Belastungsbedingungen und veränderliche Form des Querschnitts. Das Verhalten der drei Baustoffe wird mittels verschiedener nicht-linearer Gesetze beschrieben. Eine Diskretisierung der Querschnitte und numerische Integration der effektiven Dehnungen ergibt die verformte Axe der Säule für jede gegebene Belastungsbedingung. Die maximale Tragfähigkeit kann durch automatische Steigerung der Belastung ermittelt werden.

Leere Seite
Blank page
Page vide

II

Strength of Columns under Biaxially Eccentric Loads

Résistance des colonnes soumises à des charges excentrées biaxiales

Tragfähigkeit von Stützen unter zweiaxig exzentrischer Belastung

Kiyoshi OKADA
Professor
Kyoto University

Takayuki KOJIMA
Assistant Professor
Ritsumeikan University

Ikuo HIRASAWA
Lecturer
Chubu Institute of Technology

Japan

I Introduction

In the ultimate strength design of the columns, it is quite important to examine not only the ultimate strength but the ultimate deflection at the same time, especially, for the slender columns under biaxially eccentric loads.

Computer analysis[1] are made on: (1) the failure envelope of column cross-section and (2) the column deflection under biaxially eccentric load. The strength and the deflection at ultimate stage can be predicted by combining these two methods. This analysis,differently from those ever proposed, has characteristics of dealing with the change of the location of the eccentricity under biaxially eccentric load.

Based on the analysis and results of tests, the simple design procedure for slender column is proposed.

II Test of the columns under biaxially eccentric loads

Totally sixty-two short and slender columns are made and tested,[1] and the test programs for slender column are shown in Table 1.

All of the slender columns have the same rectangular cross-section of 6x9 cm and the same initial eccentricity of 3 cm. Columns of series A and B were reinforced with four and six dia. 6 mm bars, respectively. The column lengths of each group in two series were 60, 120 and 180 cm, respectively. Initial directions of eccentricities in a group were I, III and V or I, II, III, IV and V as shown in the remark in Table 1.

Fig. 1 shows the comparison of the measured deflections with the computed ones. The stress-strain relationship of concrete as assumed in the calculation is also shown in Fig. 1.

Fig.2 clearly shows the change of eccentricities with increasing load from the initial to the final locations, the final eccentricities being not located along the inclination of initial direction. These figures show that the analysis coincide well with the results of tests.

The torsional deformation due to biaxially eccentric load is not considered here, but it should be studied as an important problem in future.

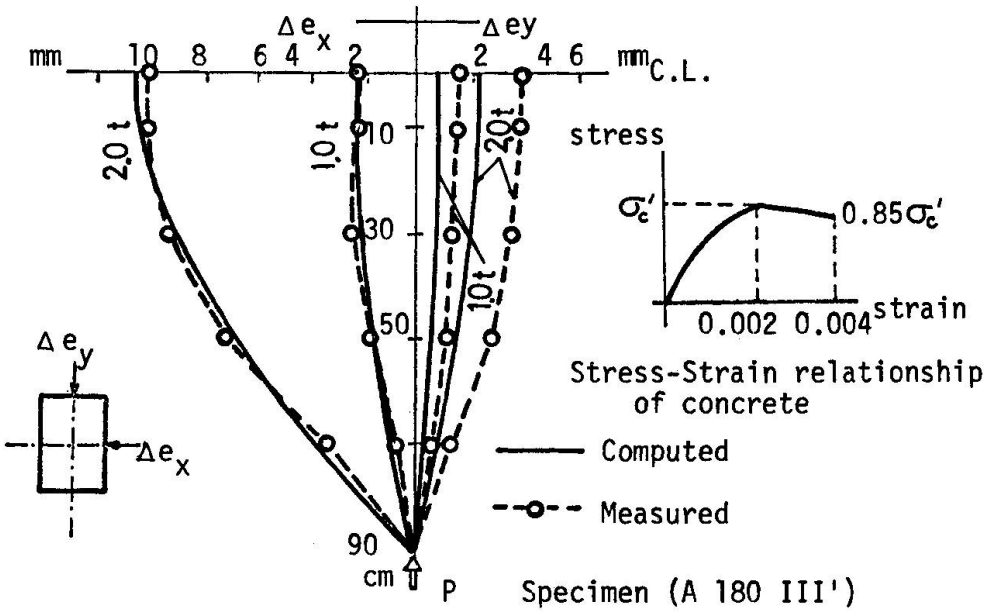

Fig. 1 Comparison of the measured deflections with the computed ones

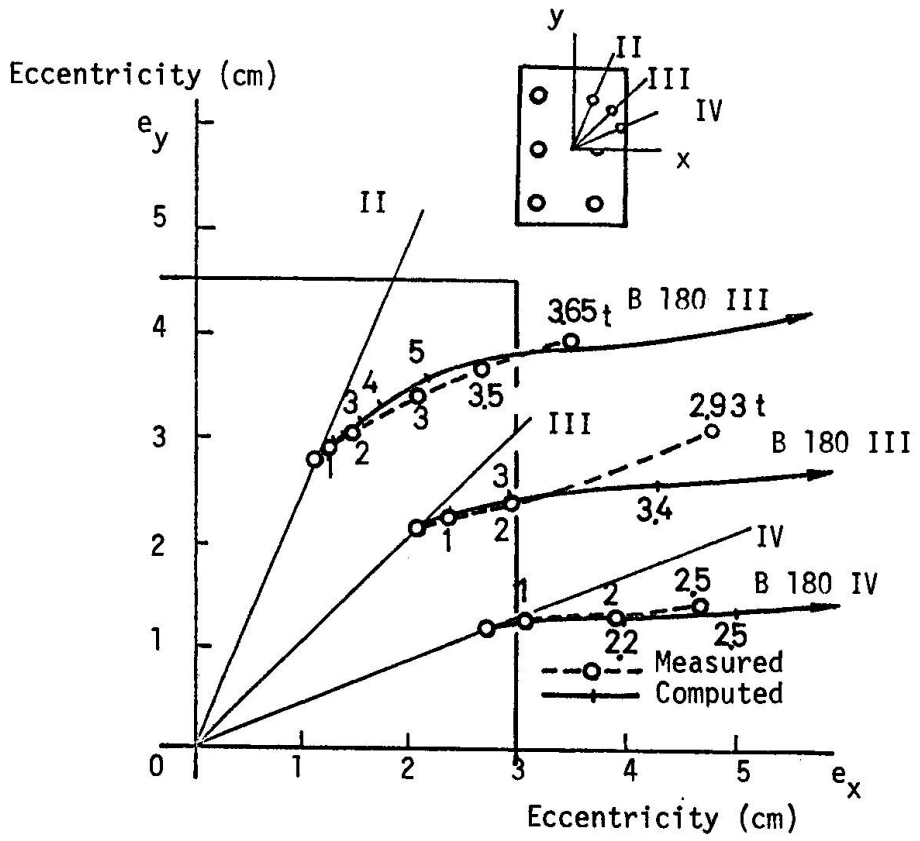

Fig. 2 Load-eccentricity relationships in the mid-height section of column

III Simple design solutions for the ultimate deflection and strength under biaxially eccentric loads

(1) Ultimate deflection and strength

A slender column when subjected to biaxially eccentric load deflects as already shown in Fig. 1 or 2.

Fig. 3 is also one of the measurements showing how the initial eccentricity of load on the critical section actually varies with increasing load for each of five slender columns subjected to uniaxially or biaxially eccentric load. The initial (e_{ro}) and final eccentricities ($e_{ro}+\Delta e_r$) projected on the e_x-e_y plane is shown in Fig. 4(a). The final eccentricities are located on the inclination (β) deviated from the initial direction (α), and P-β relationships are replotted in Fig. 4(b). Radial ultimate moments based on the final eccentricity are calculated from Fig. 4(a) and 4(b), and shown in Fig. 4(c).

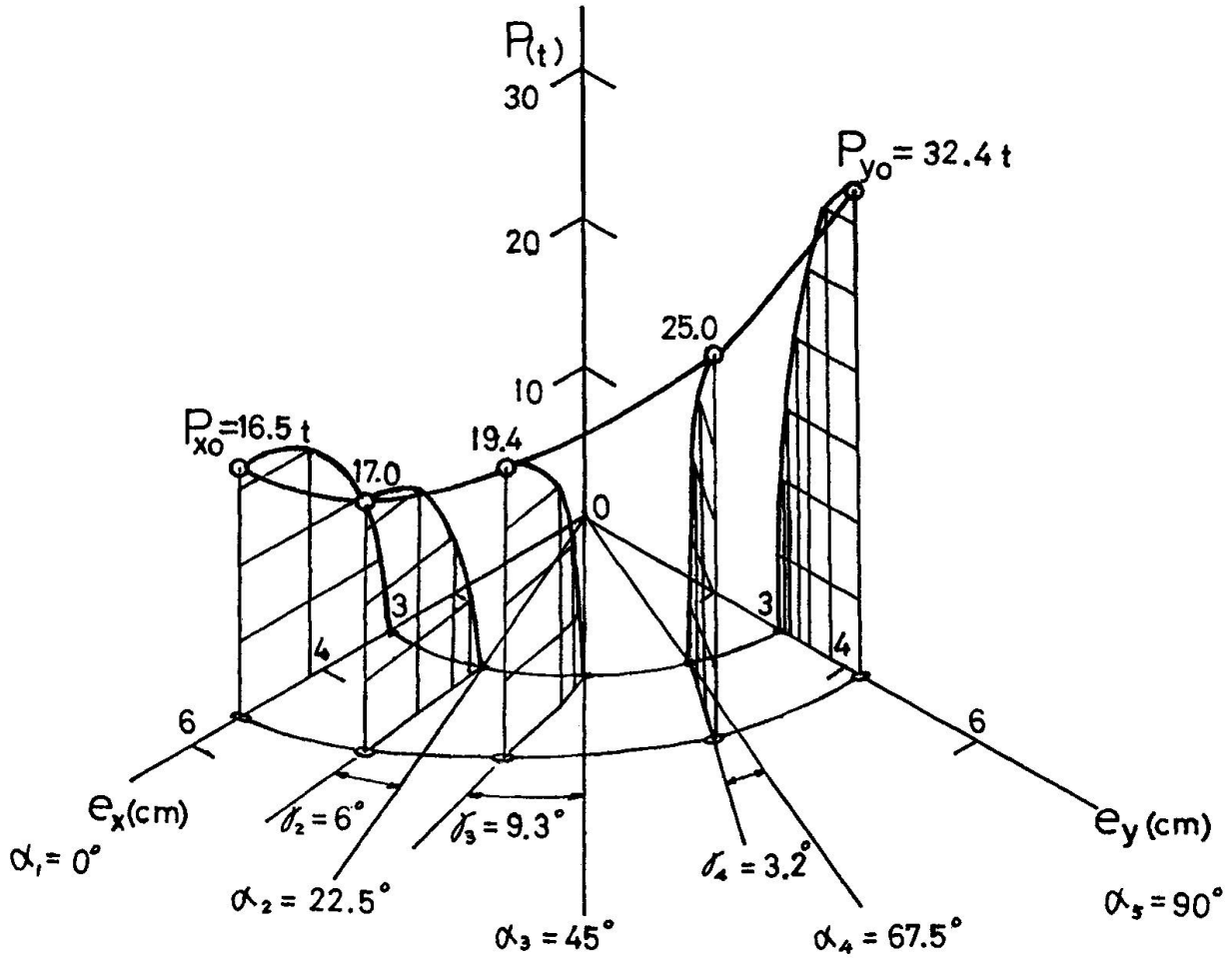

Fig. 3 Load-eccentricity relationships at the center section of biaxially loaded columns

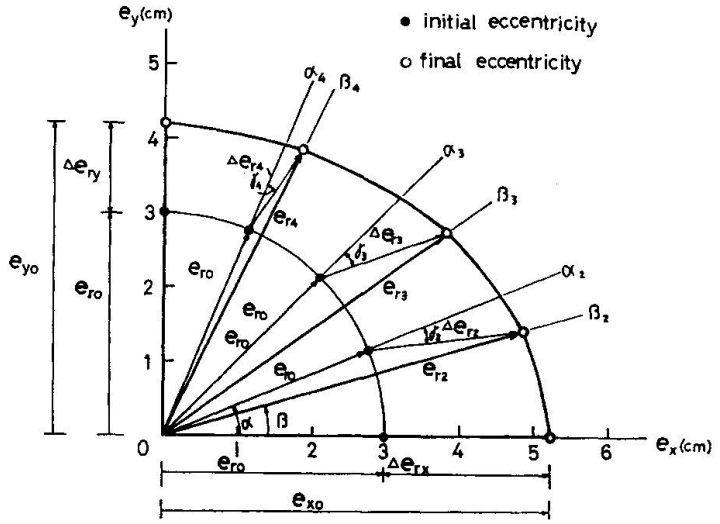

Fig. 4(a) Initial and final eccentricities projected on the e_x-e_y plane

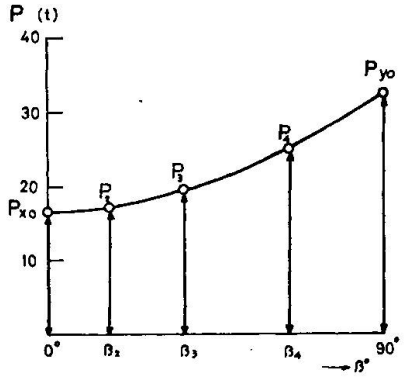

Fig. 4(b) P-β relationship

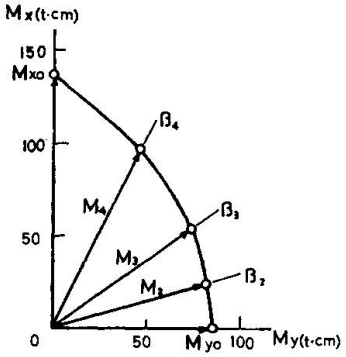

Fig. 4(c) Radial ultimate moments on final direction of eccentricity

(2) Modified additional moment method

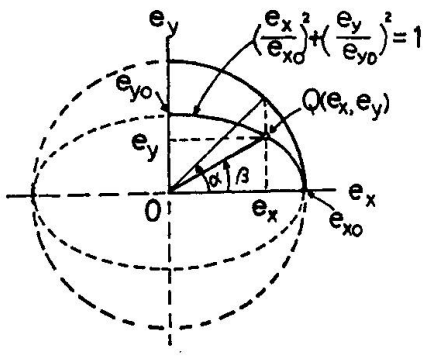

Fig. 5
Supposed radial eccentricity

Detailed calculations as illustrated in II are rather complicated, so the simple design procedure is proposed here.

It may be deduced that the radial eccentricity $Q(e_x, e_y)$ at the final stage can be approximated by the following equation, as shown in Fig. 5;

$$\left(\frac{e_x}{e_{xo}}\right)^2 + \left(\frac{e_y}{e_{yo}}\right)^2 = 1 \qquad (1)$$

The eccentricity e_x, or e_y is given by

$$e_x = e_{xo}\cos\alpha$$
$$e_y = e_{yo}\sin\alpha$$

where:
α and β in Fig. 5 are the inclinations of the lines joining the initial and final loading points (eccentricites) to the centroid of the column cross-section, respectively, and
e_{xo} and e_{yo} are the final values of uniaxial eccentricity along x and y axis, respectively.

Actual radial eccentricity at the ultimate stage is given by eq. (2):

$$e_r = \sqrt{e_x^2 + e_y^2} \qquad (2)$$

and the relation between α and β is given as follows:

$$\beta = \tan^{-1}\left(\frac{e_{yo}}{e_{xo}} \cdot \tan\alpha\right) \qquad (3)$$

Next, it may also be assumed that the outer limits of the ultimate moment corresponding to Fig. 5 is approximately given by the expression as shown in Fig. 6.

$$M_x = M_{xo}\sqrt{1 - \frac{M_y}{M_{yo}}} \qquad (4)$$

where M_{yo} and M_{xo} are the equivalent uniaxial moments for the ultimate moment about x- and y-axis, respectively, and M_y and M_x are the components of the actual ultimate radial moment M_r.

Equation(4) gives the following relations,

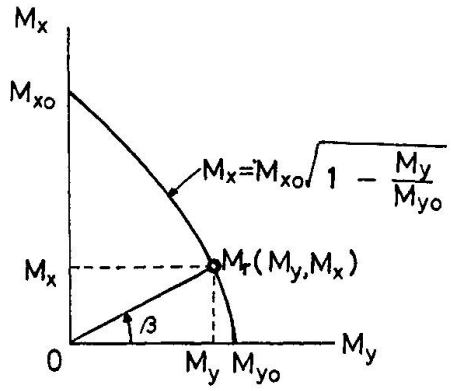

Fig. 6 Approximation for radial ultimate moment

$$M_y = M_r \cos\beta \qquad (5)$$

$$M_x = M_r \sin\beta \qquad (6)$$

$$M_r = \frac{M_{xo}}{A \sin\beta}\left[\sqrt{A+1} - 1\right] \qquad (7)$$

$$\text{where } A = 2\cdot\frac{M_{yo}}{M_{xo}}\cdot\tan\beta. \qquad (8)$$

Thus, from equations (2) and (7), the ultimate load P_r under biaxially eccentric load can be given by

$$P = \frac{M_r}{e_r}. \qquad (9)$$

(3) Comparison with tests

The detailed comparison of the proposed simple design procedures with the results of tests on actual five columns are shown, for example, in Fig. 7(a), (b) and (c), concerning the ultimate deflection (e_r), the ultimate load (P_r) and the ultimate moment (M_r), respectively.

For general use, when the uniaxial ultimate deflection and load calculated by the additional moment method introduced by Prof. Macgregor in the Preliminary Report Theme II (B.S. or FIP-CEB recomendation) are inserted into the above equations, the authors' method agreeswell with the results of tests as shown in Table 1.

Then, the simple solution proposed here for the ultimate capacities of the slender columns subjected to biaxially eccentric load may be used for design purpose.

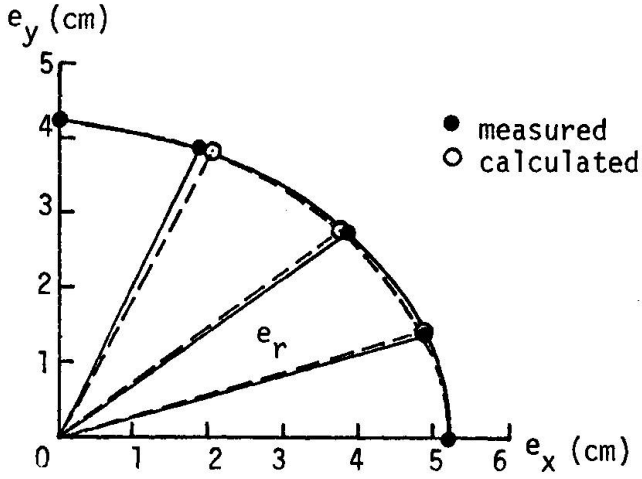

Fig. 7(a) Comparison for e_r

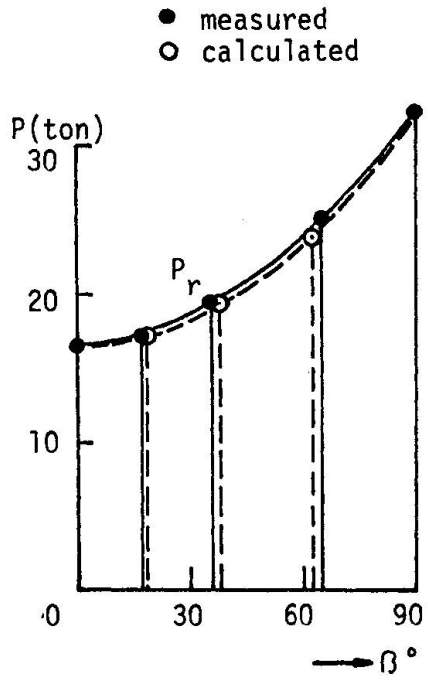

Fig. 7(b) Comparison for P_r

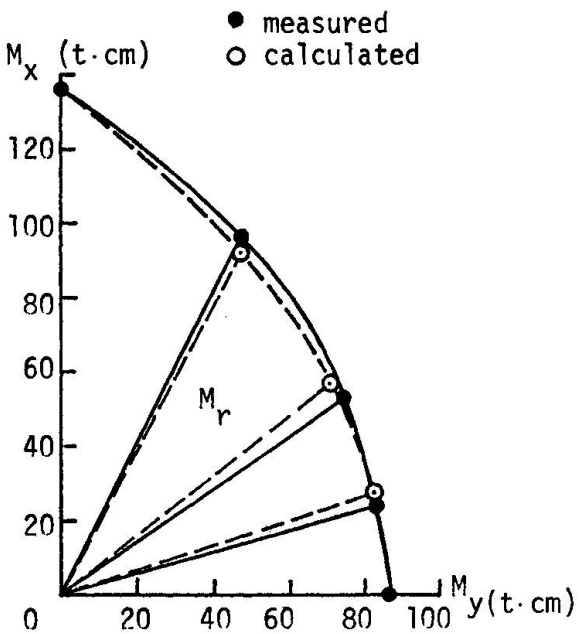

Fig. 7(c) Comparison for M_r

Table 1. Comparison between test results with calculated results

Column		l cm	b cm	h cm	d/h	σ_c' kg cm	σ_{sy} kg cm	e_{ro} cm	$e_{r\,test}$ cm	$e_{r\,cal}$ cm	$\frac{e_{r\,test}}{e_{r\,cal}}$	$P_{r\,test}$ ton	$P_{r\,cal}$ ton	$\frac{P_{r\,test}}{P_{r\,cal}}$	Remark
A 60	I	60	6	9	0.833	296	3430	3	3.30	3.16	1.044	7.75	8.59	0.902	
	III								3.30	3.22	1.025	5.35	4.36	1.227	
	V								3.47	3.29	1.055	3.95	3.54	1.116	
A 120	I	120	6	9	0.833	296	3430	3	4.20	3.65	1.151	7.40	7.96	0.930	
	III								4.50	3.88	1.160	3.65	3.10	1.178	
	V								4.17	4.10	1.017	2.68	2.37	1.131	
A 180	I	180	6	9	0.833	296	3430	3	5.46	4.57	1.195	6.00	7.02	0.855	III= 45°
	III								5.12	4.99	1.026	2.45	2.11	1.161	
	V								5.42	5.37	1.010	2.09	1.56	1.340	
B 60	I	60	6	9	0.833	318	3430	3	3.35	3.16	1.060	8.87	9.06	0.979	
	II								3.23	3.18	1.016	5.40	6.97	0.775	
	III								3.27	3.22	1.016	4.66	5.97	0.781	
	IV								3.50	3.27	1.070	4.40	5.51	0.799	
	V								3.59	3.28	1.095	4.69	5.39	0.870	
B 120	I	120	6	9	0.833	293	3430	3	4.34	3.66	1.186	6.20	8.02	0.773	
	II								4.48	3.73	1.201	4.33	5.52	0.784	
	III								4.50	3.89	1.157	4.16	4.30	0.967	
	IV								4.35	4.04	1.077	3.35	3.72	0.901	
	V								4.01	4.10	0.978	3.00	3.55	0.845	
B 180	I	180	6	9	0.833	318	3430	3	5.11	4.58	1.116	5.05	7.28	0.694	II = 22.5° III= 45° IV = 67.5°
	II								5.22	4.70	1.111	3.65	4.33	0.843	
	III								5.45	4.97	1.097	2.93	3.06	0.958	
	IV								6.45	5.24	1.231	2.90	2.52	1.151	
	V								6.25	5.34	1.170	2.73	2.37	1.152	
A 60	III'	60	6	9	0.833	333	3430	3	3.25	3.22	1.010	4.28	4.50	0.951	
A 120	III'	120							4.16	3.87	1.075	4.10	3.18	1.289	
A 180	III'	180							5.55	4.96	1.119	2.44	2.16	1.130	
B 60	III'	60	6	9	0.833	333	3430	3	3.38	3.22	1.050	4.75	6.05	0.785	
B 120	III'	120							4.25	3.88	1.095	4.40	4.44	0.991	
B 180	III'	180							5.55	4.96	1.119	3.00	3.09	0.971	
									Average		1.091			0.974	

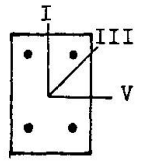

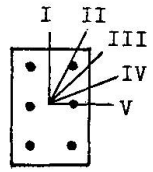

IV Conclusions

A calculating method of the ultimate capacity of concrete columns with taking into consideration the column deflection under biaxially eccentric loads is proposed.

A simple design procedure is also proposed which is developed and refined so as to achieve both simplicity in use and, as far as possible, a realistic representation of actual behavior.

This method agrees well with the results of thirty model columns.

Reference

1) OKADA,K. and HIRASAWA,I.,"Ultimate Strength of Square and Rectangular Columns under Biaxially Eccentric Loads", Review of the Twenty-third General Meeting, The Cement Association of Japan, May 1969, pp356-361.

SUMMARY

This paper deals with the design method for reinforced concrete slender columns subjected to biaxially eccentric loads. Firstly, the analysis of strength and deflection of slender column at ultimate stage is made using computer, the results are compared with the results of tests.

Next, taking into account the analysis, a simple design solution is proposed. This method agrees with tests and shows applicable for general use.

RESUME

Ce rapport présente une méthode de dimensionnement pour les colonnes en béton armé élancées soumises à des charges avec excentricité biaxiale. On procède d'abord au calcul de la résistance et de la déformation ultimes des colonnes élancées en utilisant l'ordinateur; les résultats sont comparés avec ceux des essais.

On propose ensuite, en se basant sur les calculs, une méthode simple de dimensionnement. Cette méthode concorde bien avec les résultats expérimentaux; elle est applicable dans la pratique.

ZUSAMMENFASSUNG

Der Beitrag behandelt die Bemessung von schlanken Stahlbetonstützen unter zweiaxig exzentrischer Belastung. Zunächst werden die Berechnung der Traglast und der zugehörigen Verformungen schlanker Stützen mittels Computer durchgeführt und die Ergebnisse mit Versuchsresultaten verglichen.

Als nächstes wird, unter Berücksichtigung der genauen Berechnung, eine einfache Bemessungsmethode vorgeschlagen. Diese Methode führt zu Ergebnissen, die gut mit Versuchen übereinstimmen und zeigt sich als allgemein anwendbar.

II

Slender Reinforced Concrete Columns Subjected to Biaxially Eccentric Loads

Colonnes en béton armé sous une charge d'excentricité biaxiale

Schlanke bewehrte Betonsäulen unter zweiaxig aussermittiger Belastung

N.J. GARDNER
Associate Professor

S.I. ABDEL-SAYED
Research Associate

Department of Civil Engineering
University of Ottawa
Ottawa, Canada

Over the past few years increasingly refined and accurate methods of analysis for complex structures have become available to the structural engineer. However to use such analyses more realistic imput information is needed concerning the moment-thrust-curvature characteristic of the various members comprising the structure. In general the frame analysis methods available, and their associated computer programs, have not taken account of the reduction in flexural stiffness of the columns due to axial load even though the theoretical treatment has long been available (5).

For detailing purposes the behaviour of slender reinforced concrete columns has been treated as the behaviour of a short column modified by a factor to account for slenderness effects. Currently the Building Code Requirements of the American Concrete Institute ACI 318-71 (3) require that for a slender column the moment be increased to account for slenderness and the column be designed as a short column with this increased moment. The short column axial load moment interaction is easily obtained from equilibrium considerations. Neither the moment magnifer nor the short column interaction consider strain compatibility.

The minimum characteristics needed to completely define the behaviour of a reinforced concrete column are the interrelationships between axial load-moment-curvature-strain. By integrating the moment curvature relation along the length of a given column the internal strain-lateral displacement behaviour of the column can be determined.

This paper presents a new form of interaction diagram relating the axial load, moment, maximum strain and curvature for square section corner reinforced concrete columns under uniaxial and biaxial eccentricities.

Design Method

To completely describe the behaviour of a reinforced concrete section the load, eccentricity of load about both axes, maximum strain and curvature (or position of neutral axis to determine curvature) need to be known.

(a) Section capacity calculations

Design charts have been presented by Abdel-Sayed and Gardner (1,2) for square section columns with corner reinforcement. These charts were prepared assuming a planar distribution of strain across the section, a bilinear stress strain characteristic for the steel reinforcing and Hagnestad's (4) stress strain curve for the concrete. The cross section of the column was divided into a number of elements and for a given planar strain distribution the stress on each element, either concrete or steel, determined. Hence the equilibrating force and moment due to the assumed strain distribution are determined by summing the elemental forces. The curvature implicit in the assumed strain distribution is obtained from the magnitude of the maximum strain and the perpendicular distance z between the position of maximum strain and the neutral axis.

Figure 1 is a typical interaction curve, prepared by the above described method, which relates the non-dimensional load P'_u/btf'_c, eccentricity e, maximum strain ε and location of neutral axis z (curvature) for a column with a steel ratio $pf_y/f'_c = 0.60$ and a cover ratio $g = 0.75$ for angles of eccentricity of 0^o and 45^o. Linear interpolation is used to obtain results for angles of eccentricity between 0^o and 45^o. To use the interaction curves to design columns with cover ratio's other than $g = 0.75$ a single value function F is given in Figure 2 to modify the actual eccentricity of a column with $g \neq 0.75$ to its analogous column with $g = 0.75$.

(b) Slenderness or PΔ Effects

As the axial load is constant along the length of any given column there are only a number of maximum strains and curvatures (curvature = maximum strain ε/distance to the neutral axis z) which satisfy equilibrium for a given cross section. The curvature and maximum strain are known at the ends of a column of given cross section where the load, eccentricity of the load and the angle of the eccentricity are defined. By assuming a strain and curvature of the critical section of the column the lateral deflection of that section can be calculated if the deflected shape is assumed. If the lateral deflection plus the eccentricity is greater than that possible for the chosen section then a larger section must be chosen.

Experimental Investigation

An experimental investigation into the actual behaviour of slender reinforced concrete columns under biaxial load was undertaken to verify the theoretical results.

A total of 44 columns were cast and loaded to failure. All columns were cast and tested in a horizontal position. All columns had a nominal concrete section of 6 ins. x 6 ins. (15.2 cm. x 15.2 cm.) with enlarged ends to allow loads to be applied outside the section. Two sizes of steel reinforcement #3 (0.95 cm. diam.) and #7 (2.25 cm. diam.) bars were used giving steel ratio's of 1.22% and 6.67% respectively. All reinforcement had a specified minimum yield strength of 60,000 psi (4150 bars). Two concrete cylinder strengths were used; nominally 3,000 psi (207 bars) and 5,500 psi (380 bars). To investigate length effects, two groups of specimens were made with effective lengths of 90 ins. (230 cm.) and 134 ins. (340 cm.) respectively. Columns were tested horizontally in a pinned-pinned configuration. Deflections were measured in two orthogonal directions, normal to the faces of the section at mid length of the column. The load deflection behaviour of the column was taken to failure. Unfortunately, it was not possible to obtain reliable deflections at loads near the failure load.

A summary of the experimental results and comparison with the results predicted by the method presented are given in Table 1.

Comparison shows the agreement between the measured and predicted ultimate loads to be very good with a mean of 1.065 and a coefficient of variation of 0.083. However, agreement between the measured and predicted final displacements is less good with a mean value of 0.92 and a coefficient of variation 0.129.

Example of Design Method

To illustrate the method a typical column will be designed.

Determine the section and reinforcement required for a reinforced concrete column 168 ins. (425 cm.) long monolithically cast with slabs at both ends to carry a design ultimate axial load of 150 kips (68,000 kg) and design ultimate moments of 665 kip ins. (770,000 kg. cm.) and 1000 kip ins. (1,115,000 kg. cm.) respectively about the two axes. The column is assumed bent in single curvature and a design understrength factor of 0.7 is to be used.

Assume a concrete strength of 4,000 psi (271 bars), a steel yield stress of 60,000 psi (4,100 bars), 4% reinforcement and a cover ratio of g = 0.70.

$$\frac{pf_y}{f_c'} = 0.60$$

Assume column size 13 ins. (33 cm.) x 13 ins. (33 cm.) and cover ratio 0.70.

$$P_u' = \frac{P_u}{\phi} = 214 \text{ kips } (97{,}000 \text{ kg.})$$

$$\frac{P_u'}{f_c'bt} = \frac{214{,}000}{4{,}000 \times 13 \times 13} = 0.317$$

$$e = \sqrt{(4.42)^2 + (6.67)^2} = 8 \text{ ins. } (20.4 \text{ cm.})$$

From Figure 2 with g = 0.70 and $\frac{pf_y}{f_c'} = 0.6$

$$F = 1.08$$

$$e \text{ modified} = Fe = 1.08 \times 8 = 8.64 \text{ ins. } (21.9 \text{ cm})$$

$$\theta = \tan^{-1} \frac{665}{1000} = 33.6^{o}$$

$$\frac{e}{t} = \frac{8.64}{13.00} = 0.665$$

At the ends of the column, using Figure 1, and estimating θ between $\theta = 0$ and $\theta = 45^{o}$

Maximum strain $\varepsilon = 0.0018$

$$\frac{z}{t} = 0.72 \quad \therefore z = 9.36 \text{ ins. } (23.8 \text{ cm})$$

(z is the perpendicular distance between the point of maximum strain and the neutral axis).

$$\text{curvature} = \frac{0.0018}{9.36} = 0.000193 \text{ ins.}^{-1} \; [0.000075 \text{ cm}^{-1}]$$

At mid column height the load is the same but the eccentricity and its angle are unknown.

Assume maximum strain = 0.0030. Again from Figure 1

$$\frac{e}{t} = 0.765 \quad \therefore e = 9.95 \text{ ins. } (25.2 \text{ cm})$$

$$\frac{z}{t} = 0.710 \quad \therefore z = 9.22 \text{ ins. } (23.4 \text{ cm})$$

$$\text{curvature} = \frac{0.0030}{9.22} = 0.000326 \text{ ins.}^{-1} \; (0.000128 \text{ cm}^{-1})$$

From moment area the lateral deflection about the neutral axis

$$\Delta = 1.08 \text{ ins. } (2.74 \text{ cm})$$

Hence e actual = e top + Δ = 8.64 + 1.08 = 9.72 ins. (24.6 cm)

e possible = 9.95 ins. (25.2 cm)

e possible > e actual $\therefore$ section OK.

Conclusion

An improved form of the short column axial load-biaxial moment interaction diagram is presented which also gives information concerning the maximum concrete strain and curvature necessary to develop the load capability of the section. Long column behaviour can be determined by integrating the curvature(s) along the column.

References

1. Abdel-Sayed, I. "Behaviour of slender reinforced concrete columns under biaxially eccentric loading." Ph.D. Thesis 1974, University of Ottawa.

2. Abdel-Sayed, I. and Gardner, N.J. 'Design of Symmetric Square Slender Reinforced Concrete Columns under Biaxially Eccentric Loads.' Column Symposium, ACI Fall Convention, October 1973, Ottawa.

3. Building Code Requirements, ACI 318-71, American Concrete Institute, Detroit, U.S.A., 1971.

4. Hagnestad, A. 'A study of combined and axial load in reinforced concrete members'. Bulletin #399, University of Illinois Experiment Station.

5. Livesley, R.K. and Chandler, D.B. 'Stability Functions for Structural Frameworks', Manchester University Press, 1955.

Notation

b	smaller dimension of column cross section
e	eccentricity of load, e_x about y axis, e_y about x axis
F	factor to correct for cover ratio - defined in text
f'_c	specified cylinder strength of concrete
f_y	specified yield strength of reinforcement
g	cover ratio
P_u	design ultimate load
P'_u	ultimate load
P_{exp}	experimental ultimate load
P_{ca}	calculated ultimate load
p	steel ratio
t	larger dimension of column cross-section
z	perpendicular distance from neutral axis to point of maximum strain
Δ	lateral displacement of column
ε	maximum concrete strain
ϕ	understrength factor

SUMMARY

An improved axial load biaxial moment interaction diagram including information on strain and curvature is presented. Results predicted by the proposed method are shown to be in good agreement with those measured in a companion experimental investigation. Finally, a design example using the interaction diagram is presented.

RESUME

Cette étude présente un diagramme amélioré d'interaction, donnant des informations sur la charge, les flexions biaxiales, la déformation spécifique et la courbure. Les résultats prédits par cette méthode sont en accord avec ceux de l'étude expérimentale. Un exemple de calcul employant le diagramme d'interaction est présenté.

ZUSAMMENFASSUNG

Es wird ein verbessertes Interaktions-Diagramm vorgestellt, welches neben der Beziehung zwischen Last und Exzentrizität zusätzlich Information über Dehnung und Krümmung enthält. Die nach der vorgeschlagenen Methode erhaltenen Ergebnisse sind in guter Uebereinstimmung mit Versuche. Zum Schluss wird ein Bemessungsbeispiel unter Anwendung des Interaktionsdiagramms durchgerechnet.

Set Number	Specimen Number	e_x in	e_y in	P_{exp} kip	P_{ca} kip	$\frac{P_{exp}}{P_{ca}}$	δ_{exp}	δ_{ca}	$\frac{\delta_{exp}}{\delta_{ca}}$
Set A	A1	0	2.5	62.5	64.5	0.97	0.90	0.90	1.00
90" long	A2	1.25	2.5	56.9	56.9	1.00	0.81	0.76	1.06
#7 bars	A3	2.5	2.5	46.2	44.6	1.03	0.83	0.71	1.17
	A4	0	5.0	39.2	38.8	1.01	1.1	1.28	0.86
	A5	1.67	5.0	33.8	33.7	1.00	1.0	0.95	1.05
	A6	3.33	5.0	26.7	26.5	1.01	0.96	0.87	1.11
	A7	5.0	5.0	22.0	20.9	1.05	0.94	0.79	1.19
	A8	0	7.5	29.7	29.3	1.01	1.26	1.45	0.87
	A9	2.5	7.5	23.4	22.0	1.06	1.00	1.02	0.98
	A10	5.0	7.5	22.6	20.3	1.11	0.87	0.89	0.98
	A11	7.5	7.5	15.8	15.0	1.05	0.87	0.88	0.99
Average						1.03			1.02
Set C	C1	0	2.5	48.5	56	0.87	2.41	2.42	1.00
134" long	C2	1.25	2.5	39	47.5	0.82	1.84	2.0	0.92
#7 bars	C3	2.5	2.5	36	36.6	0.98	1.82	1.72	1.06
	C4	0	5.0	31.9	31.7	1.01	3.00	3.05	0.98
	C5	1.67	5.0	28.8	28.7	1.01	2.05	2.10	0.98
	C6	3.33	5.0	20.6	20.5	1.01	1.83	1.87	0.98
	C7	5.0	5.0	17.9	17.9	1.00	1.84	1.64	1.12
	C8	0	7.5	22.6	22.4	1.01	2.41	3.14	0.77
	C9	2.5	7.5	19	17.4	1.09	1.74	1.82	0.96
	C10	5.0	7.5	14.9	14.8	1.01	1.76	1.95	0.90
	C11	7.5	7.5	13.8	13.2	1.04	1.81	1.82	0.99
Average						0.99			0.97
Set B	B1	0	2.5	44	38.4	1.14	0.8	1.06	0.76
90" long	B2	1.25	2.5	31.2	27.9	1.12	0.61	0.82	0.75
#3 bars	B3	2.5	2.5	27.2	22.5	1.21	0.65	0.78	0.83
	B4	0	5.0	18.1	14.7	1.23	0.97	1.34	0.73
	B5	1.67	5.0	16.5	14.0	1.18	0.86	1.07	0.80
	B6	3.33	5.0	12.4	11.4	1.09	0.76	1.04	0.73
	B7	5.00	5.0	10.4	9	1.15	0.75	0.97	0.78
	B8	0	7.5	10.1	8.7	1.15	1.18	1.48	0.80
	B9	2.5	7.5	9.7	8.1	1.20	1.05	1.11	0.95
	B10	5.0	7.5	8	6.95	1.15	1.02	1.09	0.94
	B11	7.5	7.5	6.4	5.2	1.23	1.03	1.04	0.99
Average						1.17			0.82
Set D	D1	0	2.5	28.5	27.7	1.03	1.4	1.67	0.84
134" long	D2	1.25	2.5	24	22.4	1.07	1.3	1.64	0.79
#3 bars	D3	2.5	2.5	16	16	1.00	1.2	1.32	0.91
	D4	0.0	5.0	14	13.4	1.04	1.99	2.34	0.85
	D5	1.67	5.0	11.9	11.5	1.04	1.51	1.95	0.78
	D6	3.33	5.0	10.7	10.4	1.03	1.41	1.85	0.76
	D7	5.0	5.0	8.3	7.9	1.05	1.46	1.59	0.92
	D8	0.0	7.5	9.8	8.20	1.19	2.19	2.33	0.94
	D9	2.5	7.5	8.7	7.38	1.18	2.23	2.29	0.93
	D10	5.0	7.5	7.7	6.84	1.12	1.83	2.11	0.87
	D11	7.5	7.5	7	6.3	1.11	1.84	1.96	0.94
Average						1.08			0.87
Overall Average						1.07			0.92

Table 1 Comparison of predicted and experimental results

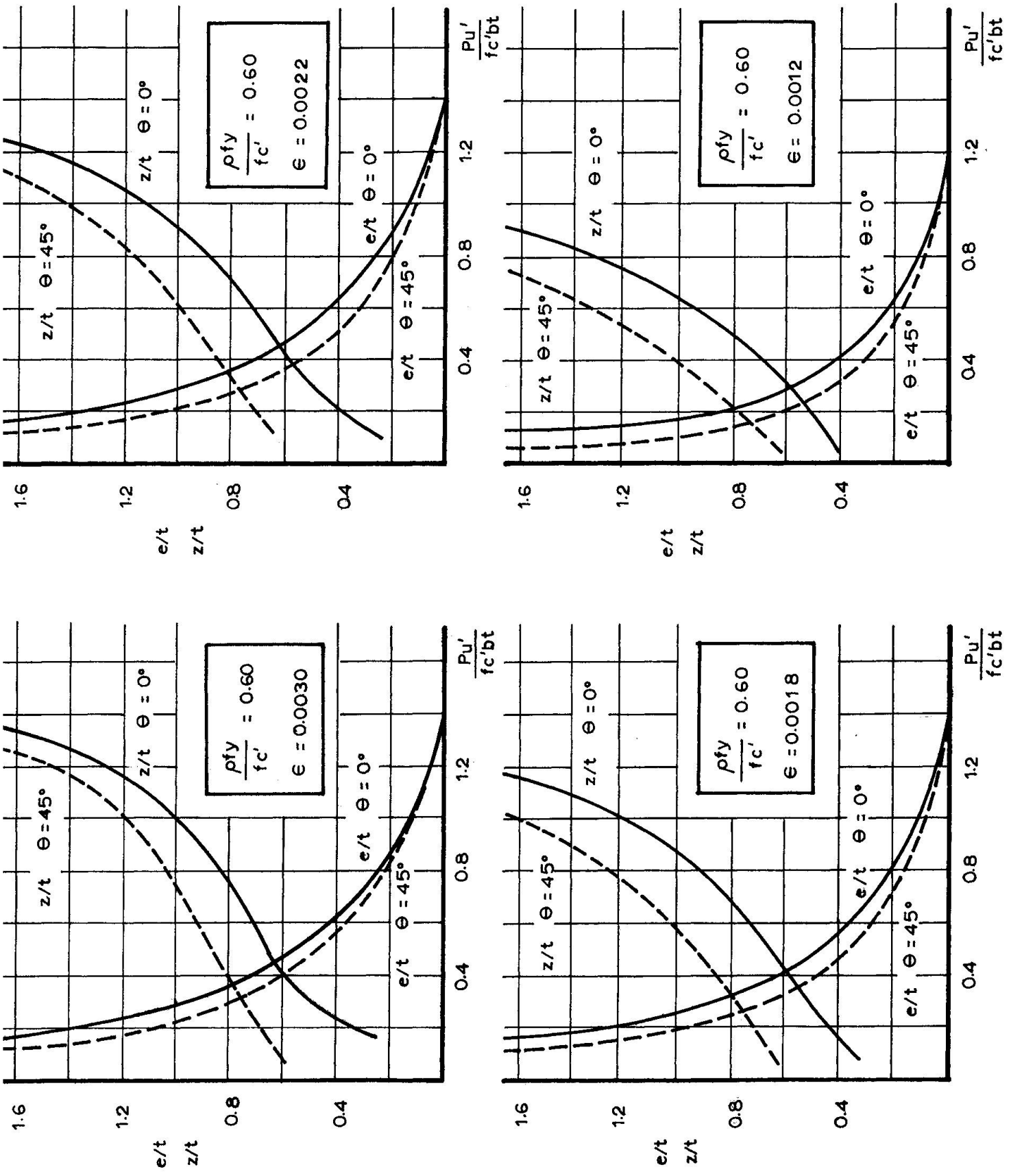

Figure 1 Interaction curves for $\frac{\rho f_y}{f_c'} = 0.60$

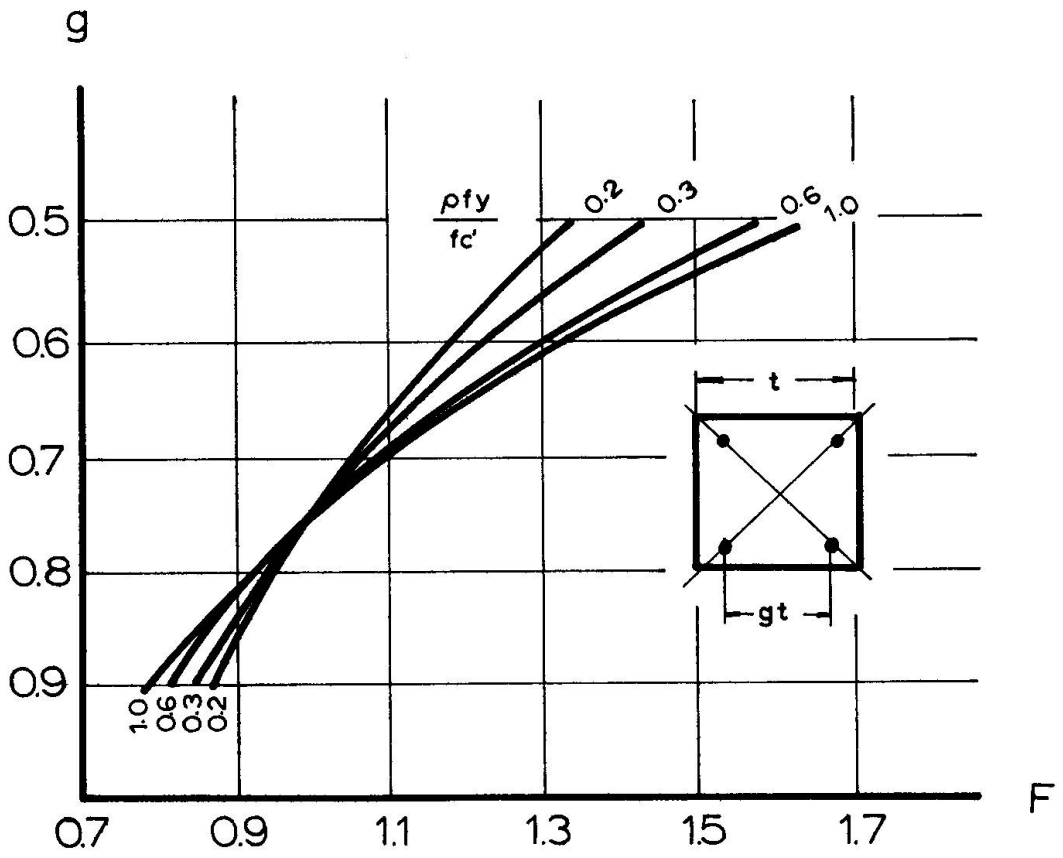

Figure 2 Factor F to modify results with a cover ratio g=0.75 to any other cover ratio

II

Analysis and Design of Reinforced Columns under Biaxial Loading

Calcul et dimensionnement de colonnes en béton armé soumises à une charge biaxiale

Berechnung und Bemessung von Stahlbetonstützen unter zweiaxiger Belastung

Wai F. CHEN
Associate Professor
Department of Civil Engineering
Fritz Engineering Laboratory
Lehigh University
Bethlehem, Pennsylvania
USA

M.T. SHORAKA
Engineer
United Engineers & Constructors, Inc.
Philadelphia, Pennsylvania
USA

INTRODUCTION: In an actual building framework, many columns are frequently subject simultaneously to bending moments about both major axes in addition to an axial compressive load, especially for corner columns. This type of loading is commonly called "biaxial loading" or "biaxial bending". The biaxial bending moments may be resulted from the space action of the entire framing system or from an axial compressive load biaxially located with respect to the major axes of the column cross section.

The mathematics of such columns is quite involved, even for the special case of relatively short columns for which the effect of lateral deflections on the magnitudes of bending moments is negligible. For the most part, analysis and design of such columns have in the past been directed toward the study of ultimate strength of reinforced concrete short columns [see for example Chap. 13, Ref. 10]. For square columns, detailed ultimate strength interaction diagrams relating axial load, and biaxial bending moments have recently been reported [7]. For the case of long columns, the present design procedure of biaxially loaded columns does not differ from uniaxially loaded columns. The 1971 ACI Building Code [1], for example, recommends to calculate the moment magnifier separately and apply to the moment about each axis independently. The long columns are then designed according to the given axial compressive load and the magnified biaxial moments. For a short column, the moment magnification factor is taken as unity.

Although this procedure has been used extensively in design computations, it does not give accurate indications of the true load-carrying capacity of a biaxially loaded column. To determine the ultimate strength of such a column, it is necessary to perform an elastic plastic stability analysis that considers the entire range of loading up to ultimate load. This is described in the present paper.

The first part of the paper discusses a rigorous method for performing elastic-plastic stability analysis of reinforced concrete columns subject to axial load combined with biaxial bending. Three classes of problems are considered: short columns, long columns under symmetrical loading, and long columns under unsymmetrical loading conditions. The ultimate strength interaction curves for symmetrical and unsymmetrical loading cases are presented in forms of charts suitable for direct analysis and design. The important factors influencing the behavior of these curves are discussed such as strength of materials, percentage of reinforcement and the magnitude of compression load.

A design method, based on the C_m factor method, is then developed. Preliminary verification indicates that maximum load carrying capacity predicted by C_m factor method for unsymmetrically loaded cases from the exact symmetrically loaded solutions is in good agreement with calculated exact unsymmetric theoretical solutions. The analytical results are also compared with the current ACI (318-71) design method for the biaxial bending case. For a standard cross section considered herein with a moderate axial compression, it is found that the ACI method gives overconservative results.

SCOPE AND ASSUMPTIONS: The columns are assumed to be isolated, simply supported, prismatic and made of rectangular cross section as shown in the insets of Fig. 3. The range of variables considered in the numerical solutions are summarized as follows:

A square cross-section with a = b = 24 in. is considered. The positioning of the reinforcement is chosen as being close to a practical average as shown in the inset of Fig. 2. Three percentages of reinforcement, A_s/ab = 1.25%, 3.25% and 8.33% are used. The stress-strain relationship is assumed to be linearly elastic-perfectly plastic [Fig. 1(b)] and Young's modulus E_s is taken at 29,000,000 psi. Three types of steel, f_y = 40, 60 and 80 ksi, are used.

Three types of concrete are considered, having compressive strengths $k_1 f'_c$ = 3, 4.2 and 5 ksi. The characteristic stress-strain curve assumed for the concrete in compression is shown in Fig. 1(a) [7]. The tensile strength and creep effect of concrete are neglected. The initial modulus of elasticity is taken as E_c = 57600 $\sqrt{f'_c}$ (normal weight concrete) [1]. The concrete strain ε'_c when concrete stress is $k_1 f'_c$ is taken at 0.002. The values of $\gamma_2 = 4$ and $\gamma_1 = E_c \varepsilon'_c / k_1 f'_c$ are used [see Fig. 1(a)]. Details of the description of the stress-strain curve are given elsewhere [7,9].

Analyses are carried out for two values of crushing strain ε_o = 0.003 (ACI [1]) and ε_o = 0.004 (note: CEB recommends 0.0035 [3]). The column is subjected to three levels of axial compressive load, $P/f'_c ab$ = 0.1, 0.5 and 1.0. The slenderness ratios, L/a considered are 0, 10, 20, 30 and 40.

The following two additional assumptions are made in the solutions: (1) plane sections remain plane after bending; and (2) lateral-torsional twisting of the column is neglected. The failure of the column is always caused by the crushing of concrete due to excessive bending curvature. In performing numerical calculations, it is further assumed that the axial compressive load P is applied first and maintained at a constant value as the biaxial bending moments increase or decrease proportionally.

In presenting the families of interaction curves the parameters L/a, $P/f'_c ab$, $M_x/f'_c ab^2$ and $M_y/f'_c a^2 b$ are chosen. The computed interaction curves are used here as a basis for (1) comparing with the C_m method; and (2) comparing with 1971 ACI moment magnifier method. The development of simple approximate interaction formulas is given elsewhere [2]. All the numerical computations are carried out in the CDC 6400 electronic digital computer.

MOMENT-CURVATURE-THRUST RELATIONSHIPS: The relations between the bending moments M_x, M_y and axial force P, and the bending curvature φ_x, φ_y and axial strain ε_o at corner 0 [Fig. 2] are of prime importance in the analysis of a long reinforced concrete column. These relationships used in the present calculations were determined by a separate program. In this program a moment vs. curvature curve was developed for a constant axial compressive load with the other moment being held constant. Typical moment-curvature relations for a square section with $P/f'_c ab$ = 0.5 are shown in Fig. 2, which has been computed from the stress-strain curves given in Fig. 1. The moment-curvature curve is obtained numerically by dividing the cross section into a large number of rectangular finite elements. Assuming linear strain distribution over the section, the strains of the elements are

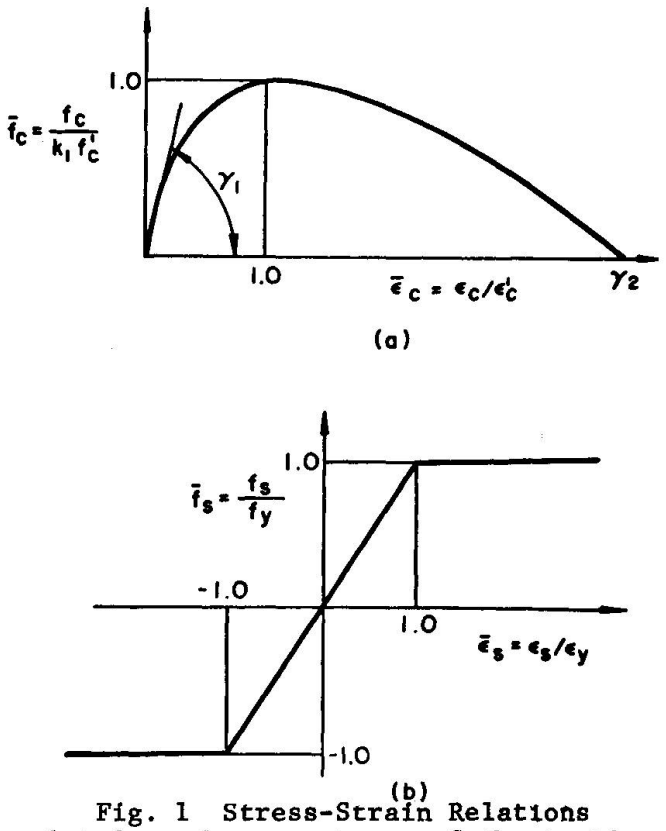

Fig. 1 Stress-Strain Relations

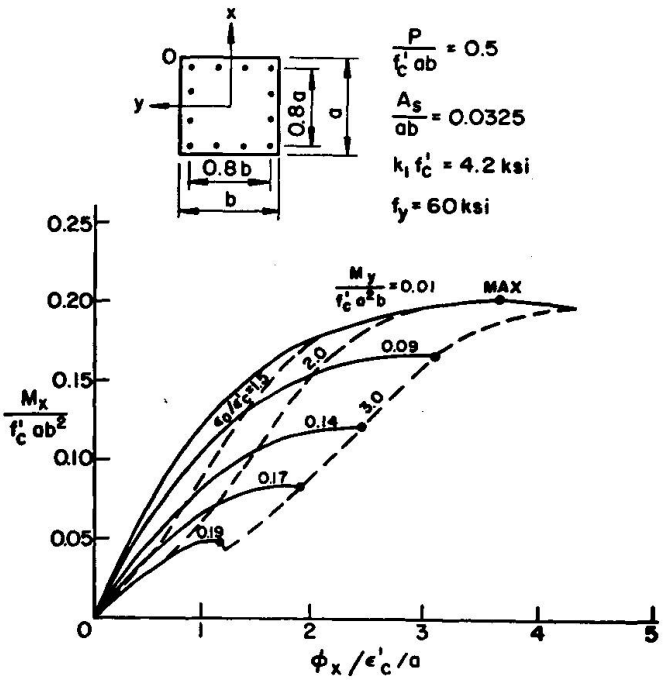

Fig. 2 Moment-Curvature Relations: Standard Case

related to the curvatures of the section. The stresses are related to the applied bending moments through the condition of equilibrium. The relationship between the applied moments and the resulting curvatures can therefore be found through the stress-strain relations shown in Fig. 1. The details of the method and the computer program are described in Ref. [7,9] for reinforced concrete sections and in Ref. [6] for steel H-sections.

In the numerical analysis, the square cross section was divided into 100 (10x10) and 400 (20x20) elements. The increase in accuracy obtained by using the finer grids was only 0.1%. A partitioning of the concrete cross section into 100 elements and steel areas into 12 elements distributed uniformly around the sides of the section are used herein. The strain and stress in each element were computed as the average value at its centroid. The allowable error in P/f'_c ab was 0.002.

METHOD OF SOLUTION: The desire response of a given column (with known length and cross sectional properties) subjected to a specified axial compressive load is the relation between an end moment and a lateral deflection. Once the complete load-deflection curve is obtained, the maximum biaxial moment that can be carried by a reinforced concrete column can be easily determined from the peak of the curve.

The numerical integration process used here is the Newmark's method [5]. The column lengths were divided into 9 segments. This degree of subdivision of column length was checked against a sub-division of 15 and 20 segments. The refined analysis leads to only an improvement of less than 1% in the results, when compared with the 9-segment solution, while the computational time was increased by more than twice.

The starting point in the Newmark's method is to assume a reasonable initial deflected shape: Herein, the elastic deflection is used with the flexural rigidity EI being computed from the approximate EI formula given by 1971 ACI Code [1]. The details of Newmark's method are described in Ref. [5].

NUMERICAL RESULTS: The interaction diagrams giving the combinations of axial compressive load and biaxial moment corresponding to maximum or ultimate load conditions are shown in Figs. 3 through 11 for symmetrically loaded cases and in Figs. 12 to 15 for unsymmetrical loading cases. The interaction curves shown in

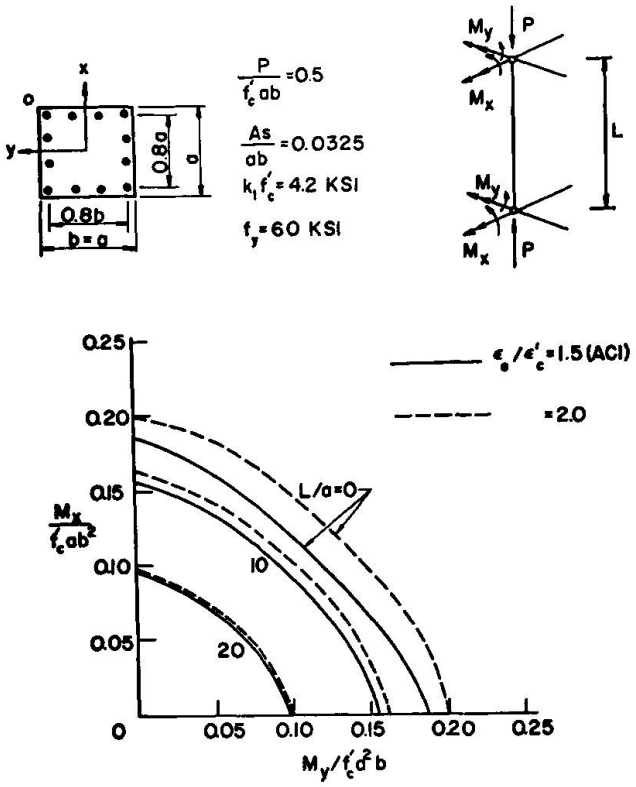

Fig. 3 Interaction Curves: Standard Case, Long Column

Fig. 3 and the moment-curvature relations shown in Fig. 2 are considered here as the standard case. Each diagram is for a particular reinforced concrete column with a given compression load. Since these interaction curves are nondimensionalized, they can be directly used in analysis and design computations and also in checking the validity of the existing design approximations. This will be described later.

Referring now to the symmetric loading cases [Figs. 3 to 11], plotted on each interaction diagram for a slender ratio are two sets of interaction curves corresponding to two different values of concrete crushing strain $\varepsilon_o/\varepsilon' = 1.5$ (solid lines) and 2.0. As can be seen, an increase in concrete crushing strain from $\varepsilon_o = 0.003$ to 0.004 significantly increases the ultimate strength of a biaxially loaded column, when the slenderness ratio L/a is less than 20. This is almost true for all the variables investigated here.

The important factors influencing the ultimate strength of a long column are the magnitude of compression load P (Figs. 3, 4 and 5), concrete quality $k_1 f'_c$ (Figs. 6 and 7), steel quality f_y (Figs. 8 and 9), and percentage of reinforcement A_s/ab (Figs. 10 and 11). The variations of these factors with respect to the standard case may be obtained by comparing Figs. 4 to 11 with Fig. 3. The shape of the interaction curves is obviously a function of these factors considered. This is discussed further in Ref. [2] where a mathematical equation is used to approximate the interaction curves.

COMPARISON WITH EQUIVALENT MOMENT METHOD (C_m-METHOD): Since the determination of the ultimate strength of reinforced concrete columns subject to biaxial bending requires lengthy computations, design aids in the form of interaction curves such as those shown in Figs. 3 to 15, or tables are needed for design in practice. However, even for the symmetrically loaded case, the range of important variables which could be considered is very large, and some restriction is necessary to keep the total number of design aids to a practical level. It is obvious that further presentation of interaction curves for various ratio of combinations of unsymmetric biaxial bending moments about each axis is too large in number to be practical. Hence, to cover adequately and comprehensively unsymmetric biaxial bending within a manageable compilation, the ultimate strength of columns to unsymmetric biaxial bending conditions must be related to its symmetric counterpart. The equivalent moment or C_m method is adopted herein to achieve this.

The C_m-method has been used extensively in the in-plane beam-column design. Direct modification of the equation recommended by AISC [4] for in-plane cases is now extended to the biaxial cases in the following manner.

$$C_{mx} = 0.6 + 0.4 \frac{M_{bx}}{M_{ax}} \geq 0.4, \qquad C_{my} = 0.6 + 0.4 \frac{M_{by}}{M_{ay}} \geq 0.4 \qquad (1a,b)$$

where M_{ax}, M_{ay}, M_{bx} and M_{by} are the end moments, and M_{ax} and M_{ay} being the larger ones. The equivalent symmetric bending moments in the two axes are

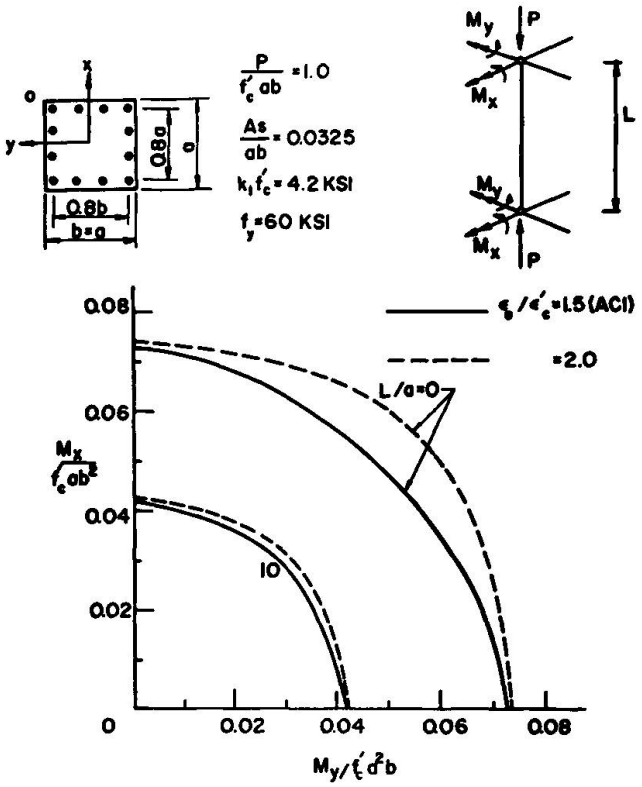

Fig.4
Interaction Curves:
Maximum Axial
Compression Force Effect

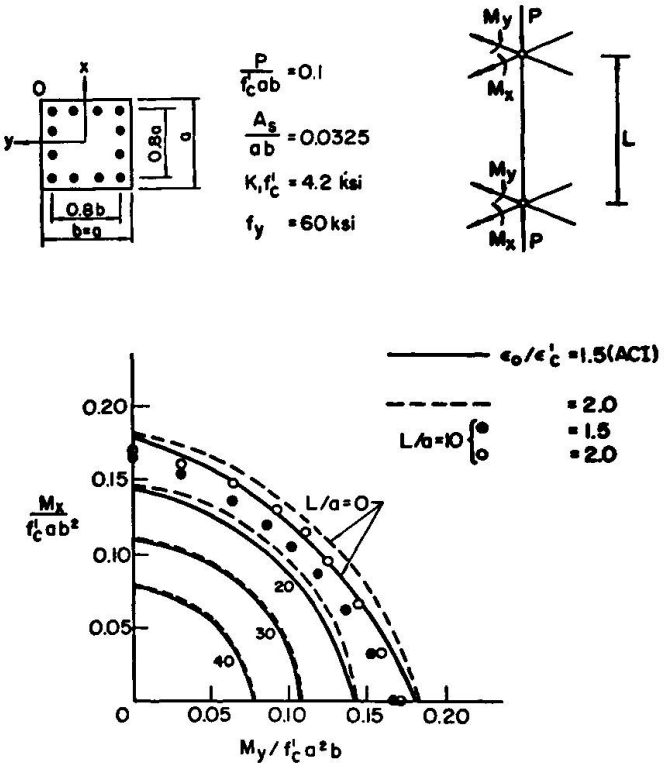

Fig.5
Interaction Curves:
Minimum Axial
Compression Force Effect

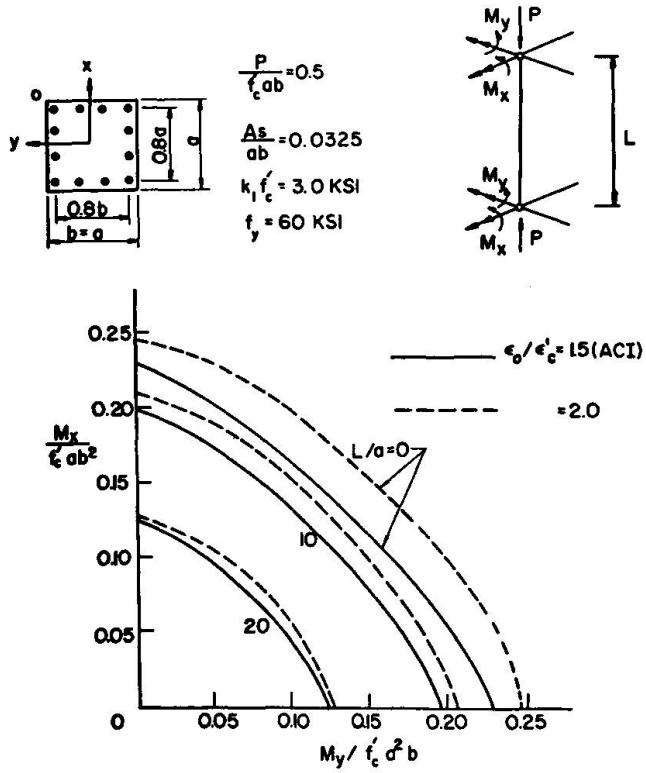

Fig.6
Interaction Curves:
Minimum
Concrete Quality Effect

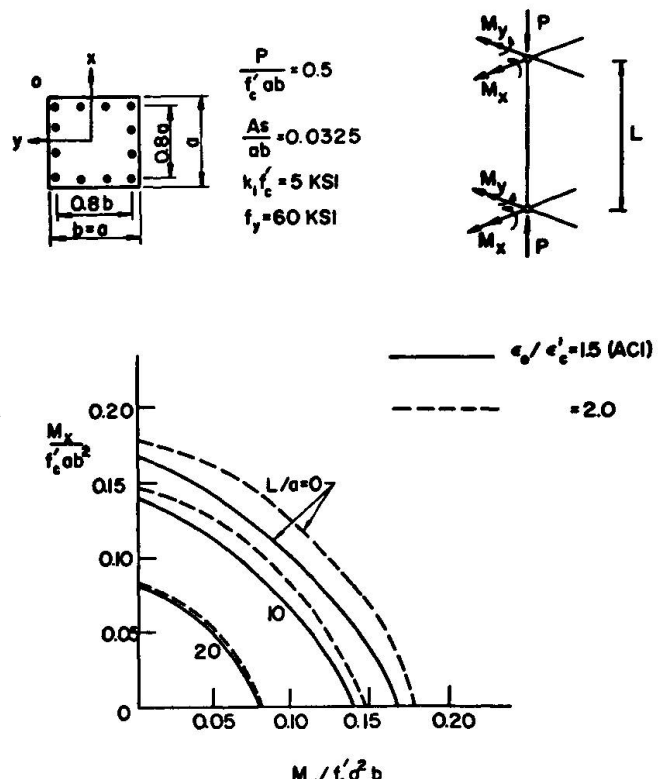

Fig.7
Interaction Curves:
Maximum
Concrete Quality Effect

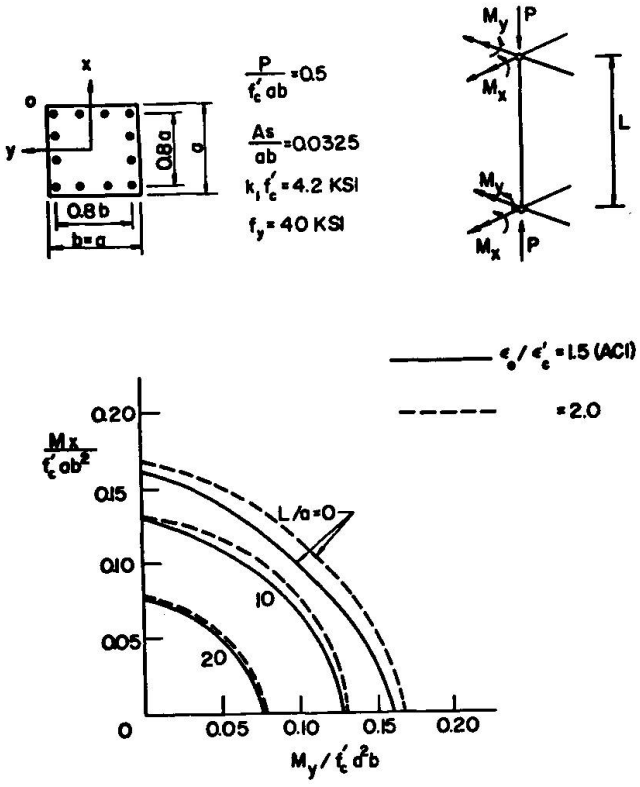

Fig. 8 Interaction Curves: Minimum Steel Quality Effect

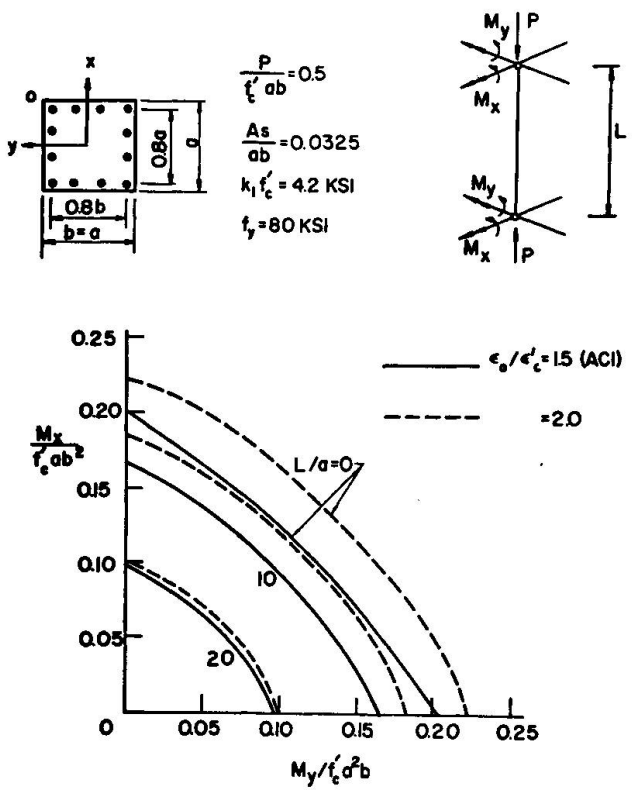

Fig. 9 Interaction Curves: Maximum Steel Quality Effect

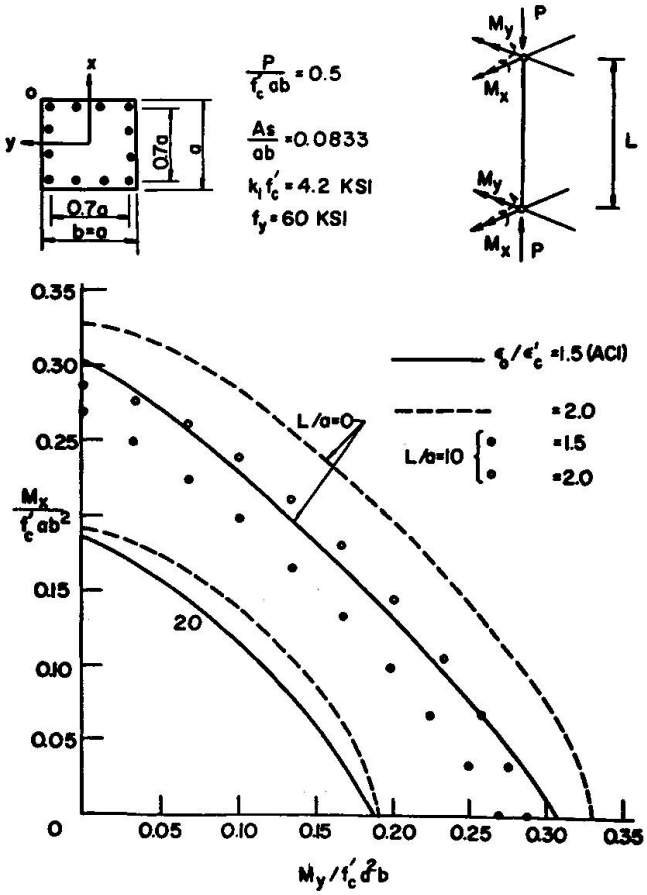

Fig. 10 Interaction Curves: Maximum Percentage of Steel

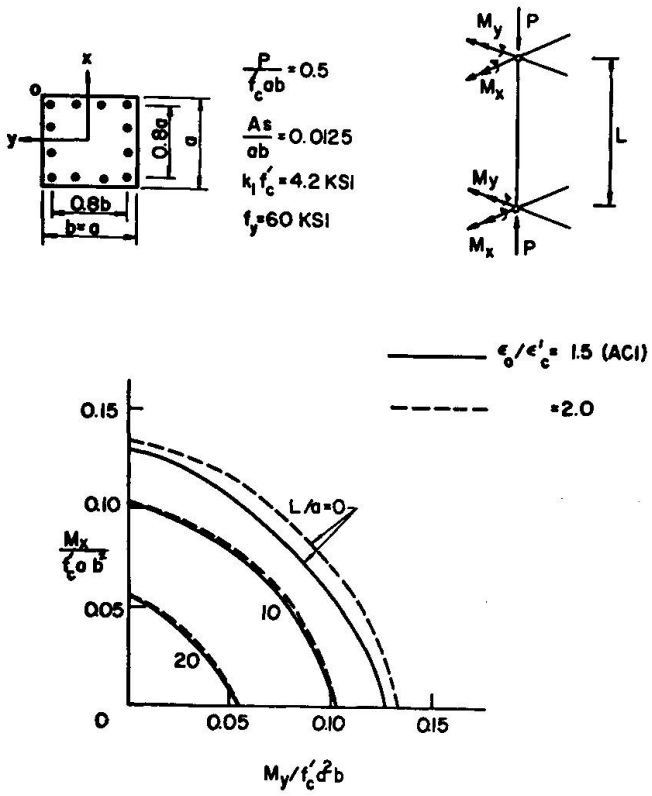

Fig. 11 Interaction Curves: Minimum Percentage of Steel

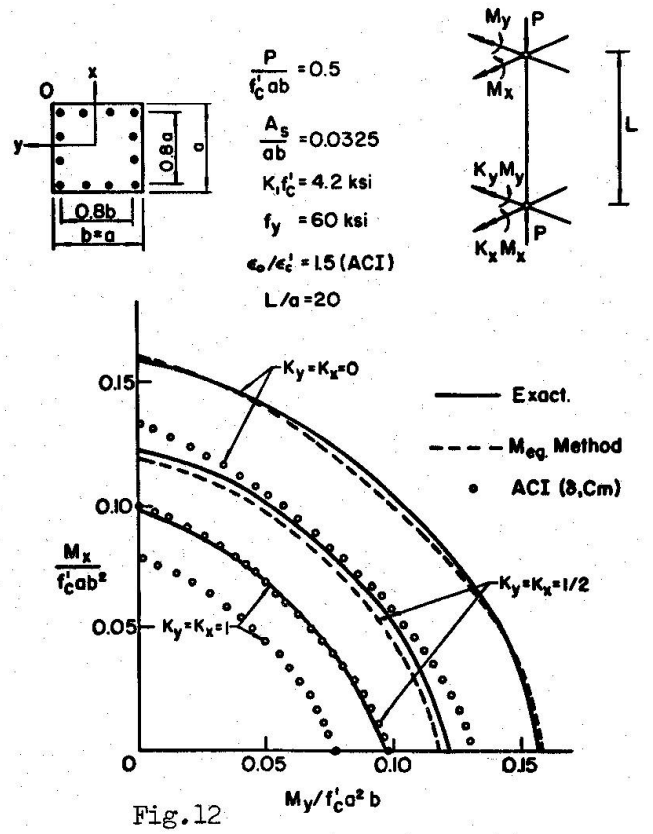

Fig.12
Comparison of Exact Solutions with Equivalent Moment Method and ACI Moment Magnifier Method

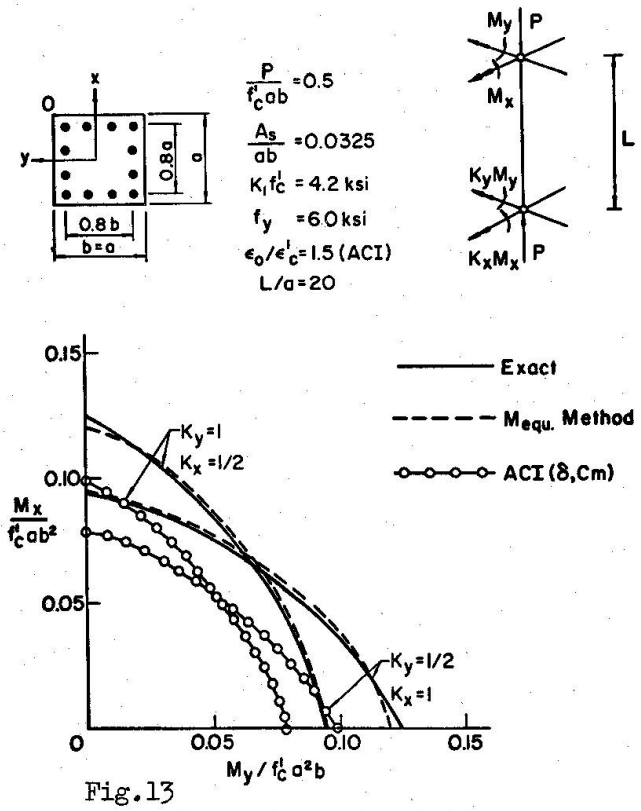

Fig.13
Comparison of Exact Solutions with Equivalent Moment Method and ACI Moment Magnifier Method

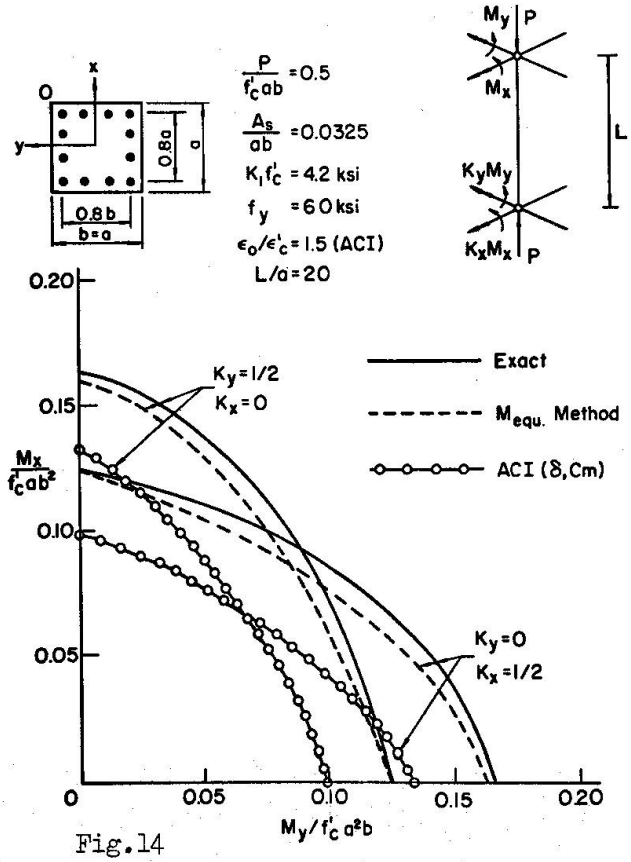

Fig.14
Comparison of Exact Solutions with Equivalent Moment Method and ACI Moment Magnifier Method

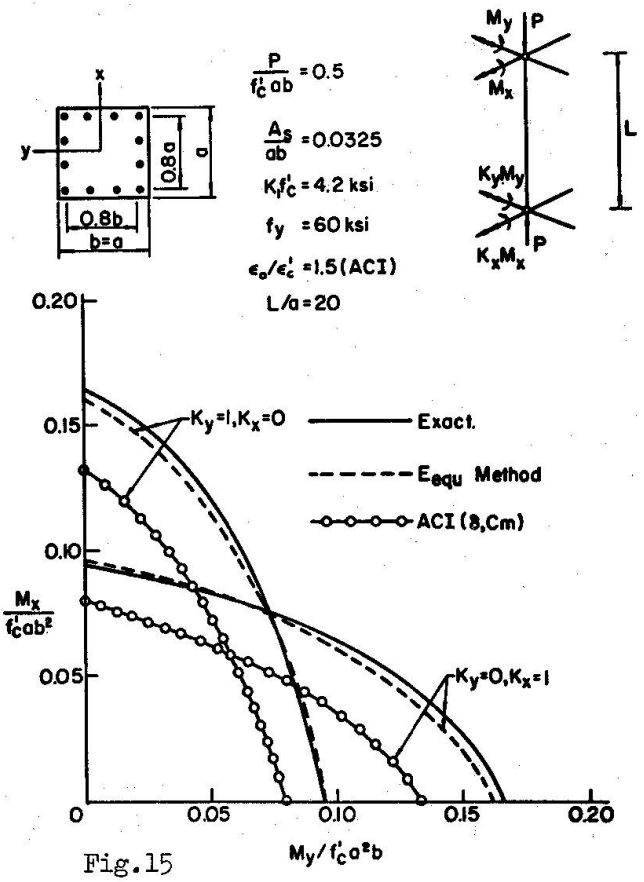

Fig.15
Comparison of Exact Solutions with Equivalent Moment Method and ACI Moment Magnifier Method

$$(M_x)_{eq} = C_{mx} M_{ax}, \quad (M_y)_{eq} = C_{my} M_{ay} \qquad (2a,b)$$

these equivalent moment values should be used in Figs. 3 to 11 when the interaction curves for the case of unsymmetrically loaded columns are sought from the corresponding interaction curves developed for the case of symmetrically loaded conditions. These results (dotted curves) are compared with the exact solutions in Figs. 12 to 15 for several ratios of combinations of unsymmetric biaxial bending moments $K_x = M_{bx}/M_{ax} = 0$, 1/2 and 1 and $K_y = M_{by}/M_{ay} = 0$, 1/2 and 1. In all cases good agreement is observed. It may be concluded from this study that the strength of unsymmetrically loaded biaxial columns may be obtained directly from Figs. 3 to 11 using the equivalent moment concept. This observation is in agreement with previous investigations on steel beam-columns [8].

COMPARISON WITH MOMENT MAGNIFIER METHOD (δ-METHOD): The formula which will be used in the comparison is Formula (10-4) given in Chap. 10 of the 1971 ACI Code [1]. In Formula (10-4), the capacity reduction factor Φ is taken as 1.0 and the creep reduction factor β_d is taken as 0. The value EI is computed from Formula (10-7) of the Code. The C_m factor as given in Eqs. (2) [or Formula (10-9) of ACI Code] is used for the case of unsymmetrical loading conditions. The maximum loads determined by the ACI formula (10-4) are compared in Figs. 12 to 15 (open circles) with the present "exact" solutions.

The moment magnifier method combined with the C_m factor is seen to give extremely conservative results for the standard case investigated. This is probably due to the fact that a more precise formula for estimating the initial stiffness is required, when a column is subjected to biaxial bending conditions.

CONCLUSIONS: Ultimate strength interaction relations for reinforced concrete columns subjected to compression combined with biaxial bending have been developed for short as well as long columns under symmetric and unsymmetric loading conditions. The results are presented in Figs. 3 to 15 in the form of interaction curves relating the axial compression, maximum biaxial moment and slenderness ratio.

The maximum biaxial moments determined by the ACI moment magnifier method have been compared with the present analytical results and are found to give overconservative results for the standard cross section considered here with a moderate axial compression. It is also found that maximum load carrying capacity predicted by C_m factor method for unsymmetrically loaded cases from the symmetric cases is in good agreement with calculated theoretical values.

ACKNOWLEDGMENTS: The research reported here was supported by the National Science Foundation under Grant GK-35886 to Lehigh University.

REFERENCES:

1. ACI Committee 318-71, "Building Code Resuirements for Reinforced Concrete", (ACI 318-71), American Concrete Institute, Detroit, 1971.
2. Chen, W. F. and M. T. Shoraka, "Design Criteria for Biaxially Loaded Concrete Columns", ASCE Structural Engineering Convention, preprint, Cincinnati, April 22-26, 1974.
3. Comite Europeen du Beton, "International Recommendations for the Design and Construction of Concrete Structures", Paris, June 1970.
4. Manual of Steel Construction, American Institute of Steel Construction, New York, seventh edition, 1970.
5. Newmark, N. M., "Numerical Procedure for Computing Deflections, Moments, and Buckling Loads", Transactions, ASCE, Vol. 108, 1943, p. 1161.
6. Santathadaporn, S. and Chen, W. F., "Tangent Stiffness Method for Biaxial Bending", J. of the Structural Division, ASCE, Vol. 98, No. ST1, January 1972, pp. 153-163.

7. Shoraka, M. T., and Chen, W. F., "Tangent Stiffness Method for Biaxial Bending of Reinforced Concrete Columns", Fritz Engineering Laboratory Report No. 391.1, Lehigh University, Bethlehem, Pa., October 1972.

8. Tebedge, N. and Chen, W. F., "Design Criteria for Steel H-Columns under Biaxial Loading", Journal of the Structural Division, ASCE, Vol. 100, No. ST3, March 1974, pp. 579-598.

9. Warner, R. F., "Biaxial Moment Thrust Curvature Relation", J. of the Structural Division, ASCE, Vol. 95, No. ST5, May 1969, pp. 923-940.

10. Wang, C. K. and Salmon, C. G., "Reinforced Concrete Design", Intext Educational Publishers, New York, second edition, 1973, pp. 469-492.

SUMMARY

Several design criteria for reinforced concrete columns subjected to compression combined with biaxial bending are discussed. The load carrying capacity of the column is presented in terms of interaction diagrams. Three classes of problems are considered: short columns, long columns under symmetrical loading and long columns under unsymmetrical loading conditions. The analytically obtained results are compared with the current ACI (318-71) design formula and also with the C_m method for the case of unsymmetrically loaded conditions.

RESUME

On examine plusieurs critères de dimensionnement pour les colonnes soumises à une charge axiale et à une flexion biaxiale. La charge que peut supporter la colonne est présentée sous forme de diagrammes d'interaction. On distingue trois catégories de problèmes: colonnes courtes, colonnes longues avec charge symétrique et colonnes longues avec charge asymétrique. On compare les résultats du calcul avec les formules de dimensionnement ACI (318-71) et avec la "C_m method" dans le cas d'une charge asymétrique.

ZUSAMMENFASSUNG

Es werden einige Bemessungskriterien für Stahlbetonstützen unter Normalkraft und zweiaxiger Biegung diskutiert. Die Tragfähigkeit der Stützen wird in Form von Interaktionsdiagrammen dargestellt. Dabei werden drei Problemgruppen berücksichtigt: kurze Stützen, lange Stützen unter symmetrischer Belastung und lange Stützen unter unsymmetrischen Belastungsbedingungen. Die rechnerisch erhaltenen Ergebnisse werden mit den Bemessungsformeln der gültigen Normen ACI (318-71) sowie - für den Fall unsymmetrischer Lastbedingungen - auch mit der C_m-Methode verglichen.

Leere Seite
Blank page
Page vide